

Knut Erik Ellingsgård Johansen

Subsea Compressor Transients

Master's thesis in Mechanical Engineering

Supervisor: Lars Eirik Bakken

Co-supervisors: Erik Langørgen, Martin Bakken and Øyvind Hundseid

July 2020

Knut Erik Ellingsgård Johansen

Subsea Compressor Transients

Master's thesis in Mechanical Engineering

Supervisor: Lars Eirik Bakken

Co-supervisors: Erik Langørgen, Martin Bakken and Øyvind Hundseid

July 2020

Norwegian University of Science and Technology

Faculty of Engineering

Department of Energy and Process Engineering



Norwegian University of
Science and Technology

MASTER WORK

for

student Knut Erik Ellingsgård Johansen

Spring 2020

Subsea Compressor Transients

Background and objective

Understanding a compressor system and its response to different operating conditions is vital. Especially subsea wet gas compressor systems represent challenges as the flow regime to the compressor inlet may change according to flow line operating condition. This includes transient behaviour as a function of liquid content and trip scenarios.

The overall objective is to test and analyse relevant wet trip scenarios to document the compressor system behaviour. Based on the NTNU test lab compressor, relevant wet trip trajectories should be established to document the impact of compressor deterioration and/or “head rise to surge”.

The following tasks to be considered:

Based on literature review and experimental work at the wet gas compressor test rig, the focus areas are:

1. Establish relevant compressor performance characteristics.
2. Review and validate how to establish different trip trajectories at dry and wet gas conditions.
3. Establish and document how different compressor performance characteristics affect the trip trajectory and related “time to surge” and “time in surge”.

Supervisor:

Lars E Bakken

Co-Supervisor(s):

Martin Bakken, Equinor
Erik Langørgen, NTNU
Øyvind Hundseid, NTNU

Intentionally left blank

Preface

You are now reading my master's thesis in Mechanical Engineering, «Subsea Compressor Transients». The submission of this thesis marks the graduation of my «Master of Science in Engineering». The work was conducted in the spring semester 2020 at the Department of Energy and Process Engineering located at NTNU in Trondheim. Five years of studies culminates in this project. In the middle of this period a special situation changed the everyday life for everyone. A global pandemic, leading to the most drastic intervention in a Norwegian's life ever in peacetime. This includes closed university and no access to the laboratory facilities. No doubt this complicates the work with the thesis. The result of this is postponement of the laboratory campaign and modifications of the scope as we go. However, I feel that I have made the best out of a challenging situation.

I want to thank my supervisors who have been of great help in this challenging period. Professor Lars Eirik Bakken for sharing his knowledge and being available and welcoming whenever I have needed guidance. I would also like to express my greatest appreciation to the co-supervisors Erik Langørgen, Martin Bakken and Øyvind Hundseid. Erik Langørgen deserves to be highlighted for his wide knowledge and steady hand running the test facility. His help during the tests have been invaluable.

Thank you for great unity in both professional and extracurricular activities to my student colleagues in the thermal energy field. Last but not least, thank you to my family, friends and my girlfriend for unlimited support during many years of studies.



Knut Erik Ellingsgård Johansen

Trondheim, 01.07.2020

Intentionally left blank

Abstract

As many of the easier accessible fields have been explored and are reaching the end of their lifetime, the petroleum industry needs new ideas to sustain production. With high focus on cost effectivity and environmental aspects the industry is led towards subsea development. Subsea wet gas compression is an important part of this. The later years valuable knowledge and experience is achieved through research and development. Still, the technology is novel, and more research is needed to understand all aspects of the operation.

The main objective of this project is to document the impact performance characteristics on compressor stability during compressor driver trip. Of specific interest is fouling, which is known to change the performance characteristics.

To investigate this, an experimental campaign divided into two parts is performed. The first part consists of establishing relevant compressor performance characteristics. This is done for the non-fouled and fouled compressor. Further, a method for replicating the performance characteristics of a fouled compressor using control techniques is established.

The second part consist of compressor driver trip tests. Here, the same three scenarios are tested; non-fouled, fouled and with imitated fouling. The results show that the wet gas effects are more prominent in the fouled compressor. This is seen as a larger deviation between the trip trajectories when varying the fluid liquid content. Further, a migration of the onset of wet gas effects is observed. Formation of a liquid film smoothing out the roughness from the fouling is suggested to be the cause.

Regarding compressor stability, the results demonstrate a positive impact of fouling. The wet gas cases show an increase in time to surge, which is attributed to a higher PRTS found in the performance tests. Also, a reduce time in surge is observed, which are consistent for all fluid liquid contents tested. This is attributed to a higher minimum flow rate after driver trip.

Intentionally left blank

Sammendrag

Mange av de lett tilgjengelige feltene på norsk sokkel er utforsket og nærmer seg slutten på sin levetid. Nye ideer med fokus på kosteffektivitet og miljø har ledet utviklingen mot undervannsteknologi, hvor våtgass undervannskompresjon er en viktig brikke. De siste årene har verdifull erfaring blitt tilegnet gjennom forskning og utvikling, men fremdeles er teknologien relativt ny og mer forskning er nødvendig for å forstå alle aspekter ved drift av våtgasskompressor.

Formålet med dette prosjektet er å dokumentere innvirkningen beleggdannelse har på kompressorstabilitet ved ikke-stasjonær drift som tap av drivkraft. Dokumentasjonen gjøres gjennom en todelt kampanje av eksperimenter. I den første delen etableres relevante ytelseskaraktistikker som inkluderer karakteristikk både med og uten beleggdannelse. I tillegg etableres en metode for å gjenskape karakteristikk til en degradert kompressor ved hjelp av ulike kontrollteknikker. Deretter reproduseres den degraderte ytelseskaraktistikken ved hjelp av denne metoden.

Den andre delen av kampanjen består av ikke-stasjonære tester med hovedvekt på tap av drivkraft. Testene gjøres med og uten beleggdannelse og ved hjelp av metoden for replikasjon av beleggdannelse. Målet er å dokumentere effektene beleggdannelse har på stabilitet ved nedkjøring. Spesielt nyttig er det å dokumentere tiden det tar for kompressoren å nå ustabilitetsområdet og hvor lenge den oppholder seg der.

Resultatene tilsier at våtgasseffektene er mer fremtredende når kompressoren er degradert. Observasjoner tyder også på at grensen hvor våtgasseffektene er tilstede har migrert mot høyere væskeinnhold. Dette forklares med at det dannes en væskefilm i diffusoren som glatter ut ujevnhetene i belegget. Kompressorstabiliteten er også funnet å være bedre, i form av redusert tid i ustabilitetsområdet. Denne effekten tilskrives et høyere minimumsnivå for volumstrøm. For våtgass er også tiden det tar å nå ustabilitetsområdet økt, som forklares med en økt bratthet i ytelseskaraktistikken.

Intentionally left blank

Contents

Preface	iii
Abstract	v
Sammendrag	vii
Contents	ix
List of Figures	xii
List of Tables	xvi
Nomenclature	xvii
1 Introduction	1
1.1 Background	2
1.2 Scope	4
1.3 Delimitation	5
1.4 Structure	5
2 Compressor Fundamentals	7
2.1 Principle of Operation	7
2.2 Performance Evaluation	9
2.2.1 Polytropic Performance	10
2.2.2 Performance Testing	11
2.2.3 Affinity Laws	12
2.3 System Characteristics	13
2.3.1 Control Methods	13
2.3.2 Surge	14
2.4 Performance Deterioration	17
2.5 Wet Gas Impact	18
2.5.1 Multiphase Flow	18
2.5.2 Wet Gas Performance	23
2.6 Summary	25
3 Compressor Driver Trip	26
3.1 Impact of System Characteristics	27
3.1.1 Polar Moment of Inertia	27
3.1.2 Rate of Power Decay	30
3.1.3 Trip Delay	31

3.1.4	Suction and Discharge Volumes	32
3.1.5	Characteristics of Protection Systems	33
3.2	Impact of Performance Characteristics	34
3.2.1	Reduced Performance Steepness	35
3.2.2	Increased Performance Steepness	36
3.3	Impact of Wet Gas	37
3.4	Tuning of Trip Trajectory	38
3.5	Summary	40
4	Test Facility	41
4.1	Compressor System	42
4.1.1	Suction	42
4.1.2	Variable Inlet Guide Vanes	43
4.1.3	Compressor	43
4.1.4	Discharge	44
4.2	Instrumentation	45
4.2.1	Pressure	45
4.2.2	Temperature	46
4.2.3	Flow rate	46
4.3	Summary	47
5	Experimental Campaign - Compressor Performance	48
5.1	Compressor Performance - Base Case	50
5.1.1	Test Objective	50
5.1.2	Results and Discussion	51
5.2	Compressor Performance - Fouling	53
5.2.1	Test Objective	53
5.2.2	Results and Discussion	54
5.3	Replicated Fouling	56
5.3.1	Test Objective	56
5.3.2	Results and Discussion	58
5.4	Uncertainty and Sources of Error	59
5.5	Summary	59
6	Experimental Campaign - Compressor Transients	60
6.1	Driver Trip - Base Case	62

6.1.1	Test Objective	62
6.1.2	Results and Discussion	64
6.2	Driver Trip - Fouling	68
6.2.1	Test Objective	68
6.2.2	Results and Discussion	68
6.3	Driver Trip - Replicated Fouling	71
6.3.1	Test Objective	71
6.3.2	Results and Discussion	72
6.4	Uncertainty and Sources of Error	74
6.5	Summary	75
7	Conclusion	76
8	Further Work	77
	Bibliography	78
	Appendix A: Additional Results	ii
	Appendix B: Test Procedures	x
	Appendix C: Wet Gas Compressor Test Facility	xiii
	Appendix D: Orifice Plate	xiv
	Appendix E: Data Processing	xvi
	Appendix F: Simulation Model	xvii
	Appendix G: Schultz' Approach	xix
	Appendix H: Risk Assessment	xxi

List of Figures

1	Illustration of a complete subsea factory	1
2	Illustration of the two available solutions for subsea compression systems.	3
3	View of the main parts of a compressor seen from a cross-sectional and axial view. . .	7
4	Velocity diagrams at inlet and outlet for a centrifugal compressor stage.	8
5	Various impeller vane designs.	9
6	Polytropic compression process in specific enthalpy-entropy diagram	10
7	Effect of inlet swirl on compressor inlet velocity diagram.	13
8	Effect of inlet swirl on compressor characteristic.	13
9	Behaviour during a deep surge cycle	15
10	Compressor system with anti-surge and hot gas bypass.	16
11	Fouled impeller of a compressor, NTNU Test Facility.	17
12	Flow regimes in horizontal flows.	18
13	Flow regime map for horizontal flows.	18
14	Impeller outlet water jet, NTNU Test Facility.	20
15	Multiphase speed of sound in air/water mixture at 20°C and 1 atm.	22
16	Static pressure ratio versus volume flow rate for varying GMF.	23
17	Polytropic head versus volume flow rate for varying GMF.	23
18	Polytropic efficiency versus volume flow rate for varying GMF.	24
19	Polar inertia impact impact on rundown trajectory	29
20	Power decay time impact on rundown trajectory.	30
21	Driver trip signal delay impact on trip trajectory	31
22	Suction volume impact on the trip trajectory.	32
23	Discharge volume impact impact on the trip trajectory.	32
24	Anti-surge system capacity impact on the trip trajectory.	33
25	Compressor performance characteristics of new machine, Troll Kollsnes.	34
26	Compressor performance characteristics with internal leakage, Troll Kollsnes.	35
27	Compressor performance characteristics with fouling, Troll Kollsnes	36
28	Expected effect on the trip trajectory of varying the individual tuning parameters. . .	39
29	Wet gas compressor suction side, NTNU Test Facility.	41
30	VIGV-unit, NTNU Test Facility.	43
31	P&ID, NTNU Test Facility.	44

32	Piezoelectric pressure sensors mounted along the radius of the diffuser.	45
33	Temperature and pressure sensors at the compressor inlet.	45
34	Flow measurement by differential pressure over an orifice plate.	47
35	Normalized pressure ratio versus normalized total volume flow, base case.	51
36	Normalized polytropic head versus normalized total volume flow, base case.	52
37	Normalized polytropic efficiency versus normalized total volume flow, base case.	52
38	NTNU Test Facility diffuser.	53
39	NTNU Test Facility diffuser with fouling.	53
40	Normalized pressure ratio versus normalized total volume flow, fouled.	54
41	Normalized pressure ratio versus normalized total volume flow, base case versus fouled GMF 0.97.	55
42	Normalized pressure ratio versus normalized total volume flow, base case versus fouled GMF 0.90.	55
43	Normalized polytropic head versus normalized total volume flow, fouled.	55
44	General trend in performance characteristics of clean and fouled compressor at same valve opening.	56
45	Three steps of replicating fouling using compressor control techniques.	57
46	Normalized pressure ratio versus normalized total volume flow, various IGV angles GMF 1.00.	58
47	Normalized pressure ratio versus normalized total volume flow, IGV angle 5° GMF 1.00.	58
48	Normalized pressure ratio versus normalized total volume flow, various IGV angles GMF 0.97.	59
49	Normalized pressure ratio versus normalized total volume flow, various IGV angles GMF 0.90.	59
50	Effect of tuning the rundown trajectory using the discharge throttle valve.	62
51	Valve sequence tool used to tune the rundown trajectory, NTNU Test Facility.	62
52	Trip trajectory, base case without tuning.	64
53	Trip trajectory, base case.	65
54	Normalized rotational speed versus time, base case.	66
55	Total volume flow versus time, base case.	66
56	Pressure ratio versus time, base case.	66
57	Trip trajectory, fouled.	69

58	Trip trajectory for GMF 1, fouled versus non-fouled.	70
59	Trip trajectory for GMF 0.90, fouled versus non-fouled.	70
60	Trip trajectory, replicated fouling.	72
61	Trip trajectory for GMF 1, fouling versus replicated fouling.	73
62	Trip trajectory for GMF 0.90, fouling versus replicated fouling.	73
63	Change in GMF during trip test, starting at three different GMF's.	74
64	Trip trajectory with delay.	ii
65	Response from pressure pulses.	iii
66	Response from pressure pulses, zoomed in.	iii
67	Trip trajectory after correcting for delay.	iv
68	Normalized polytropic head versus normalized total volume flow, fouled.	v
69	Normalized polytropic efficiency versus normalized total volume flow, fouled.	v
70	Normalized polytropic efficiency versus normalized total volume flow, base case versus fouled GMF 0.97.	v
71	Normalized polytropic efficiency versus normalized total volume flow, base case versus fouled GMF 0.90.	v
72	Trip trajectory for all GMF's, base case (*).	vi
73	Trip trajectory for all GMF's, fouled (*).	vi
74	Trip trajectory for all GMF's, replicated fouling (*).	vi
75	Trip trajectory for all scenarios, GMF 1 (*).	vi
76	Trip trajectory for all scenarios, GMF 0.97 (*).	vi
77	Trip trajectory for all scenarios, GMF 0.90 (*).	vi
78	Pressure ratio versus time, GMF 1 (*).	vii
79	Pressure ratio versus time, GMF 0.97 (*).	vii
80	Pressure ratio versus time, GMF 0.90 (*).	vii
81	Total volume flow versus time, GMF 1 (*).	vii
82	Total volume flow versus time, GMF 0.97 (*).	vii
83	Total volume flow versus time, GMF 0.90 (*).	vii
84	Consistency in test scenario #4 (*).	viii
85	Consistency in test scenario #5 (*).	viii
86	Consistency in test scenario #6 (*).	viii
87	Consistency in test scenario #10 (*).	viii
88	Consistency in test scenario #11 (*).	viii

89	Consistency in test scenario #12 (*).	viii
90	Consistency in test scenario #16 (*).	ix
91	Consistency in test scenario #17 (*).	ix
92	Effect of correcting the discharge coefficient for Reynolds' number.	xv
93	HYSYS simulation model.	xvii

List of Tables

2	Wet gas impact on transient system performance.	37
3	Fluid properties of test fluid and natural gas/condensate.	42
4	Test matrix, compressor performance - base case.	50
5	Test matrix, compressor performance - fouling.	53
6	Test matrix, effect of various VIGV-angles on performance characteristics in wet and dry conditions.	57
7	Test matrix, driver trip - base case.	63
8	Stability performance, base case(*).	67
9	Test matrix, driver trip with fouled diffuser.	68
10	Change in stability performance from base case to fouled (*).	70
11	Test matrix, driver trip with replicated fouling.	71
12	Change in stability performance going from fouling to replicated fouling.	73
13	Main dimensions, NTNU Test Facility.	xiii
14	Instrumentation accuracy, NTNU Test Facility.	xiii
15	Simulation model specifications.	xviii

Nomenclature

Latin Letters

Symbol	Description	Units
c	Absolute velocity	m/s
f	Head correction factor	-
Fr	Froude number	-
H	Head	J/kg
I	Polar moment of inertia	kgm^2
\dot{m}	Mass flow	kg/s
M	Mach number	-
MW	Molar weight	kg/kmol
n	Polytropic exponent	-
N	Rotational speed	rpm
P	Pressure	bar
Pr	Pressure Ratio	-
R	Gas constant	$kJ/kmol \cdot K$
Re	Reynolds number	-
St	Stokes number	-
t	Time	s
T	Temperature	K
u	Peripheral velocity	m/s
w	Relative velocity	m/s
We	Weber number	-
X	Compressibility function	-
Y	Compressibility function	-
Z	Compressibility factor	-

Greek Letters

Symbol	Description	Units
α	Gas volume fraction	-
β	Gas mass fraction	-
κ	Isentropic exponent	-
η	Efficiency	-
μ	Dynamic viscosity	Ns/m^2
Ω	Rotational speed	rad/s

Subscripts

Subscript	Description
1	Inlet/suction
2	Outlet/discharge
c	Compressor
C	Constant
d	Droplet
i	Initial
mp	Multiphase
o	Orifice
P	Polytropic
tot	Total
T	Temperature
v	Valve
V	Volume

Abbreviations

Index	Description
ASME	The American Society of Mechanical Engineers
ASV	Anti Surge Valve
BEP	Best Efficiency Point
FT	Flow Transmitter
GMF	Gas Mass Fraction
GVF	Gas Volume Fraction
HGB	Hot Gas Bypass
HRTS	Head Rise To Surge
HS	High Speed
IGV	Inlet Guide Vanes
IOR	Improved Oil Recovery
ISO	International Organization for Standardization
LS	Low Speed
NCS	Norwegian Continental Shelf
NG	Natural Gas
NTNU	Norwegian University of Science and Technology
PDT	Pressure Differential Transmitter
PT	Pressure Transmitter
PMMA	Polymethyl methacrylate
PRTS	Pressure ratio Rise To Surge
P&ID	Process and Instrument Diagram
RMS	Root Mean Square
TIS	Time In Surge
TT	Temperature Transmitter
TTS	Time To Surge
VIGV	Variable Inlet Guide Vanes
VSD	Variable Speed Drive

1 Introduction

Since the first oilfield in Norway was found in 1969, the activity on the Norwegian Continental Shelf (NCS) has been high. Enormous values have been created for Norway and the companies involved. Today, large parts of the easier accessible fields in the NCS has been explored. As many of these fields are approaching the end of their lifetime, new ideas are needed to sustain production and meet the demand for energy and petroleum products. Development of gas/condensate fields, increasing tail end production from existing fields, marginal field development, exploration of reserves in harsh conditions and remote locations might all contribute to resolving this challenge. To achieve sustainable production of these reserves technological progress is needed. This has led the industry in the direction of subsea development. Ahead companies have been placing equipment on the sea bed since the early 1960s [1]. The first subsea development was a shallow water well by Shell in the Gulf of Mexico. Since then it has been a thriving evolution on the field and from the 1980s equipment have been placed on great depths in the North Sea and Brazil. Figure 1 depicts a potential subsea factory concept.

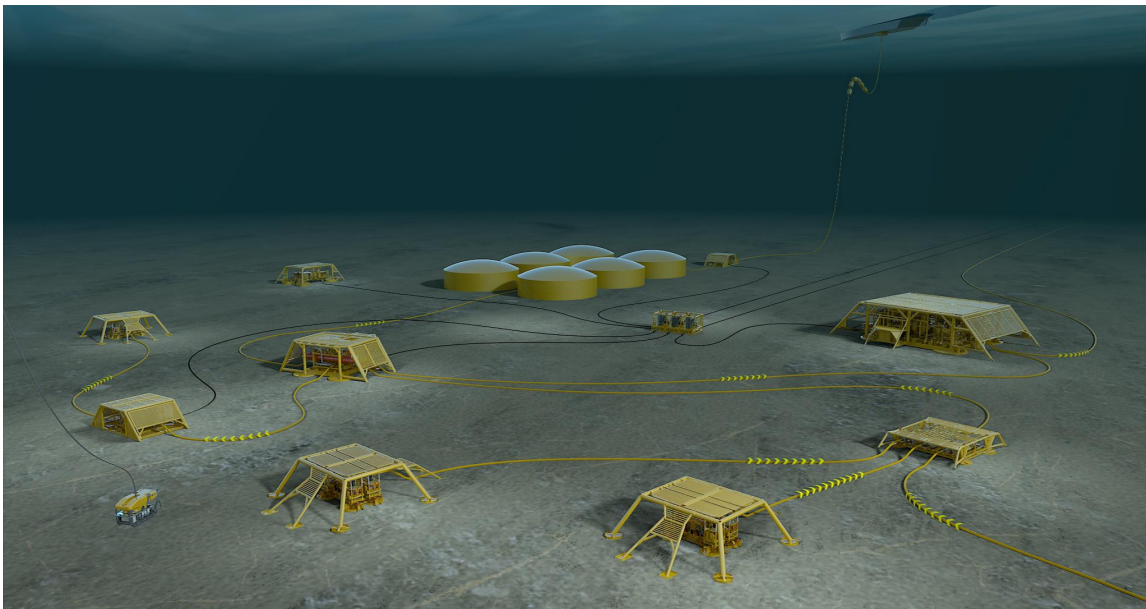


Figure 1: Illustration of a complete subsea factory [2].

In many cases, placing equipment subsea can be less resourceful than the alternatives. This is due to tie-in possibilities to existing infrastructure, reduced dimensions of the surface structures and low maintenance requirements. The latter is also one of the main challenges in the design phase. Maintenance of subsea placed equipment is expensive and time consuming, hence it must be robust and able to operate for years without maintenance. This sets very high standards for design, choice of materials and redundancy. Until now, only parts of the processing equipment have been placed subsea. Looking at the past years technological progress, complete factories subsea replacing surface structures is not unthinkable in the future.

1.1 Background

Compression as a way of increasing flow rate and total recovery from a reservoir is a well-known and proven successful technique. Introducing subsea wet gas compression expands the area of application of the technique. Further, it might lead to feasible development of the mentioned reserves. It could also be an important milestone in the journey towards complete subsea factories. Compared to compression topside, there are several advantages of subsea placement of the compressor system. The most obvious is the proximity to the reservoir. This makes lower suction pressure possible, which results in increased recovery. Subsea wet gas compression can also increase the flow rate and enable control of the flow regime in the multiphase flow lines [3]. This can prevent instabilities like slugging, which can be a severe problem for the receiving facilities and complicate stable production. Changes in flow regime can be expected to occur during the lifetime of a field due to changes in reservoir conditions. Even though designed for subsea placement, the technology is also attractive for topside structures. This is due to the reduced weight, compact design and reduced need for maintenance.

Today there are two available solutions for subsea compression systems:

1. Subsea separation with single-phase compression and pumping
2. Wet gas compression of unprocessed well stream

The Norwegian energy company Equinor operate systems of both categories on the NCS. In 2015 the world's first subsea compressor system commenced operation at the Åsgard field in Norway. The system is of type 1 with separation, single-phase centrifugal compression and pumping before mixing in the pipeline. It has shown a regularity of almost 100% until now and is expected to increase the recovery rate from 62% to 74% from Åsgard[4]. The same year the world's first system of type 2 was installed on the Gullfaks field, also in Norway [5]. This is a wet gas compressor utilizing contra-rotating compressor technology to handle unprocessed well stream.

In this thesis, systems of type 2, wet gas compression are in focus. An illustration of both types of systems is shown in Figure 2.

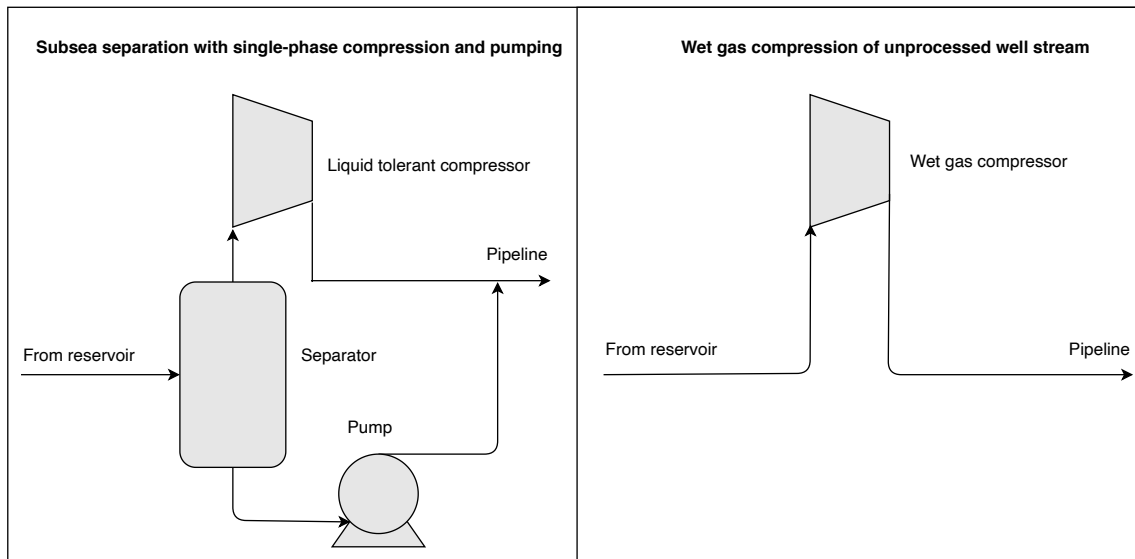


Figure 2: Illustration of the two available solutions for subsea compression systems.

This thesis will emphasize the centrifugal compressor. The choice is done based on the centrifugal compressor available at the NTNU test facility and its high relevance for industrial application. The industry's preference for this type of compressor is based on its operating characteristics, large tolerance for process fluctuations and higher reliability compared to other types of compressors [6].

The past twenty years research on design and operation of wet gas compressors has been performed. A select few from NTNU and Equinor have been the main drivers of a large part of these projects together with the compressor manufacturers and oil service industry. Still there are many aspects in need of consideration to better understand the interaction between multiphase flows and the compressor. The desire for subsea placement reinforces the need to understand all aspects of the operation. When doing maintenance is avoided at all cost, this understanding is vital to reduce the risk.

The subject of this project is compressor transients in wet gas operation, with emphasis on compressor driver trip. Of specific interest is the impact of wet gas and compressor deterioration on the trip trajectory and related stability performance.

Driver trip is a critical event for the compressor system which is avoided at all cost. However, sometimes the occurrence is inevitable due to e.g. power outage. This accentuates the need to understand the system behaviour during driver trip. This is well documented in dry gas operation but, limited research is done on the effects of compressor deterioration and fluid liquid content. Also, the potential negative effects of compressor instabilities are documented for dry gas. There is nothing to my knowledge that implies that these are less severe for wet gas operation, knowing that the intensity of surge is proportional to the fluid density [7]. The relevance for subsea compressors is high. In the case of outage, the consequences are greater for subsea placed equipment. Maintenance of subsea systems requires special vessels, equipment and personnel. The weather is also a limiting factor during these operations. Enormous potential for lost production highlights the importance of understanding every aspect of subsea wet gas compression.

1.2 Scope

Understanding a compressor system and its response to different operating conditions is vital. Especially subsea wet gas compressor systems represent challenges as the flow regime to the compressor inlet may change according to flow line operating condition. This includes transient behaviour as a function of liquid content and trip scenarios. The overall objective is to test and analyze relevant wet trip scenarios to document the compressor system behaviour. Based on the NTNU test lab compressor, wet trip trajectories should be established to document the impact of compressor deterioration and/or «head rise to surge».

The following tasks to be considered:

Based on literature review and experimental work at the wet gas compressor test rig, the focus areas are:

1. Establish compressor performance characteristics.
2. Review and validate how to establish different trip trajectories at dry and wet gas conditions.
3. Establish and document how different compressor performance characteristics affect the trip trajectory and related «time to surge» and «time in surge».

1.3 Delimitation

- The transients in this project is limited to the compressor driver trip phenomenon. This is due to time limitations and scientific relevance.
- This project focuses on the operational point of view of the compressor. Hence, design of systems or specific components is not considered.
- Compressor performance analysis is not the main focus of this project. The objective of the performance part of the experimental campaign is to establish relevant performance characteristics to form a basis for driver trip tests. Hence, only short, basic analysis will be given in the compressor performance experimental campaign.
- Dynamic simulations in HYSYS will not be done during the project due to complexity and time limitations.
- This thesis will only consider the centrifugal compressor. Other types of dynamic compressors and positive displacement were shortly presented in the project thesis but are not found relevant for further discussion.

1.4 Structure

The following chapters will start with an introduction for the reader to get an overview of the contents. If a chapter contain especially important concepts and results these will be summarized at the end of the chapter.

The chapter contents are:

- **Chapter 1: Introduction**

This is the introduction chapter which aim is to put this project into perspective and give the reader an overview of the industry and its history, challenges and possibilities. Further, the subsea wet gas compression technologies are presented alongside its associated advantages and challenges. The chapter ends with the scope of the thesis, delimitations and the structure of the report.

- **Chapter 2: Compressor Fundamentals**

This chapter contains the most fundamental theory related to centrifugal compressors. The contents are chosen to be in compliance with the thesis subject. This includes the principle of operation of a compressor system, compressor performance, system characteristics and

deterioration mechanisms. Further, wet gas impact on compression performance is analyzed through fundamental multiphase theory and a literature review.

- **Chapter 3: Compressor Driver Trip**

This chapter documents compressor transient phenomena, with emphasis on driver trip. The main focus is on the trip trajectory and the impact of system characteristics, performance characteristics and wet gas. Lastly, a method for tuning of the trip trajectory is presented.

- **Chapter 4: Test Facility**

This chapter contains a presentation of the wet gas compressor test facility at NTNU, where the experiments in this thesis is conducted. A description of the relevant equipment and dimensions are included. Further, the simulation tool HYSYS alongside the simulation model used in this project is presented.

- **Chapter 5: Experimental Campaign - Compressor Performance**

This chapter contains the compressor performance experimental campaign. This includes performance tests done in dry and wet conditions for the clean and fouled compressor. Further, a method for tuning the performance characteristics is established and used to replicate the fouled characteristics. Test objectives, results and basic analysis of the most important trends are given.

- **Chapter 6: Experimental Campaign - Compressor Driver Trip**

This chapter contains the compressor driver trip experimental campaign. Here, the impact of wet gas and fouling on the trip trajectory is investigated. This includes test objectives, results and discussion.

- **Chapter 7: Conclusions and Further Work**

This chapter contains the most important conclusions and suggestions for further work based on findings in this project.

Most of the figures in this thesis is made by the author with inspiration from various sources. This is to standardize the format and improve readability. It also ensures consistency with respect to symbols, nomenclature and abbreviations. Figures that are not made by the author has a reference included in the caption.

2 Compressor Fundamentals

This chapter contains fundamental theory relevant for this project. The principal of operation for the machine and the different parts of the compressor and their role in the machine is explained. This is followed by compressor performance evaluation and testing, compressor deterioration, system characteristics and wet gas impact on the compressor system.

2.1 Principle of Operation

The centrifugal compressor is a rotating machine which purpose is to increase the pressure of a fluid. It is versatile and in use for a wide variety of applications, ranging from small combustion engines to large scale hydrocarbon transport. A detailed view of the main parts of a compressor is seen in Figure 3.

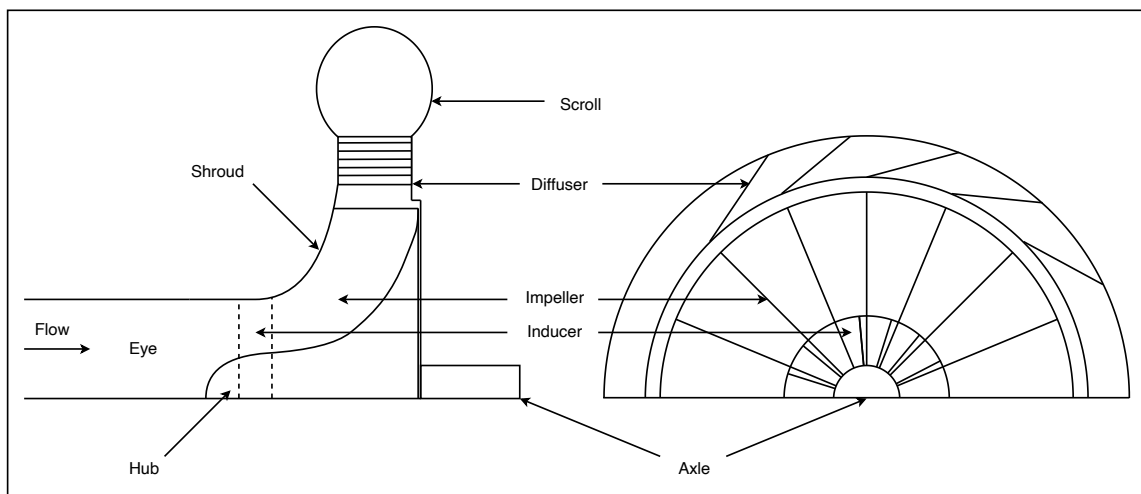


Figure 3: View of the main parts of a compressor seen from a cross-sectional and axial view.

The gas enters the compressor through the center, known as the eye. The flow has an angle of β_1 to the axial direction and relative flow velocity w_1 . Further, the flow approaches the rotating part of the machine, the impeller. The first section of the impeller is the inducer which blades changes the flow direction from the inlet angle to the axial direction. The inducer has an important role in the compressor, providing larger operational area. The impeller consists of carefully designed airfoils, which turns and accelerates the gas in the radial direction. Leaving the impeller, the gas

has an angle of β_2 to the axial direction and a relative velocity w_2 . Both the static pressure and the velocity is increased in the impeller before it exits into the static diffuser. This is a flow channel of increasing area which purpose is to convert the kinetic energy of the gas into pressure energy. From the diffuser the gas exits in radial direction into the volute. Here the flow is collected and directed to the outlet, or to the next stage if the compressor has multiple stages.

The described changes in flow angle and velocity in the impeller is illustrated in the velocity diagrams in Figure 4. Here the velocity triangle is drawn without inlet swirl, $C_{\theta 1} = 0$. This is the best efficiency point (BEP).

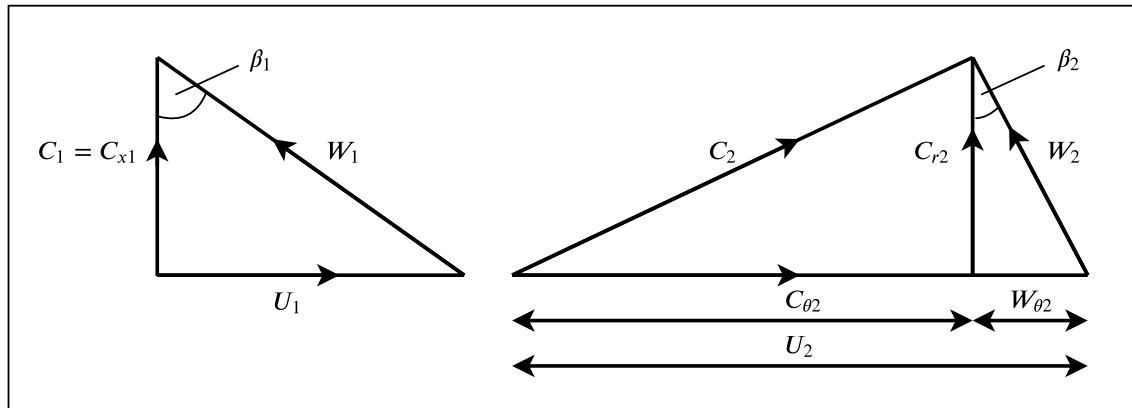


Figure 4: Velocity diagrams at inlet and outlet for a centrifugal compressor stage.

The impeller design is normally a result from a compromise between pressure ratio, efficiency and stability. The angle of the impeller vanes dictates the impeller exit Mach number and the pressure ratio. Backwards swept impellers reduce the Mach number and the pressure ratio. Forward swept impellers have the opposite effect, increased impeller exit Mach number and increased pressure ratio. The latter is associated with larger losses in the diffuser [6]. Today, most compressors have backward swept impellers, including the NTNU Test Facility. This improves the flow stability of the compressor and increases the operational range. The reduced pressure ratio can be accounted for by increasing the rotational speed. This will increase the Mach number, but less than the reduction from impeller design [8].

An illustration of the mentioned impeller designs can be seen in Figure 5.

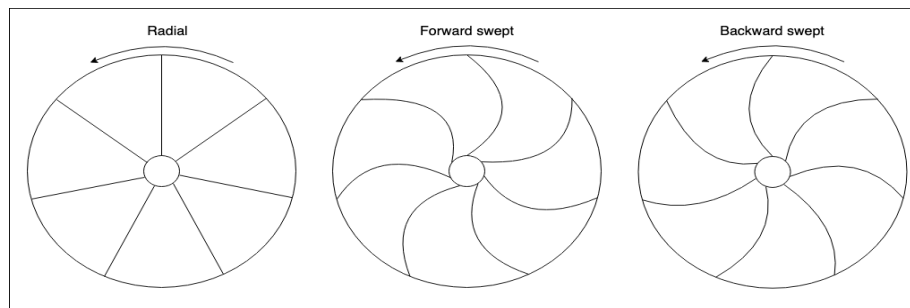


Figure 5: Various impeller vane designs.

Also, diffuser design involves similar compromises. An increase in efficiency of a stage by 2-4 percentage points can be achieved by improving diffuser design. However, the cost of increased efficiency can be reduced operational range [6].

2.2 Performance Evaluation

The compressor performance is the relation between flow rate in terms of mass or volume, head in terms of enthalpy or pressure and efficiency. To visualize the operational range of the compressor these variables can be plotted in a characteristic map. These plots commonly have the head term on the vertical axis and the flow rate on the horizontal axis. It can also include lines of constant speed and contours of constant efficiency.

Such a map is given for a machine of known size, fixed working fluid and constant inlet conditions. The operating area of the map has two constraints. Surge to the left and choke to the right. Surge will be further presented later in this chapter. Choke is also known as stonewall. This is the maximum flow through the compressor, due to the flow velocity reaching the speed of sound.

The general behaviour of a centrifugal compressor at constant rotational speed is that high flow yields low head. This gives the operating lines at constant speed the shape of concentric circles. For practical purposes, maps can often be limited to the area around BEP, which is the combination of flow and pressure/head which gives the highest compressor efficiency. If looking at the compressor in isolation, this is the optimal area of operation. Compressor performance is evaluated through rigorous testing according to international standards.

2.2.1 Polytropic Performance

The polytropic process follows the real compression path, dividing it into a large number of small isentropic processes. By definition a polytropic process satisfies equation (2.1).

$$pv^n = C \quad (2.1)$$

An illustration of a polytropic compression process can be seen in Figure 6.

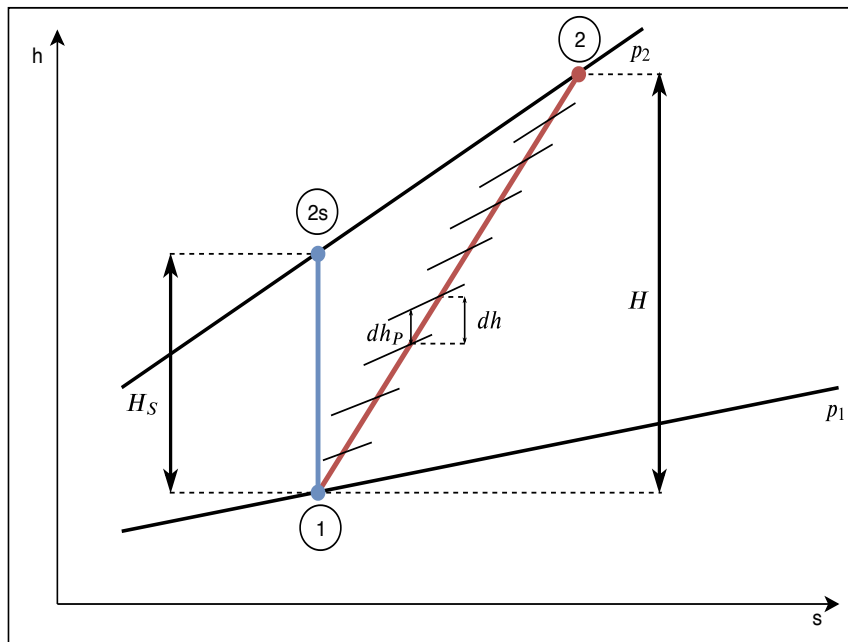


Figure 6: Polytropic compression process in specific enthalpy-entropy diagram

Here, H is the head which is a measure of the amount of energy needed to increase the pressure of the gas from p_1 to p_2 . In equation (2.2) the relation between the actual head and the polytropic head and efficiency is shown.

$$H = \frac{H_P}{\eta_P} \quad (2.2)$$

The polytropic head, H_p , is the sum of the enthalpy changes in all the small stages and η_P is the polytropic efficiency.

Traditionally the thermodynamic design and test evaluation of centrifugal compressors is frequently based on polytropic analysis employing perfect-gas relations [9]. In many cases this does not provide satisfactory accuracy. To improve the accuracy John M. Schultz derived real-gas equations for polytropic analysis. The compressibility factor Z was supplemented by two additional functions, X and Y . These functions correct the polytropic exponents for the change in temperature and pressure through the process. Also, a correction factor equal for both isentropic and polytropic analysis was given to fully account for changes along the compression path. The polytropic head including Schultz' correction factor is given in equation (2.3).

$$H_p \approx f \frac{n_v}{n_v - 1} \frac{Z_1 R_0 T_1}{MW} \left[\left(\frac{p_2}{p_1} \right)^{\frac{n-1}{n}} - 1 \right] \quad (2.3)$$

By using Schultz' work the accuracy of the polytropic analysis is improved. It must be pointed out that there are four different methods of implementing Schultz' in the polytropic performance evaluation. Hundseid et al. [10] reviewed these methods and found errors of more than 4% in polytropic head. Further, the authors suggested a direct integration method enabling updating of fluid and thermodynamic properties along the compression path for the future. A more detailed description of Schultz' work is attached in Appendix G.

2.2.2 Performance Testing

The industry standards for performance testing of centrifugal compressors are the ASME PTC 10 - «Performance Test Code on Compressors and Exhausters» and ISO 5389 - «Turbocompressors - Performance Test Code». In this thesis, references will be given to the ASME standard which contains two types of tests:

- Type 1 - Test is conducted with the specified gas at or very near the specified operating point. Seven variables need to be within permissible deviations given in the standard. Amongst these are inlet pressure, inlet temperature speed and molecular weight.
- Type 2 - Test is conducted at different point than the specified operating point and substitute gas might be used. Rotational speed of the machine is adjusted to obtain similarity [11]. Four variables need to be within permissible deviations given in the standard. These are specific volume ratio, flow coefficient, Machine Mach number and Machine Reynolds number.

In performance evaluation these standards use the polytropic process as reference, with the modifications done by Schultz' included. At this time there is no current standard for performance testing of wet gas compressors. Mæland and Bakken [11] concluded that requirements for wet gas simili-

tude conditions needs to be incorporated in future standards. This includes defining dimensionless parameters suitable for wet gas. Examples are Reynolds number, Stokes number and Weber number. This makes a test of type 1 the safer option so far. Research on wet gas compression shows that the compressor performance is highly influenced by the amount of liquid and its properties [12]. This highlights the need for specific wet gas parameters.

2.2.3 Affinity Laws

The affinity laws, also known as the fan laws, relate changes in rotational speed to the change in compressor performance. Given that the operating point before the change is known, these equations can be used to estimate the flow rate, head and power of the machine. The three fan laws are:

$$\frac{Q_2}{Q_1} = \frac{N_2}{N_1} \quad (2.4)$$

$$\frac{H_2}{H_1} = \left(\frac{N_2}{N_1}\right)^2 \quad (2.5)$$

$$\frac{P_2}{P_1} = \left(\frac{N_2}{N_1}\right)^3 \quad (2.6)$$

Here, Q is volume flow rate, H is head, P is power, and N is rotational speed. The accuracy of the affinity laws depends on the operating conditions and the compressor system. Constant efficiency is assumed and the accuracy of the estimates decreases with increasing molecular weight and the number of compression stages [13]. Also during transients like run down of a compressor, the fan laws might deviate greatly from the actual operating point [14]. This will be further discussed in Chapter 3.

2.3 System Characteristics

2.3.1 Control Methods

For the compressor to meet the exact system requirements different control techniques can be used. Suction and discharge throttling, recycling, variable compressor speed and variable inlet guide vanes are examples of this. Regardless of the large losses associated with some of these methods they are frequently used in the industry. Johansen [7] suggested that the reasons for the use of inefficient methods could be related to the vulnerability of the surrounding process, risk and cost related to modification and outage. The most energy-efficient, yet expensive way of controlling a compressor is by a variable speed drive (VSD). Considering a fixed speed drive, inlet guide vanes (IGV) is the most effective control method [15]. Today the control techniques for a dry gas compressor is also considered suitable for wet gas flow. However, considerations for each method and how they are affected by liquid content must be done.

Especially relevant for this project is the inlet guide vanes. These are airfoils placed in front of the compressor impeller with purpose of changing the impeller inlet flow direction. In terms of velocities, this means changing the tangential component of the absolute velocity $C_{\theta 1}$, often referred to as adding pre-swirl. This can be done with the direction of rotation, positive pre-swirl or in the opposite direction, negative pre-swirl or counter-swirl. The effect on the compressor performance is a change in head, flow and efficiency. Some of these are illustrated in Figure 7 and Figure 8.

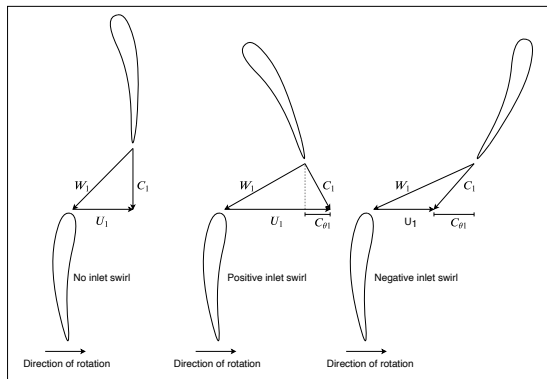


Figure 7: Effect of inlet swirl on compressor inlet velocity diagram.

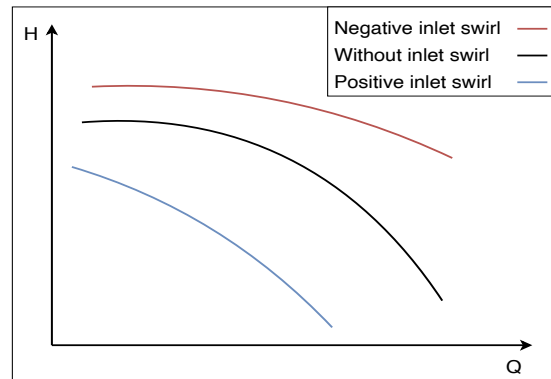


Figure 8: Effect of inlet swirl on compressor characteristic.

Considering equation (2.7), the effect of adding pre-swirl on the theoretical compressor head can be seen. Counter-swirl increases the head, while pre-swirl decreases the head.

$$H_t = U_2 C_{\theta 2} - U_1 C_{\theta 1} \quad (2.7)$$

A challenge proposed for the IGV is the ability it has to deflect the flow when liquid is introduced. Vigdal [15] investigated the IGV impact on compressor performance in dry and various wet conditions. This included the relative impact on the pressure ratio and volume flow. The volume flow rate variation possible with IGV was found to be 6% at GMF = 0.4 and 16% at GMF = 1.0. The same numbers for pressure ratio was respectively 1.7% and 4.1% [15]. The conclusion from this work is that the relative effect the IGV has on the compressor performance is decreasing when the liquid content is increasing.

The pressure loss over the IGV also increase with liquid content. Vigdal [15] found that a GMF of 0.4 reduced the turning ability of the IGV such that it could not compensate for the losses.

2.3.2 Surge

Surge is known as a critical instability challenge for a compressor system. It occurs when the compressor is not able to deliver the energy required by the system [13]. The cause can be aerodynamic instabilities like stall, which is the event when flow is reduced to a critical point where it detaches from the airfoil. At the onset of surge, the upstream system volume has a higher pressure than the compressor discharge. The flow follows the pressure gradient which implies a flow reversal. This induces a pressure reduction downstream of the compressor which continues until the positive pressure gradient is restored. Now positive flow is restored, but the compressor is operating in the unstable area to the left of the stability line. If no actions are taken, the cycle repeats itself. Compressor driver trip is an event where the flow rate is reduced very fast due to the impeller speed decay. If upstream flow capacity is not provided immediately, the pressure ratio will remain constant. The consequence of this is an abrupt and sudden migration into the unstable region.

The criticality for the compressor depends on system pressure, system volumes and safety systems. Also, the intensity of surge is proportional to the density of the fluid [13]. This is of specific relevance for this project where wet gas is involved. Observations during surge are high frequency oscillations in pressure and flow, increased temperature, vibrations and high loads on the bearings. In Figure 9 an example of a deep surge cycle can be seen, and an explanation of the figure is given below.

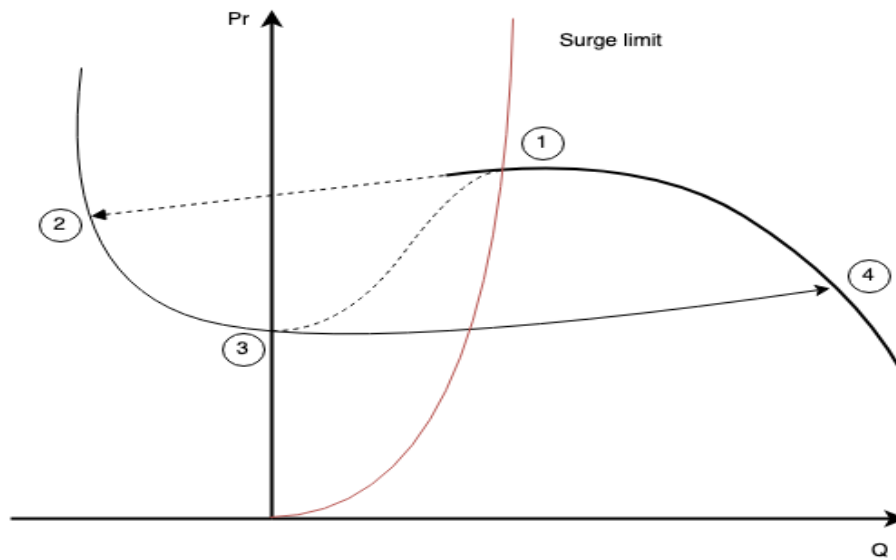


Figure 9: Behaviour during a deep surge cycle

- 1 → 2: Operation point is moving towards the surge limit where the flow becomes unstable. This is the flat part of the characteristic, a small change in pressure ratio leads to a large reduction in flow rate and the operating point jumps to 2.
- 2 → 3: Flow is reversed and leads to a reduction in pressure ratio until zero flow is achieved.
- 3 → 4: Positive flow is restored and operation point jumps to point 4.
- 4 → 1: The compressor follows the characteristic to point 1. The cycle repeats if no measures are implemented.

As mentioned, the left limit in the compressor characteristic map is the surge limit. To avoid the occurrence of surge the compressor is usually operated with a margin to this line. This margin can be expressed in terms of head, pressure ratio or other variables. Two of these can be seen in equations (2.8) and (2.9). The subscript «surge» denotes the point at the surge line.

$$\text{Head Rise To Surge (HRTS)} = \frac{H_{surge} - H}{H} \quad (2.8)$$

$$\text{Pressure ratio Rise To Surge (PRTS)} = \frac{Pr_{surge} - Pr}{Pr} \quad (2.9)$$

In between the surge limit and the operating point several lines are defined. These are surge control lines. When the operating point reaches these lines, various protective measures are activated. This is normally done by an anti-surge system. This is a parallel loop connecting the outlet to the inlet, with a flow control valve which can open if needed and avoid surge. In contrast, a hot gas bypass is the last resort. This system has an open/close valve and draws off the flow before passing through the discharge cooler of the system. This is a faster acting system which immediately increases the flow capacity downstream of the compressor. These systems are illustrated in Figure 10.

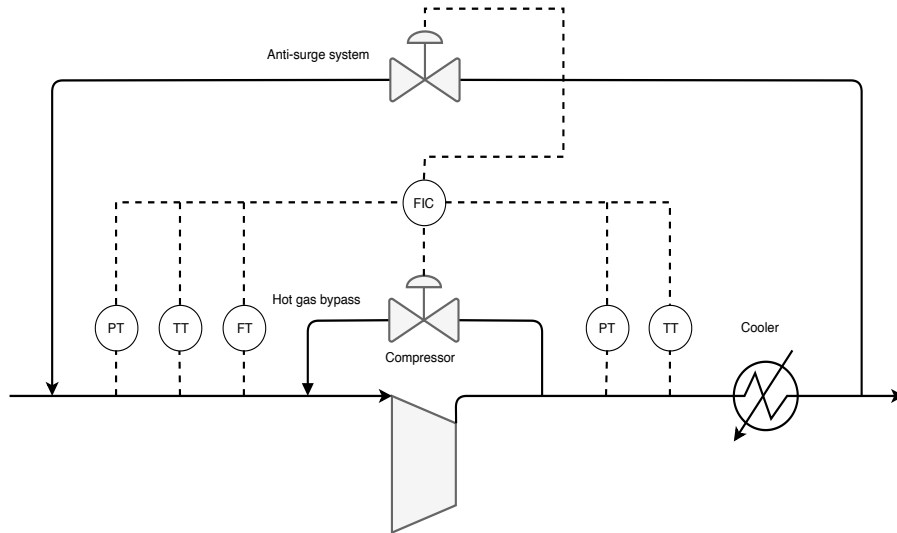


Figure 10: Compressor system with anti-surge and hot gas bypass.

The main challenge with surge is the time scale of the phenomenon. Time to surge (TTS) is the time it takes for the compressor to enter surge from a given operating point in the characteristic map [16]. TTS depends on factors like the steepness of the performance characteristic at the operating point. The shortest TTS is normally related to compressor driver trip. Here, factors like impeller speed decay rate is vital. The TTS provides useful information from a machine safety point of view in addition to the margins given in pressure, head or flow. By knowing the smallest TTS of the operational area, this sets the exact minimum criteria for the safety systems.

Time in surge (TIS) is the time from the compressor enters the surge area to the operating point is back in the stable area. This depends on factors like suction/discharge volumes, the capacity and response time of the safety systems. From a stability point of view a long TTS and short TIS is favorable. This would indicate a stable system with effective safety systems.

2.4 Performance Deterioration

Different deterioration mechanisms are observed in centrifugal compressors. Some of these are corrosion, erosion, fouling and leakages. These mechanisms affect the compressor performance in various ways. Both fouling and leakages are known to have an impact on the slope of the performance characteristics. This is of specific interest for this project, where the impact of fouling on the trip trajectory and stability performance is to be investigated.

The labyrinth seals objective is to prevent flow from the discharge to the inlet of a compressor stage. These seals allow for a minor leakage to reduce friction. In a normal situation this does not affect the compressor performance significantly. Although, deterioration of the impeller, balance piston or shaft labyrinths can increase the internal leakage of the compressor [17]. Also, the event of excessive vibration occurring during compressor surge can increase the leakage through these seals. This can reduce the compressor performance, which is seen as a reduction in head in the compressor characteristics. The slope of the curve is markedly reduced.

Fouling is the event when various contaminant particles from the flow adhere to the inside surfaces of the compressor. These particles are typical salts and heavy hydrocarbons. Fouling decreases the surface area and increases the surface roughness. The result is flow disturbances, changed aerodynamics and increased losses. In the performance characteristics this appears as reduced head and efficiency. In contrast to some of the deterioration mechanisms fouling is not always permanent. In some cases, the fouling can be washed off the surfaces by liquid injection. A fouled impeller is depicted in Figure 11.



Figure 11: Fouled impeller of a compressor, NTNU Test Facility.

2.5 Wet Gas Impact

Wet gas is commonly defined as a flow with a gas content ranging from 95-100% on a volume basis [18, 19, 20]. Implications of wet gas in the compressor includes changes in both the thermodynamics and aerodynamics of the machine. Wet gas effects include flow deflection, phase change, heat transfer between phases, increased surface roughness and reduced flow area due to liquid film formation.

2.5.1 Multiphase Flow

The presence of both liquid and gas in the same flow results in complex multiphase behaviour. The interaction between the different phases contribute to momentum, heat and mass transfer [12]. Some of the challenges related to multiphase flows are phase slip, transient flow phenomena and complex friction/pressure drop relations.

Multiphase flows are commonly classified into flow regimes based on observed flow behaviour and transport mechanisms. An illustration of the flow regimes observed in horizontal flows can be seen in Figure 12.

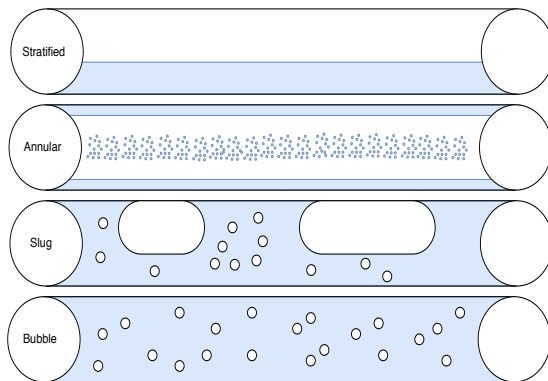


Figure 12: Flow regimes in horizontal flows.

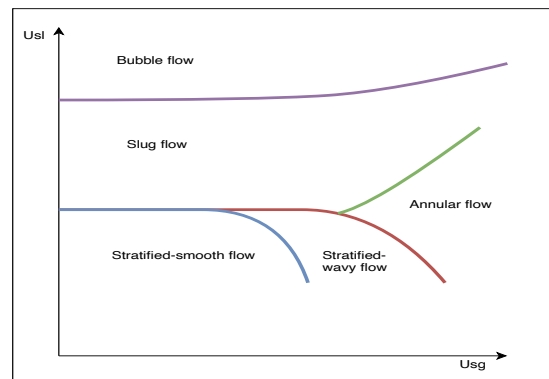


Figure 13: Flow regime map for horizontal flows.

The two main categories are separated flows and dispersed flows. In dispersed flows bubbles or droplets are dispersed in a continuous phase, with no distinct interface. In contrast to this, the separated flows are characterized by a distinct interface separating the phases. However, this does not rule out the possibility of gas in the liquid phase and vice versa. For horizontal flows the dispersed regimes are bubble and slug, while the separated are stratified and annular.

For a given multiphase flow, the different flow regime regions can be visualized in a flow regime map like in Figure 13. These maps can have e.g. gas and liquid superficial velocities on the axes. This is the volume flow per pipe area, which would be the velocity if the phase were alone in the pipe. The definition of the superficial gas velocity is given in equation (2.10).

$$U_{sg} = \frac{Q_g}{A} \quad (2.10)$$

Generalizing these maps are challenging because of a high number of non-dimensional groups, a large span in dominating forces and the phase mixing can be dependent on surface active components. The flow regime is also sensitive to flow inclination, hence vertical and horizontal flows have separate flow regime maps. This is because gravity acts as a stratifying force in horizontal flows. An illustration of a typical map can be seen in Figure 13.

In the area of application of a wet gas compressor system a typical flow has low liquid content and high gas velocities. By looking at Figure 13, such a flow will be placed in the lower part of the map. This is where the stratified and annular flow regimes are found. When Hundseid et al. [12] did wet gas compression tests the flow regime in the tests were described as annular. This is a separated flow regime where the liquid transport is due to film at the wall and a droplet field in the gas phase.

At the NTNU test rig, stratified flow is the regime observed during «normal operation». At high flow rates and nozzles dispersing the injected water finely, significant transport of droplets is also observed in the gas phase. Stratified flow is a result of gravity being the dominant force. Here, a clear interface between the phases is observed. The interface can be smooth or wavy depending on the pressure.

Also, slug flow can be induced in the lab by having high water injection rates, pipe inclination or S-shaped piping. Regardless of the inlet flow regime, the liquid is ripped into small droplets and dispersed into a mist when it reaches the hub of the compressor. The transparent sections of the test rig also allow for visual observations of the impeller flow regime. A distinct water jet is observed on the pressure side at the impeller outlet along with droplets on the back wall.

In Figure 14, a picture of the flow can be seen where a stroboscope was used to «freeze» the impeller. Note that every other water jet is larger due to the inducer having half as many blades as the impeller.



Figure 14: Impeller outlet water jet, NTNU Test Facility.

The complex behaviour of multiphase flows are commonly simplified by the use of the total fluid model. This model treats the flow as a homogeneous fluid but includes fluid and thermodynamic properties of all components through modified multiphase variables.

$$H_{P,mp} = \frac{n}{n-1} (p_2 v_2 - p_1 v_1) \quad (2.11)$$

An example of such a multiphase variable is the multiphase density which is weighted by the gas and liquid volume fractions.

$$\rho_{mp} = \alpha \rho_g + (1 - \alpha) \rho_l \quad (2.12)$$

The gas fraction is an important parameter when describing wet gas behaviour. The definitions on a volume basis (GVF) and on a mass basis (GMF) is given in equations (2.13) and (2.14).

$$GVF = \alpha = \frac{\dot{Q}_g}{\dot{Q}_g + \dot{Q}_l} \quad (2.13)$$

$$GMF = \beta = \frac{\dot{m}_g}{\dot{m}_g + \dot{m}_l} \quad (2.14)$$

In most conditions liquids have considerable higher density than gases. However, gas density strongly depends on temperature and pressure. Higher gas density raises the drag between liquid and gas which leads to an increased homogeneity of the fluid. Hence, the density ratio gives an indication of the homogeneity of the flow and the tendency of phase separation [12]. The density ratio (δ) is defined in equation (2.15).

$$\delta = \frac{\rho_g}{\rho_l} \quad (2.15)$$

For atmospheric air/water, the density of water is in excess of eight hundred times the density of air. With such a density ratio a GVF of 95% will equal a GMF of just 2%. For high pressure hydrocarbons the density ratio will be considerably closer to unity and the tendency for homogeneity will be larger.

The Stokes number is the ratio of the characteristic times of the gas and the droplet. In practice, the tendency a droplet has to follow the gas stream it is suspended in. In a wet gas compressor this dimensionless quantity is useful for understanding the droplet trajectory over the airfoils. This could improve wet gas performance and predict locations of droplet erosion. A low Stokes number means that the droplets will follow the streamlines of the gas. In a high Stokes number flow, the droplet will tend to continue along the trajectory it initially had because of its dominating inertia.

$$St = \frac{\tau_d}{\tau_g} = \frac{\rho_d r_d^2}{18\mu_g} \quad (2.16)$$

The Weber number is a useful relation when studying the interface between two fluids. It is the ratio of the inertial effects to the surface tension effects. When this ratio reaches a critical value, the droplet will break into smaller droplets. In wet gas flow, the droplet size can be an important variable. Here, the Weber number provides information about the occurrence of droplet breakup.

$$We = \frac{\rho_g v_g}{\frac{\sigma_d}{l}} \quad (2.17)$$

For single phase flows, $M = 1$ is the critical speed where shockwaves and compressibility effects appear. These phenomena are associated with losses. For multiphase flows, the sonic speed may not coincide with the critical speed. This means that the onset can be at Mach numbers different than one [12]. Calculation of multiphase speed of sound can be done in various ways. Woods' model is one approach, which uses homogeneous flow assumptions. The model is seen in equation (2.18) and applied in Figure 15.

$$a_{mp} = \sqrt{\frac{1}{\rho_{mp} \left(\frac{\alpha}{\rho_g a_g^2} + \frac{1-\alpha}{\rho_l a_l^2} \right)}} \quad (2.18)$$

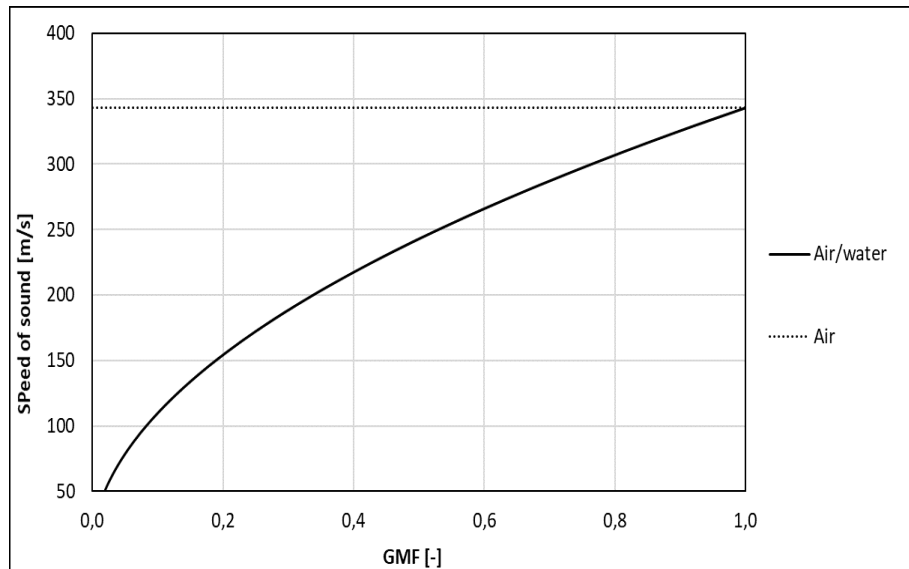


Figure 15: Multiphase speed of sound in air/water mixture at 20°C and 1 atm.

When the GMF is reduced further the multiphase speed of sound will again increase towards the speed of sound in water. This is well outside of what is relevant for wet gas compression.

2.5.2 Wet Gas Performance

The studies done by Hundseid et al. [12], Bertoneri et al. [20], M. Bakken et al. [21], Brenne et al. [22] and Fabrizzi et al. [23] all investigate the wet gas impact on compressor performance. One of the performance indicators mentioned in all studies is the compressor pressure ratio. The results from four of the studies show a trend of increasing pressure ratio when increasing liquid content. This is observed only for medium to low flow rates. This might indicate that the benefits from increased density and cooling effects outweighs the negative effects from aerodynamic distortion at low flow rates [23]. At high flow rates the pressure ratio measured in the wet gas tests are lower than for dry gas conditions. M. Bakken et al. explained the finding by an increased droplet deposition and momentum transfer. The same author found a steadier increase in pressure ratio towards surge for the low GMF cases. This is where the dry gas curve flats out and enters the positive part of the characteristic associated with unstable operation. The fifth study mentioned, by Fabrizzi et al., deviates from the others. The results show an increase in pressure ratio only for $GMF > 0.9$ and low flow rates. The increase in pressure ratio is attributed to changes in compressibility [12], increased Mach number [20] and increased density [20, 22, 23].

Findings regarding polytropic head in all the mentioned studies were consistent and showed a significant reduction in polytropic head. When introducing a liquid, which is practically incompressible compared to a gas, the change in specific volume through the compressor will be greatly reduced. This effect is clearly larger than the modest increase in pressure ratio observed. This is expected according to equation (2.11) when fluid liquid content increases. An interesting observation done by M. Bakken et al. is that for wet gas the HRTS is greatly reduced, while the PRTS is not. See Figure 16 and Figure 17.

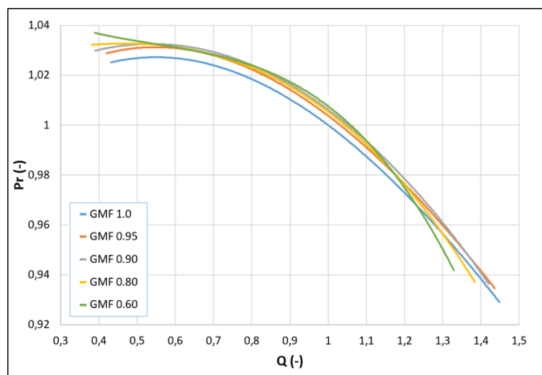


Figure 16: Static pressure ratio versus volume flow rate for varying GMF [21].

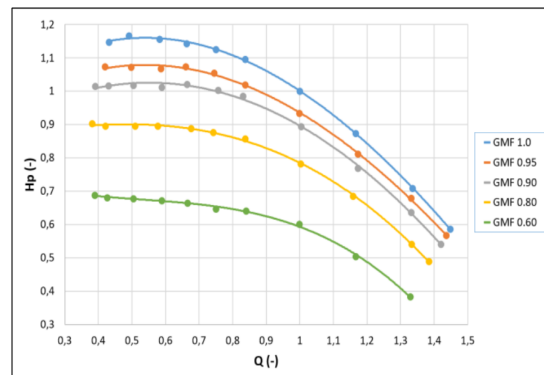


Figure 17: Polytropic head versus volume flow rate for varying GMF [21].

HRTS is the governing factor when setting the left limit of the operating range of the compressor. Adapting this method to wet gas compression could greatly reduce the operating range compared to dry gas. However, Ferrara et al. [24] found that liquid does not restrict the operating range of the compressor, but rather had a stabilizing effect. From these findings it seems that HRTS is not suitable to set surge margins in wet gas operation.

Consistent findings were also done for polytropic efficiency. A clear trend of reduced polytropic efficiency was observed when increasing the fluid liquid content. The results from M. Bakken et al. [21] is seen in Figure 18.

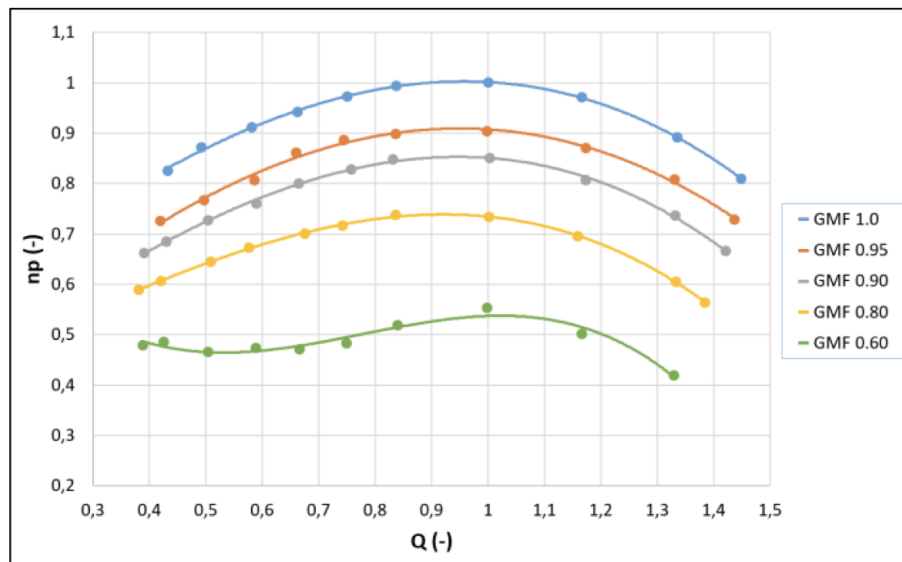


Figure 18: Polytropic efficiency versus volume flow rate for varying GMF [21].

The reduction in polytropic efficiency is attributed to increased internal losses which causes an increase in power consumption [20, 23]. For the experiments with high pressure hydrocarbons the losses are more pronounced at lower suction pressures. This is explained by a higher density ratio which implies a lower GMF for the same GVF [12, 22, 23]. The net effect of the reduction in polytropic head and reduction in polytropic efficiency is an increase in actual head.

Temperature measurements in multiphase flow is a well-known challenge also relevant for wet gas compression. The challenge is that there is no guarantee of thermal equilibrium between the phases. The consequence is that the temperature in both phases must be measured. This is complicated because of the non-uniform distribution of gas and liquid on the cross section of the pipe, which also changes according to the flow regime. Regardless of difficulties measuring the temper-

ature accurately, Bertoneri et al. [20] and Brenne et al. [22] investigated the temperature ratio in their experiments. Both studies found reduced temperature ratios and that the largest part of the decrease occurred at the highest GMF test. Further increase in liquid content led to a modest reduction in temperature ratio. The reduced temperature ratio is explained by heat transfer between the phases and evaporative cooling. Bertoneri et al. [20] also checked the flow for thermal equilibrium by measuring the temperature at several locations downstream the compressor. The conclusion was that thermal equilibrium occurred inside the machine.

The droplet size impact on wet gas performance has been investigated by Brenne et al. [22] and Fabrizzi et al. [23]. The first study found no substantial effect on wet gas performance suggesting that the compressor inlet served as a mixing element, making the flow pattern inside the impeller independent of the injection pattern [22]. Similar observations were done by Fabbrizzi et al. [23] reporting only a small increase in performance when the droplet size was reduced. A possible explanation is that the injected droplets coalesce into a liquid film in the inlet pipe with a droplet field in the center.

2.6 Summary

- Fundamental theory regarding centrifugal compressors was presented in this chapter. Starting with a walk-through of the different parts of the compressor and the principle of operation.
- Compressor performance testing is done according to the international standards ASME PTC-10 and ISO-5389. The thermodynamic basis is the polytropic process with the works of Schultz included.
- At this time there does not exist a standard for performance testing of wet gas compressor systems, hence the mentioned standards are only valid for dry gas.
- Surge is a critical event for compressors and great measures are done to avoid it. Compressor driver trip is one event where surge is likely to occur.
- The steepness of the compressor characteristics can change due to compressor deterioration mechanisms like fouling and leakages.
- Wet gas impact on compressor performance is documented in several studies. In these, general observations are increased pressure ratio, decreased polytropic head and decreased polytropic efficiency.

3 Compressor Driver Trip

This chapter contains a presentation of the driver trip phenomena and the impact of relevant factors on the trip trajectory. Of specific interest is different system characteristics, changes in performance characteristics and wet gas impact. In the last part of the chapter a method for tuning the trip trajectory from affinity-like to the shape observed in large-volume, high pressure systems. The method described, utilizes the discharge throttle valve and 3 control parameters are varied to obtain the wanted effect.

A driver trip is when the compressor experiences an immediate shutdown. In general, there are two types of driver trips.

- Driver trips initiated by the driver itself
- Driver trips initiated by the surrounding process

Trips initiated from the driver itself can be due to e.g. power outage, excessive vibration or lack of lubrication. Process shutdowns can be due to any event in the surrounding process which requires the compressor to shutdown. Especially critical is the driver trips which are so sudden, that a controlled rundown is impossible. Such a trip can occur due to power outage or extensive failures which requires the compressor to stop immediately.

For the compressor system such an event is challenging due to a large, sudden reduction in flow rate. If the pressure ratio is not reduced in time by fast-acting safety systems, the compressor will approach surge. The factors affecting the occurrence and the severity of surge will be discussed in this chapter.

3.1 Impact of System Characteristics

Several studies have been performed on different system characteristics effect on rundown trajectory. Three of these [14, 25, 26] are done on Troll Kollsnes ¹ by Tveit et al. and L.E. Bakken et al. The system characteristics investigated are:

- System polar inertia
- Protection system characteristics
- Rate of power decay
- Trip delay
- Suction/discharge volumes

These factors were studied by the use of dynamic simulations based on earlier trip tests where the model was validated against actual plant tests and operating data.

3.1.1 Polar Moment of Inertia

For a compressor the polar inertia can be regarded as the machine's ability to keep rotating when the driver stops providing power. By this, the rate of compressor speed decay depends on the polar inertia. A low rate of speed decay is highly wanted because positive throughput can be maintained for longer reducing the pressure ratio and providing time for the safety systems to act.

The power provided by the driver in steady state is the sum of the power consumed by the fluid passing through the compressor and the losses due to friction in bearings and seals.

$$P_{dr} - P_{fluid} - P_{losses} = 0 \quad (3.1)$$

The kinetic energy stored in the impeller is a function of the total polar inertia of the machine and the rotational speed.

$$KE_{tot} = \frac{1}{2} I_{tot} \omega_c^2 \quad (3.2)$$

¹Kollsnes is a gas processing plant on the coast of Norway treating the gas from the Troll field among others.

The derivative of the kinetic energy with respect to time is:

$$\frac{dKE}{dt} = \frac{d}{dt} \left(\frac{1}{2} I_{tot} \omega_c^2 \right) \quad (3.3)$$

The time-derivative of the kinetic energy is the power, hence combining (3.1) and (3.3) gives:

$$\frac{d}{dt} \left(\frac{1}{2} I_{tot} \omega_c^2 \right) = P_{dr} - P_{fluid} - P_{losses} \quad (3.4)$$

The polar inertia does not change with time, thus when the driver stops providing power the result is equation (3.5).

$$\frac{d}{dt} (\omega_c^2) = -2 \frac{P_{fluid} + P_{losses}}{I_{tot}} \quad (3.5)$$

This equation shows that when the driver stops providing power, the fluid power requirement and losses will start to decelerate the impeller. The polar inertia is constant, and a larger value implies a slower deceleration of the compressor. This shows that the impeller speed decay will be at its fastest at peak fluid power. Since the fluid power is the product of mass flow and head, it also implies that wet gas flow will lead to a faster impeller speed decay.

In Tveit et al. [14] an equation for the rotational speed during rundown were defined. This was based on the equations above and the fan laws. In addition to the effect of polar inertia, equation Equation (3.6) shows the effect of the power mentioned above.

$$N_{dr} = \frac{1}{\frac{1}{N_{dr,i}} + \frac{P_i}{I_{tot}} \frac{1}{N_{dr,i}^3} \left(\frac{60}{2\pi} \right)^2 t} \quad (3.6)$$

Note that this equation assumes no losses and that rundown of a compressor operating in large-volume, high-pressure systems does not necessarily follow the fan laws.

L.E. Bakken et al. [25] performed simulations in which the impact of polar inertia was investigated. A low, medium and high polar inertia case was established. This is shown in Figure 19.

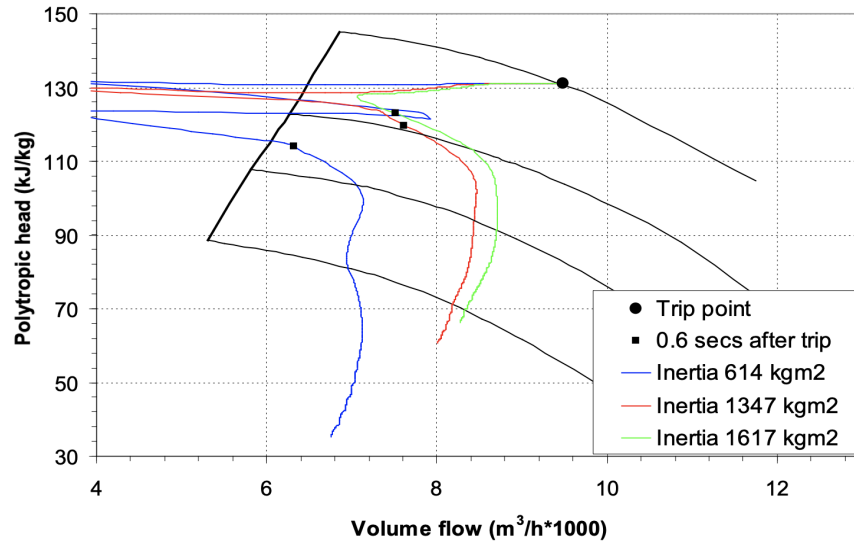


Figure 19: Polar inertia impact on rundown trajectory [25].

The results show that the polar inertia could be decisive in whether the compressor enters surge or not during driver trip. Both the low and medium inertia cases demonstrate an abrupt leap into surge, while the high inertia case never enters the surge area. The response from safety systems provides enough flow capacity for both cases to leave surge, however the low inertia case turns abruptly and moves straight back into surge. This demonstrates the significant effect of the train polar inertia. Regardless of the effect, the polar inertia for an existing system is set by the hardware and redesign is needed to change it. Another aspect is that the torque requirement would increase together with the polar inertia.

3.1.2 Rate of Power Decay

For an electric drive, the power decay rate is instant after a trip signal or power loss. This is not the case for gas turbines and steam turbines which can have varying power decay due to time delay from the fuel/steam valves [14]. In Figure 20 a simulation of driver trip with varying power decay times is shown.

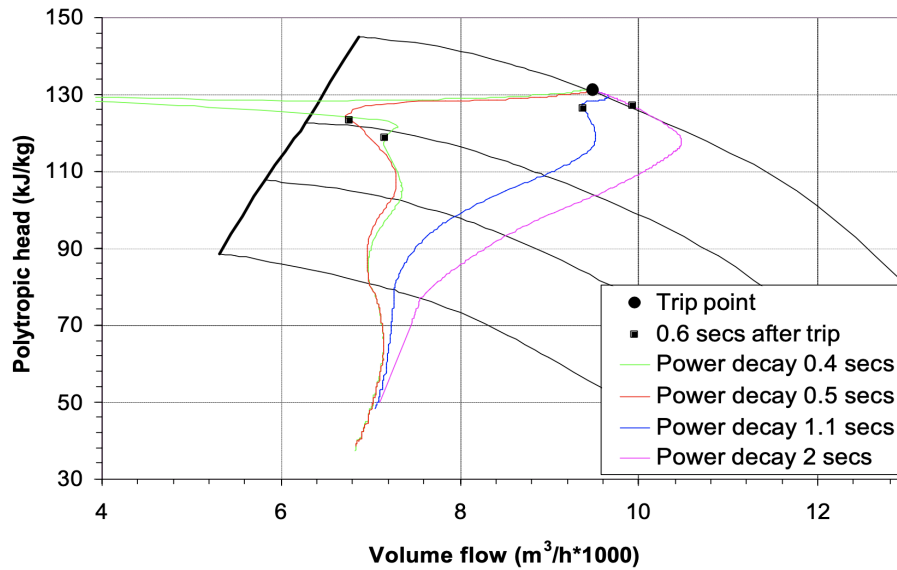


Figure 20: Power decay time impact on rundown trajectory [14].

The delay was varied from 0.4 to 2 seconds and a significant effect of increasing the power decay time can be seen. The effect is that the impeller will rotate for a longer time, providing positive throughput and giving safety systems time to increase downstream flow capacity. This is important information for understanding all the aspects of driver trips. However, the power decay time is not easily changed for electric drives.

3.1.3 Trip Delay

Driver trip events which is not due to power outage may have possibilities for setting a trip signal delay. The purpose of this feature is to provide time for the safety systems to act before the speed decay starts. Providing extra flow capacity downstream of the machine in advance of the power drop can prevent the compressor from entering surge during rundown.

Tveit et al. simulated the effect of trip postponement at the Kollsnes plant. The trip trajectory is seen in Figure 21. It shows that for this system, postponing the trip by just 60ms can give the safety systems enough time to prevent surge.

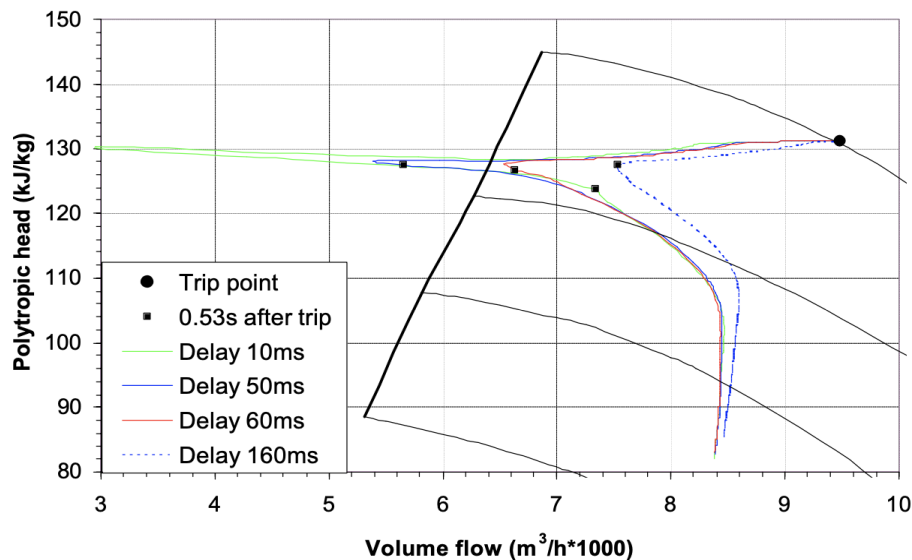


Figure 21: Driver trip signal delay impact on trip trajectory [14].

The events where this type of measure is appropriate is during process trip or alarms from the machine regarding e.g. high bearing temperature or excessive vibration. All of these events are possibly critical, but a delay of 1-2 seconds will usually not aggravate the situation markedly. What these few seconds can do is give the systems for recycling and hot gas bypass (HGB) time to act and reduce the energy requirement of the system.

Modern compressors are driven by electric motors, which requires a stable supply of power from the electrical grid. An example of the criticality of stable power supply was observed at the Kollsnes plant. A power supply voltage drop below 80% trips the driver, and if it lasts for more than 150 ms the compressor may enter surge [14].

3.1.4 Suction and Discharge Volumes

Both the suction and discharge volume of the compressor plays an important role in the system behaviour during rundown. Reducing the pressure ratio as fast as possible is vital for surge avoidance. The suction volume affects how fast the suction pressure increases, while the discharge volume affects how fast the discharge pressure decreases [26]. This is the amount of fluid which needs transport through the safety systems to reduce the pressure ratio over the compressor. For a given dimension of bypass system this can be done faster when these volumes are small. This is favorable from a rundown perspective. These volumes consist of pipelines and vital equipment like scrubbers and coolers. Nevertheless, limiting these volumes is possible in some cases. One solution is installing check valves or revising the location of existing ones [26].

Figure 22 and Figure 23 show simulations where the impact of both suction and discharge volumes on the transient response during driver trip was tested.

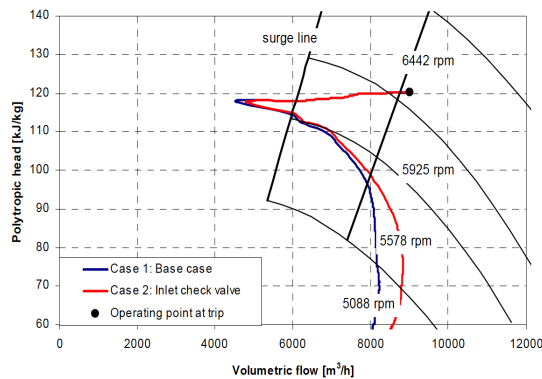


Figure 22: Suction volume impact on the trip trajectory [26].

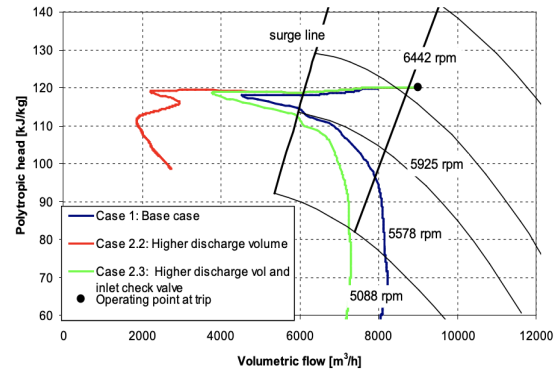


Figure 23: Discharge volume impact on the trip trajectory [26].

These tests involved a very large suction volume. The result of this is that the reduction in pressure ratio over the compressor was based almost solely on the reduction in discharge pressure. Tveit et al. [26] did a simulation with the suction volume reduced to approximately 10% of the original volume. The results, seen in Figure 22, show a very modest improvement of the trip trajectory. The flow reduction after trip is slightly lower and the flow increase from the safety system slightly higher. Reducing the suction volume even further, to approximately 6% of the original was also investigated. This did not give any major improvement. The conclusion is that the HGB-system is the bottleneck in the current setup, hence reducing the suction volume further has limited effect.

3.1.5 Characteristics of Protection Systems

For a compressor system the time to surge can be very short. Hence, the protection systems need to be fast acting and able to reduce the pressure ratio quickly. Important factors for the performance of the protection systems are time from trip signal to valve actuator response, valve characteristics and system capacity.

The response time from trip signal to valve actuator starts moving is of vital importance for the protection system. Schjøberg et al. [27] did simulations of the Hammerfest LNG-plant using the D-SPICE dynamic simulator. In this study, rundown with different anti-surge valve (ASV) dead time was simulated. It showed that applying a dead time of only 200 ms significantly changed the shape of the trip trajectory to the worse. Also, the capacity of the protection systems is an essential factor. The Kollsnes plant has both anti-surge and HGB installed. The latter is to account for scenarios where the operating point moves fast towards surge like e.g. driver trip. For these scenarios anti-surge systems might not be sufficient. Tveit et al. [26] simulated the impact of protection systems characteristics. This included three cases. The base case is both anti-surge and HGB, while the two other cases are only anti-surge system and one with 5 times increased anti-surge system capacity and reduced valve opening time.

The last case is to simulate the effect of installing a on/off valve in parallel with the ASV to be activated only during driver trip. The simulation is depicted in Figure 24.

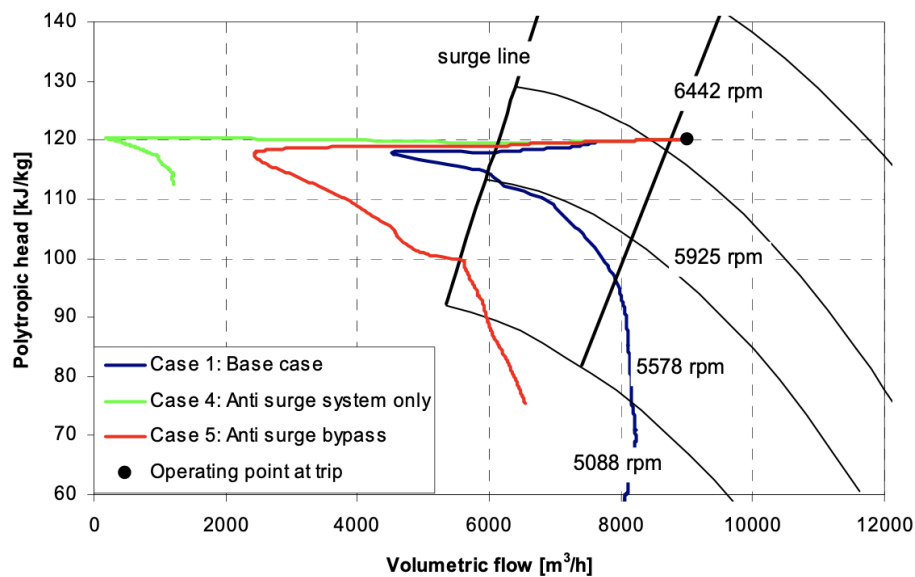


Figure 24: Anti-surge system capacity impact on the trip trajectory [26].

The results demonstrate limited effect of increasing the capacity of the anti-surge system. From this the authors pinpoint that this system would need to be dimensioned above any normal limits to protect the compressor. It clearly shows the limitations of anti-surge systems during driver trip and highlights the need for hot/cold gas bypass.

3.2 Impact of Performance Characteristics

The performance characteristics of the compressor influences the margin from the operating point to surge. Following, the steepness of the characteristic curve is essential for the surge occurrence and duration. A commonly used margin is the before-mentioned HRTS.

Tveit et al. [17] and L.E. Bakken et al. [25] studied the impact and sensitivity of compressor deterioration. The former tested two types of deterioration in centrifugal compressors leading to a change in head rise to surge. A simulation model validated against trip tests and operational data from the Kollsnes gas processing plant was used to acquire the data. The trip trajectory of the machine in new condition is seen in Figure 25. This is the base case for the two following figures.

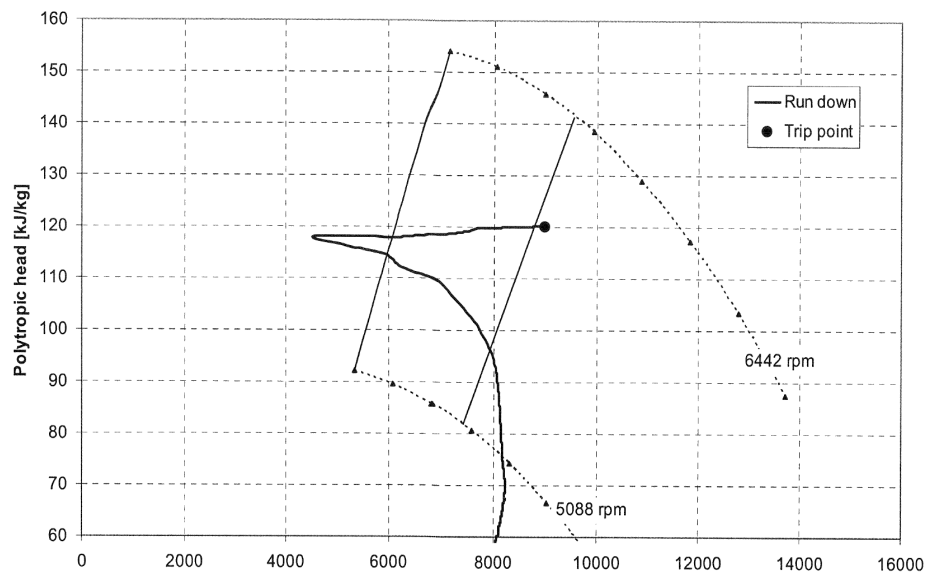


Figure 25: Compressor performance characteristics of new machine, Troll Kollsnes [17].

3.2.1 Reduced Performance Steepness

Compressor deterioration can reduce the performance steepness, seen as a reduced slope of the performance curve. The consequence can be that the system is more vulnerable to surge due to reduced surge margins. The reduction in performance steepness can be due to e.g. increased internal leakages in the compressor. One of the cases in the study by Tveit et al. [17] was a simulation of internal leakage based on plant experience. The results can be seen in Figure 26.

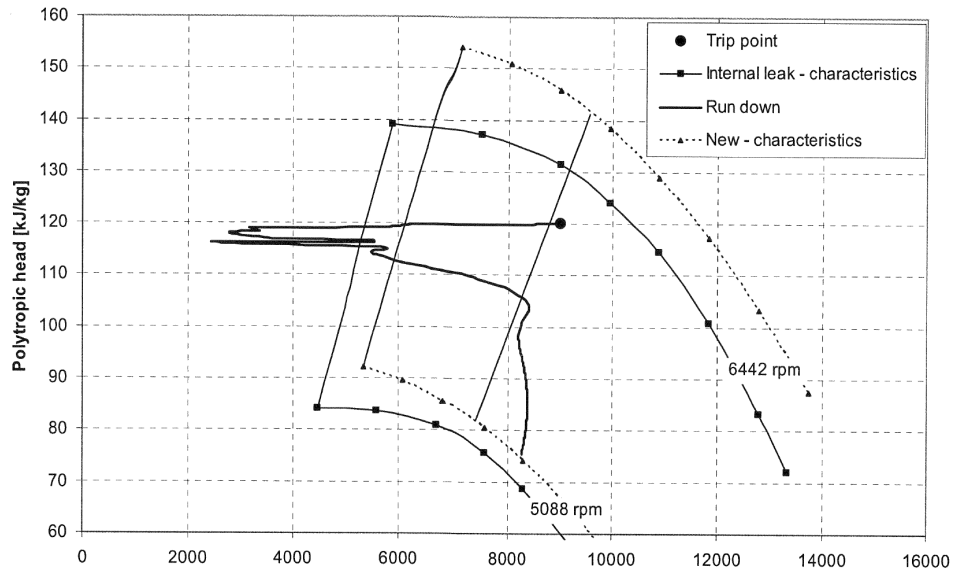


Figure 26: Compressor performance characteristics with internal leakage, Troll Kollsnes [17].

In this case the slope reduction is markedly from the surge control line to surge. In this area the slope is approximately 2/3 of the slope of the new compressor. This leads to a reduction in HRTS. When the driver trip is initiated the trajectory travels horizontal into surge with almost no reduction in head requirement. Compared to the new compressor the case with reduced HRTS travels significantly longer into surge and also show an increased time in surge because of flow pulsations. L.E. Bakken et al. [25] did simulations of the same plant with a reduced HRTS. The markedly reduction in HRTS was observed from the surge control line to the surge line also here. Similar results are observed, with an abrupt leap into surge and increased time in surge.

3.2.2 Increased Performance Steepness

Compressor deterioration can also increase the performance steepness. In [17] it is suggested that fouling can lead to an increase in HRTS and improve the surge stability. Paulsen and Haugen [28] found a minor increase in HRTS during experiments with a fouled inducer section. The effect is visible from medium to high flow rate. Tveit et al. [17] simulated driver trip scenarios in a fouled compressor, seen in Figure 27.

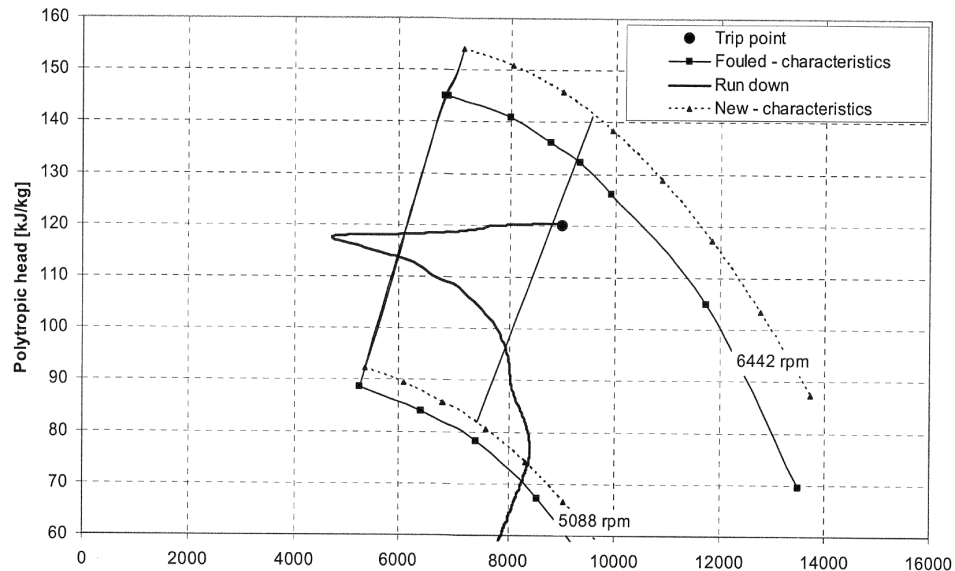


Figure 27: Compressor performance characteristics with fouling, Troll Kollsnes [17].

The compressor characteristic entailed a slightly increased head rise to surge, with the majority of the effect in the high flow rate area. The same tendency was demonstrated by Paulsen and Haugen [28]. Comparing the slope from the surge control line to surge in Figure 27, these two seems to be perfectly parallel. This indicates that the fouling is not the bottleneck in the low flow rate area. If looking at the trip trajectory of the new machine and the fouled machine almost identical behaviour is observed. However, the fouled case seems to have a slightly reduced time in surge.

3.3 Impact of Wet Gas

Most of the research done on compressor driver trip is from dry gas operation. The consequence of this is that there is little knowledge regarding the effect of fluid liquid content on the trip trajectory. Limited research is done on compressor transients in wet gas flow. However, two studies are conducted at NTNU by M. Bakken et al. [29] and Navarsete [30]. M Bakken et.al [29] executed driver trip tests for 3 different GMF's. The shape of the trip trajectory found in this study is in close compliance with what is predicted by affinity laws. Also, there is no visible change in the shape of the trip trajectory due to liquid content. However, a faster reduction in impeller speed was observed. This led to a faster reduction in both flow rate and pressure ratio. The increased impeller speed decay for wet gas is due to the higher density fluid increasing the flow inertia. As mentioned in 3.1.1, this is negative from a stability point of view because it reduces the compressor's ability to maintain positive throughput. Almost identical findings were done in [30]. In addition, the results showed a longer fluid response time for the wet gas. A summary of the results and their impact on compressor rundown is given in Table 2. From looking at other studies, M. Bakken et al. [21] concluded that the liquid content does not alter the surge point location or ruin the surge stability margin.

Variable	From dry to wet	Impact on compressor rundown
Impeller speed	Faster speed decay	Negative impact on throughput, positive impact on pressure ratio
Pressure ratio	Faster reduction	Positive impact, high pressure ratio is one of main causes of surge
Flow rate	Faster reduction and increased response time	Negative impact, faster reduction after driver trip and slower increase through protection systems. Reduced time to surge and increased time in surge.

Table 2: Wet gas impact on transient system performance [30].

3.4 Tuning of Trip Trajectory

Compressor driver trip tests at the NTNU Test Facility has demonstrated an affinity-like trip trajectory. This is a result of single impeller, atmospheric air suction, and small suction/discharge volumes. Attempts of tuning the trip trajectory at the NTNU Test Facility has been done. This is to obtain a behaviour more similar to large-volume, high-pressure systems like Troll Kollsnes, seen in Figure 25. Navarsete [30] investigated this through an experimental campaign in 2019. The approach consists of increasing the system resistance by throttling the discharge valve. This will reduce the compressor throughput and maintain the pressure ratio over the compressor. The operating point of the compressor will move left towards surge. Further, re-opening of the discharge valve will increase the downstream flow capacity, reduce the pressure ratio and move the operating point out of surge. This simulates the system response to an active safety system. Precise and repeatable tuning is achieved by the use of a valve sequencing tool where three different variables can be controlled. These variables are the ramp time, end position and hold time. The expected impact of each of the variables is presented below.

Ramp time

The ramp time is the valve travel time from the initial position to the new position. This is seen as the slope of the trajectory. The ramp down time affects how fast the throughput is reduced. A fast reduction in throughput will maintain the pressure ratio and the operating point will travel horizontal to the left in the characteristics. The ramp up time affects how fast the throughput is restored. This is the effect of protection system capacity in an industrial system.

Discharge throttle valve end position

The discharge throttle valve end position affects the degree of throughput reduction in the system. This dictates how far to the left the operating point travels.

Hold time

The hold time is how long the valve is held at the end position. This variable affects the duration of the maximum reduction in throughput. This is the how far the operating point travels along the left system resistance line before the turning point. In an industrial system this is the effect from the safety system response time.

First these variables were tested one by one to document the respective effect each had on the trip trajectory. The findings were in compliance with the ones illustrated in Figure 28, but with some markedly differences.

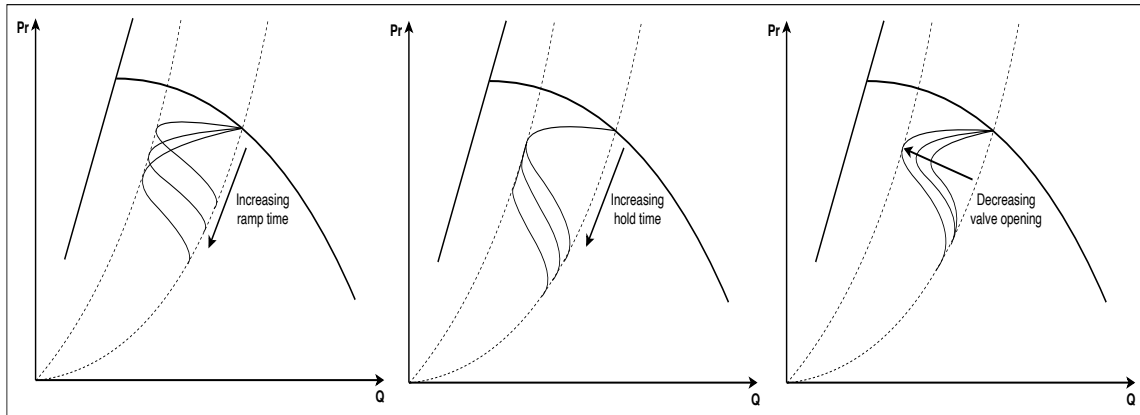


Figure 28: Expected effect on the trip trajectory of varying the individual tuning parameters.

An important observation is that the pressure ratio is not maintained at an adequate level if compared to e.g. the compressor at Troll Kollsnes. This is probably related to not being able to distinguish between ramp up/down time in the current setup. The result is a too slow reduction in throughput, and a less abrupt leap into surge. Based on the findings in the first part, different combinations of the variables were systematically tested. The objective was to find a suitable tuning regime to achieve a system behaviour similar to the ones observed in industrial scale systems. The most important results from this work will be reviewed and validated in this project. Further presentation of the valve sequencing tool and expected outcome of the tuning follows in Chapter 6.

3.5 Summary

In this chapter transient behaviour of the compressor system during a driver trip has been presented. The emphasis was on the different factor's effect on the trip trajectory. The factors investigated was system characteristics, compressor characteristics and wet gas. This shows a very complex challenge with a large number of factors involved. Lastly, a method for tuning the trip trajectory was presented.

- System characteristics like polar inertia, protection systems, power decay rate, trip delay and system volumes have significant effect on transient behaviour during driver trip.
- Changes in compressor performance characteristics due to deterioration can affect the compressor stability during driver trip. This includes the related time to surge and time in surge.
- Research on the field mostly come from simulations validated from operational data. True transient response of the compressor system during driver trip might deviate from the simulation models. This is a weakness of simulations which require large amounts of data to give adequate results. Further, the effect of unknown factors influencing the transient response will not be revealed.
- Experimental work by a master student at NTNU have shown that the trip trajectory can be tuned from an affinity-like shape to match trajectories of large volume, high pressure systems. This is done by the use of only the discharge throttle valve. Valve opening, ramp time and hold time were the variables adjusted to obtain the wanted outcome.
- Regarding driver trip in wet gas operation the research is limited and more needs to be done to fully understand the impact on TTS and TIS.

4 Test Facility

The Wet Gas Compression Test Facility is located in the basement of the Thermal Engineering Laboratory at NTNU. The rig facilitates research and tests in wet gas flow for manufacturers, operators and students. The main objective of the facility is to validate a wet gas compression system and to determine capabilities and constraints related to the impact of impeller stage performance [31]. Examples of research areas are fouling, digital twin and various transients.

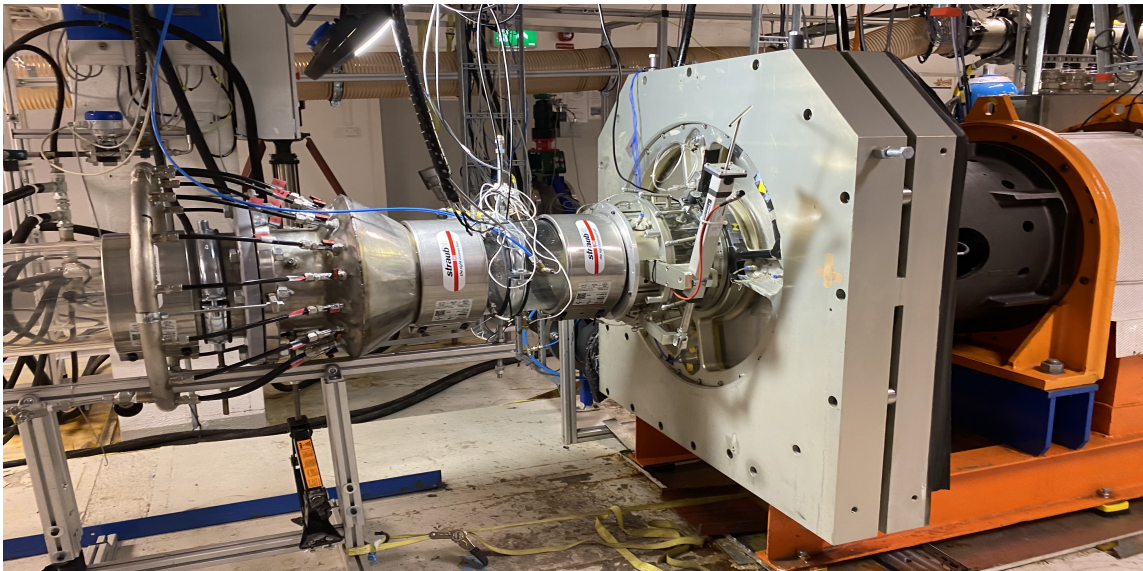


Figure 29: Wet gas compressor suction side, NTNU Test Facility.

The compressor operates in an open loop with air and water at atmospheric pressure. Gr uner and Bakken [32] found that the general performance trends in high-pressure hydrocarbon tests were reproducible with atmospheric air/water tests. This makes the research facility relevant for the petroleum industry. Despite the similarities in the general performance trends there are also major differences. The expected droplet size and Stokes' number is expected to be several orders of magnitude larger for air/water. This has a significant negative effect on the ability the droplet has to follow the flow path of the gas. Also, the density ratio of the air/water will make the compressor more sensitive to changes in GMF. In general the tests done in air/water will be more sensitive to liquid content and the effects will be more pronounced [15]. This includes phase slip, flow segregation and compressor losses.

Relevant fluid properties of air/water and natural gas/condensate can be seen in Table 3.

Variable	Air/Water	NG/Condensate
Gas pressure	1 bar	70 bar
Density ratio	0.00114	0.1887
Viscosity ratio	0.0181	0.525
Surface tension	0.072	0.02
GMF	0.8	0.8
GVF	0.99985	0.977
Gas constant	287	618

Table 3: Fluid properties of test fluid and natural gas/condensate [15].

4.1 Compressor System

The rig has been designed with the use of a transparent material that allows for visual observation. This design was based on results from tests performed on the previous rig. These results demonstrated the importance of visual observation of the flow path for the understanding of performance in wet gas conditions.

4.1.1 Suction

The compressor suction duct is placed in the same room as the compressor. At the start of this duct an orifice flow element measures the suction flow. Downstream of the flow element a throttle valve is installed which permits suction throttling. The inlet section has a diameter of 250 mm and length of approximately 30 meters. In the section closest to the compressor the inlet flow regime can be observed through the transparent pipe.

To obtain wet gas flow, water is injected. The injection can be done in different locations and with different droplet sizes. This is achieved by the use of movable injection modules with adjustable nozzles. Previous tests show that when the injection point is far enough upstream, the droplet size is not essential for the performance. This is assumed to be because of coalescence before the droplets reach the compressor. By varying the water injection rate and nozzle configuration various wet gas conditions and flow regimes can be tested.

4.1.2 Variable Inlet Guide Vanes

In front of the compressor an inlet guide vane unit with variable airfoil angle is mounted. It consists of 14 airfoils mounted in a transparent pipe which allows for visual observation of the flow over the airfoil during operation. The guide vanes are attached to an adjustable ring which enables angles from -20° to 40° at root mean square. One of these airfoils is equipped with a position transducer, measuring the airfoil position. The design of the unit is a trade-off between adjustment options and a gentle turning of the flow and flow control [33]. The VIGV unit is seen in Figure 30.

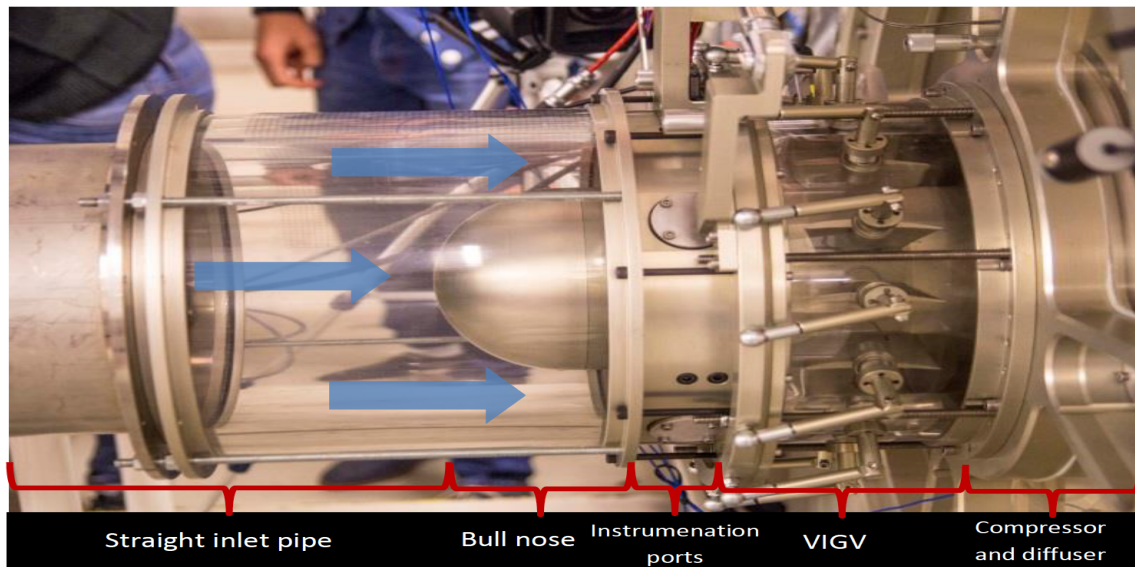


Figure 30: VIGV-unit, NTNU Test Facility [33].

4.1.3 Compressor

The heart of the facility is a centrifugal compressor driven by a 450-kW electric motor. The motor is equipped with a variable speed drive (VSD) allowing for a maximum speed of 11 000 rpm. Instruments mounted on the shaft measure the rotational speed and the torque. The compressor is equipped with a shrouded, backward swept impeller, a vaneless diffuser and a circular symmetrical volute. Also, parts of the diffuser and volute are made of transparent materials. This enables visual observation of the whole width of the diffuser, but limits the pressure to 1.5 bar [31].

4.1.4 Discharge

The outlet piping of the compressor is 200 mm in diameter and has a length of approximately 6 meters. Here the discharge throttle valve is located. This is a hydraulic operated ball valve. The ball has a V-shape cut to be able to open and close in a controlled manner. The cut is oriented downwards to avoid liquid accumulation in case of e.g. stratified flow. The outlet piping ends in an open separator.

A Process and Instrument Diagram of the rig configuration used in the tests of this project can be seen in Figure 31.

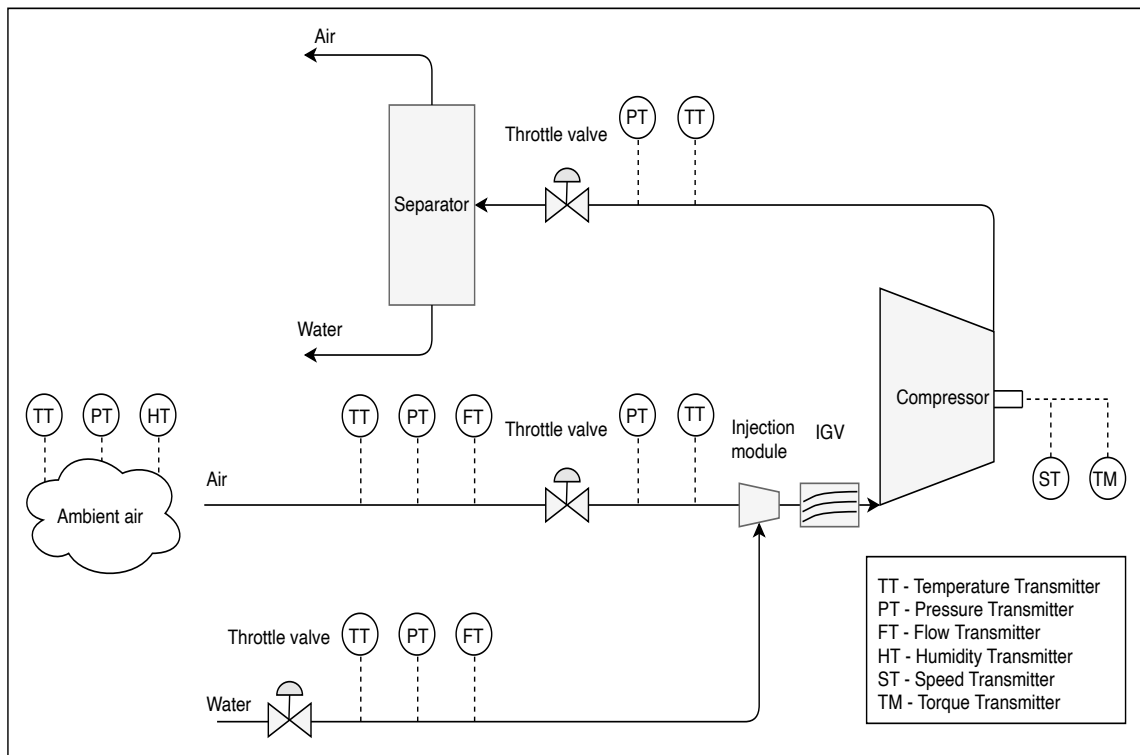


Figure 31: P&ID, NTNU Test Facility.

4.2 Instrumentation

The instrumentation of the test rig is done in accordance with ASME PTC-10.

4.2.1 Pressure

The inlet of the compressor has 4 pressure sensors spread across the perimeter of the pipe. These sensors are located approximately 0.5 meters from the compressor. The same setup is used for the outlet, approximately 1.5 meters from the compressor discharge. From these sensors the compressor pressure ratio, defined in equation (4.1), is calculated. The inlet pressure instrumentation can be seen in Figure 33, marked with red circles.

$$Pr = \frac{P_2}{P_1} \quad (4.1)$$

The diffuser also has 4 rows of 3 slots each for instrument insertion. One of these rows have dynamic pressure gauges installed, seen in Figure 32, spread radially on the diffuser. These are piezoelectric sensors which can measure small changes in pressure.

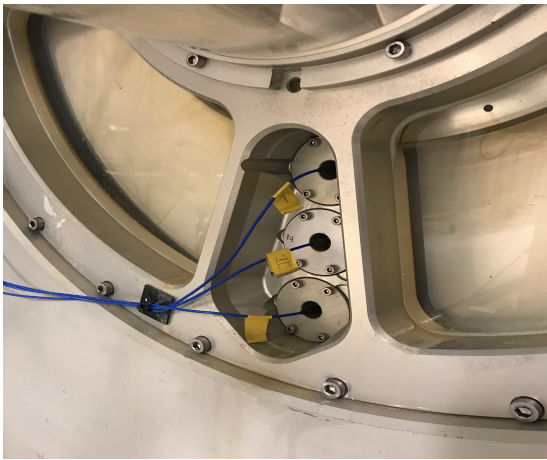


Figure 32: Piezoelectric pressure sensors mounted along the radius of the diffuser.

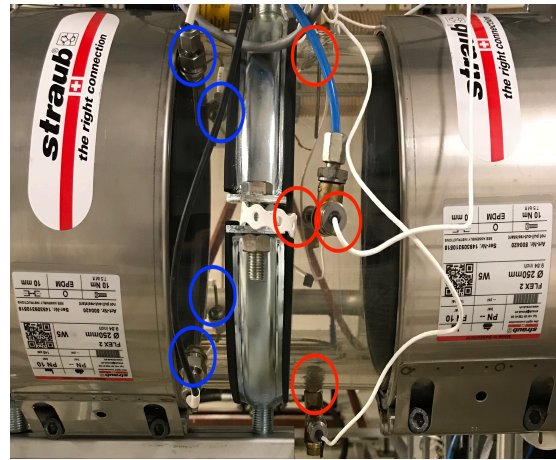


Figure 33: Temperature (blue) and pressure (red) sensors at the compressor inlet.

4.2.2 Temperature

The inlet and outlet of the compressor has temperature sensors in the same setup as for pressure. 4 sensors on both sides, spread across the perimeter of the pipe. To avoid disturbing the trailing pressure sensors, the temperature sensors are rotated 45° relative to the pressure sensors. For wet gas operation the temperature measurement of the outlet is associated with large uncertainties. There is no guarantee that thermal equilibrium between the phases is achieved, hence the gas temperature might be greater than the liquid temperature. Using water with approximately the same temperature as the air limits the heat transfer between the phases. This can improve the accuracy of the temperature measurement. This is achieved by storing the water in a tank in the room for several days before the test. However, there will still be heat transfer due to evaporative cooling.

4.2.3 Flow rate

The water injection volume flow rate is measured using an electromagnetic induction flow device while the air mass flow rate is measured by an orifice plate flow element. The plate creates an obstruction in the pipe, which leads to a pressure drop. Measuring the pressure drop over the orifice, the flow velocity can be calculated by Bernoulli's principle. However, this is only accurate for fully laminar, incompressible and inviscid flows. Correcting for these effects the coefficients C and ϵ are included. The coefficient of discharge C , accounts for the dissipation of energy by viscosity and turbulence, while the expansion factor ϵ , accounts for the compressibility of the flow. Both these factors are a function of the orifice type as well as the location of the measurement tubes. The full equation for calculating mass flow over an orifice plate according to ISO 5167-2 can be seen below.

$$\dot{m} = C\epsilon\rho A_1 \sqrt{\frac{2\Delta p}{\rho(1-\beta^4)}} \quad (4.2)$$

The coefficients of equation (4.2) and the calculation approach is described in Appendix D. Both the air and the water is measured on the suction side of the compressor. The sum of the water and air suction flow is the total volume flow rate. This is seen in equation (4.3)

$$Q_{tot} = Q_{air} + Q_{water} \quad (4.3)$$

The measurement principle for the flow orifice is illustrated in Figure 34.

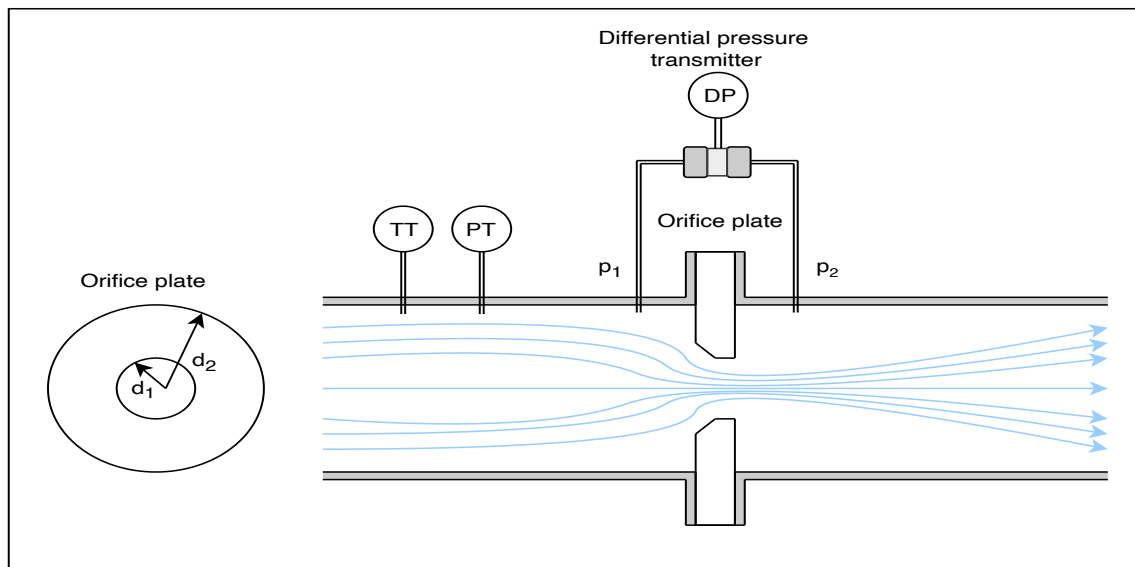


Figure 34: Flow measurement by differential pressure over an orifice plate.

The main dimensions of the compressor and the test facility instrument accuracy can be found in Appendix C.

4.3 Summary

In this chapter a brief presentation of the Wet Gas Compressor Test Facility at NTNU was given. This includes information regarding equipment, instrumentation and operation of the lab. The relevance for the industry was highlighted and research showing that results from air/water experiments are comparable to those from high pressure hydrocarbons were presented. Of specific relevance for groundbreaking research is the transparent rig design and liquid tolerant compressor which facilitates research on wet gas. Note that the lab is subject to frequent modifications which means that this information only reflects the current setup.

For a more detailed description of the test facility, see «Integrated Wet Gas Compressor Test Facility» by Hundseid and L.E. Bakken [31].

5 Experimental Campaign - Compressor Performance

This chapter contains the experimental campaign for the compressor performance testing of this project. This includes test objectives, procedures and test matrices. Further, results will be presented, and short analysis of the general trends will be given.

The tests done in this project have been planned in consultation with the supervisor and the lab engineer. To ensure the safety of both equipment and personnel a risk assessment has been performed in advance of the experimental activities. This is attached in Appendix H and is valid also for the next chapter.

The main objectives of this experimental campaign are:

- Establish compressor performance characteristics for the base case
- Establish compressor performance characteristics for the compressor with fouling
- Establish a method for tuning the compressor performance characteristics
- Replicate compressor performance characteristics of the compressor with fouling using the established method

The guidelines from ASME PTC-10 are the basis for the tests in this experimental campaign. According to this standard at least 5 operating points should be recorded when establishing performance curves for the compressor. The operating points stated by the standard are:

- One point near overload
- One point near best efficiency point
- Two points between best efficiency point and surge
- One point near surge

ASME PTC-10 sets requirements for temperature and pressure fluctuations during performance testing. The temperature in Kelvin and pressure in psia should not change with more than respectively $\pm 0.5\%$ and $\pm 2\%$ in 15 minutes. The standard also states that for low temperature rise machines an acceptable standard must be developed by uncertainty analysis. Here, the discharge temperature of the compressor is the bottleneck and the time for the system to obtain stability can be very long.

Especially for dry gas tests. Because of time constraints, the compressor torque will be used in the performance calculations instead of the outlet temperature. This method has been validated against calculations using the discharge temperature. To ensure acceptable stability, each operating point will be run for 30 minutes. For wet gas operation, stability is achieved faster due to the high specific heat of the injected water. Since there is no current standard for performance testing of wet gas compressors, each operating point is run for 5 minutes. This is based on experience from the test facility.

In this chapter all results are normalized against the best efficiency point from the dry gas base case. In equations (5.1) to (5.4) data from this point is denoted with a star.

$$\text{Normalized total volume flow} = \frac{Q_{air} + Q_{water}}{Q_{air}^*} \quad (5.1)$$

$$\text{Normalized static pressure ratio} = \frac{Pr}{Pr^*} \quad (5.2)$$

$$\text{Normalized polytropic head} = \frac{H_P}{H_P^*} \quad (5.3)$$

$$\text{Normalized polytropic efficiency} = \frac{\eta_P}{\eta_P^*} \quad (5.4)$$

Before each test is conducted a still test and reference point test is done. These preparations are described in Appendix B. Some test procedures will be given in this chapter for illustrative purposes, the rest is found in Appendix B.

5.1 Compressor Performance - Base Case

5.1.1 Test Objective

The objective of this test is to establish base case compressor performance characteristics for dry and wet conditions. In addition, gain understanding of the general behaviour of the compressor system and the wet gas impact. The results will form a basis for later comparison and analysis.

The dry gas performance test starts with the operating point closest to surge, and then increasing the valve opening to achieve the rest of the operating points. By starting at this end, stability for the later points will be achieved faster. In the wet gas tests, the same valve openings as for dry gas are used. This means that the volume flow rate for the test points will be slightly lower for the wet gas cases due to higher density and increased losses. The GMF's are chosen to be in compliance with the driver trip tests planned later in the project and other relevant studies on the subject. The test matrix for both dry and wet gas tests is seen in Table 4.

Compressor speed	GMF	Operating point	Compressor condition
9000 rpm	1.00	Close to choke - 100%	Non-fouled
	0.97	Intermediate A - 75%	
	0.90	BEP - 54%	
		Intermediate B - 42%	
		Close to surge - 30%	

Table 4: Test matrix, compressor performance - base case.

The detailed test procedure is seen below.

1. Perform start-up procedure
2. Start logging
3. Adjust discharge throttle valve to obtain wanted operating point
4. Open water injection valve and adjust water valve to obtain wanted GMF
5. Run for minimum 5 minutes for wet gas or 30 minutes for dry gas
6. Stop logging
7. Close water injection valve
8. Repeat steps 2-6 until five operating points is recorded according to the test matrix
9. Repeat steps 2-7 for all GMF's according to the test matrix

5.1.2 Results and Discussion

In the following figures, the wet gas cases entails a reduced volume flow rate for the medium and high valve openings. There might be several causes of this phenomena. One of them is droplet deposition creating a liquid film on the internal surfaces, reducing the effective flow area in the system. At high flow rates this becomes a bottleneck. Other studies have reported the same trend [12, 20, 21]. Explanations were increased losses and reduced flow area due to liquid film formation [12], increased system resistance [20], droplet deposition and momentum transfer [21].

In Figure 35 static pressure ratio versus total volume is plotted. This shows an increased static pressure ratio for wet gas. The exception is at high flow rates where the dry and wet gas cases are almost inseparable.

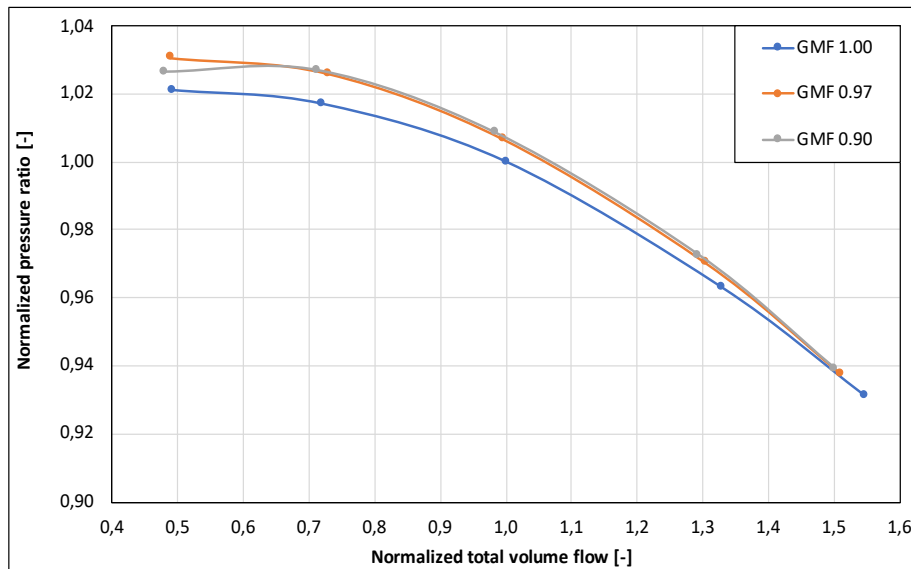


Figure 35: Normalized pressure ratio versus normalized total volume flow, base case.

This might be related to increased losses which outweighs the advantageous effects of the wet gas on the pressure ratio. Frictional losses are proportional to the density and the velocity squared. Furthermore, decreased flow area induces higher pressure losses. A similar increase in pressure ratio is seen for both GMF's tested. Further, it seems to be the immediate effect of introducing liquid which increases the pressure ratio. No significant increase is observed between GMF 0.97 and 0.90. The result of the reduced flow range and increased pressure ratio is a steeper curve. This translates to an increase in PRTS which indicates better stability performance.

The polytropic head in Figure 36 shows the opposite tendency of the pressure ratio. The polytropic head decreases consistently with increasing liquid content. By the theory and former studies this is expected. The difference is largest at low flow rates and decreasing towards choke. These findings implicate a reduction in HRTS in contrast to the increased PRTS. As discussed earlier, this indicates that HRTS is not suitable to establish stability margins in wet gas compressors.

Figure 37 shows the polytropic efficiency. The results show a polytropic efficiency which is consistently decreasing with decreasing GMF. This is in agreement with previous research [12, 20, 22, 23]. This is explained by increased losses due to mechanisms mentioned earlier.

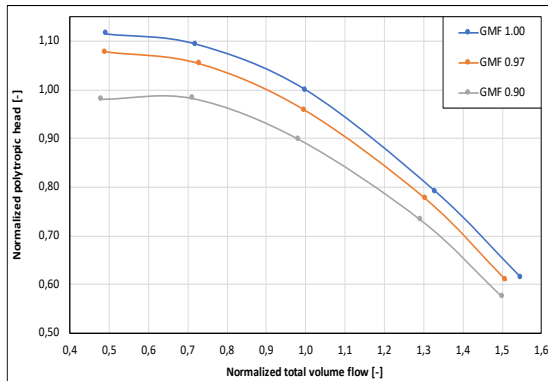


Figure 36: Normalized polytropic head versus normalized total volume flow, base case.

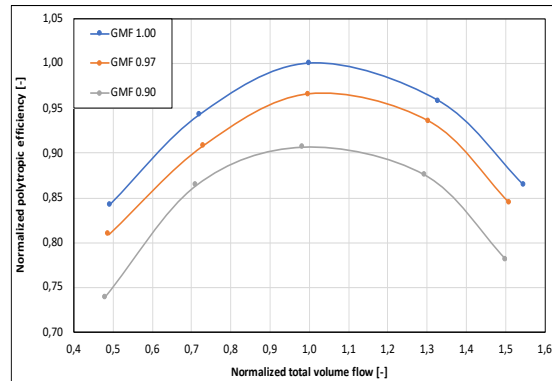


Figure 37: Normalized polytropic efficiency versus normalized total volume flow, base case.

Through the transparent sections at the compressor inlet stratified flow was observed in the wet gas tests. Recognized by a clear interface between liquid flowing at the bottom of the pipe and gas at the top. In addition, a part of the liquid transport is observed as a droplet field in the center of the pipe. The distribution between the liquid transport mechanisms depends on the flow rate of air and the GMF. Higher air flow rate increases the liquid entrainment in the flow and leads to more liquid transport in the droplet field. The trend for decreasing GMF is that more liquid is transported at the bottom of the pipe. Approaching the impeller, this liquid is ripped into droplets and dispersed into the compressor. The water exits the impeller as a jet on the pressure side of the impeller and on the back wall.

5.2 Compressor Performance - Fouling

This part of the experimental campaign is done in cooperation with another master student. Here, the compressor diffuser is coated with a mixture of paint and fiberglass particles to replicate fouling. Apart from that, this test is identical to the base case and the same test procedure is used. The diffuser before and after coating was applied is depicted in Figure 38 and Figure 39.



Figure 38: NTNU Test Facility diffuser.

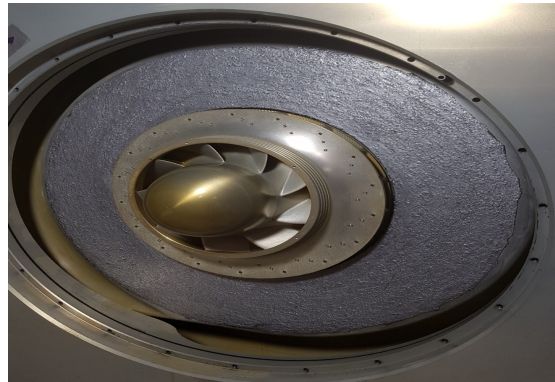


Figure 39: NTNU Test Facility diffuser with fouling.

5.2.1 Test Objective

The main objective of this test is to establish performance characteristics for the compressor with a fouled diffuser. Comparing the results with the base case the relative effects of diffuser fouling can be analyzed. Further, this will form a basis for driver trip tests later in the project. The related test matrix is seen in Table 5.

Compressor speed	GMF	Operating point	Compressor condition
9000 rpm	1.00	Close to choke - 100%	Fouled
	0.97	Intermediate A - 75%	
	0.90	BEP - 54%	
		Intermediate B - 42%	
		Close to surge - 30%	

Table 5: Test matrix, compressor performance - fouling.

5.2.2 Results and Discussion

The general observations going from non-fouled to fouled is a reduction in total volume flow rate, pressure ratio, polytropic head and polytropic efficiency. This corresponds well with the theory and the results from Haugen and Paulsen [28]. Similar to the base case, the effect is not equal in all operating points. Especially the flow reduction is largest in the medium to high flow rate region.

The wet gas cases also appear to diverge from each other at high flow rates, while converging at low flow rates. This is the opposite of what is observed in the base case. The same behaviour was also demonstrated by Haugen and Paulsen [28] with a fouled inducer.

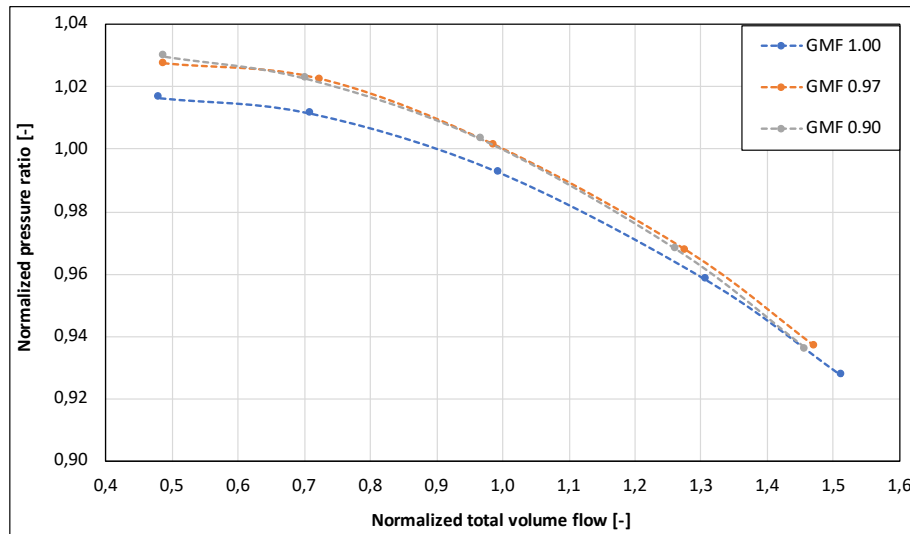


Figure 40: Normalized pressure ratio versus normalized total volume flow, fouled.

The wet gas impact is also observed to be more prominent for the fouled compressor than the non-fouled. This is seen as a higher pressure ratio increase and higher reduction in volume flow when going from dry to wet.

Comparing the results from non-fouled to fouled in Figure 41 and Figure 42 a general trend regarding is observed. A markedly increase in steepness is observed for the fouled cases in wet gas flow. The effect is found in the low flow rate area and leads to a steady increase in pressure ratio towards surge. This translates to an increase in PRTS.

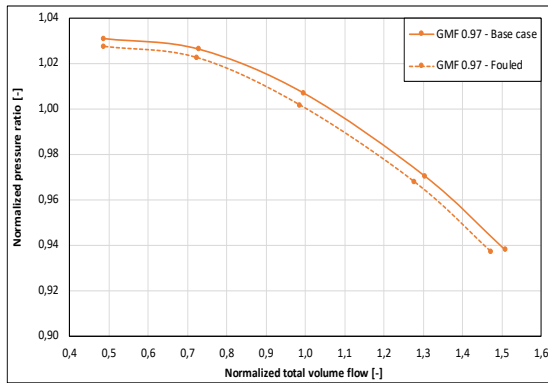


Figure 41: Normalized pressure ratio versus normalized total volume flow, base case versus fouled GMF 0.97.

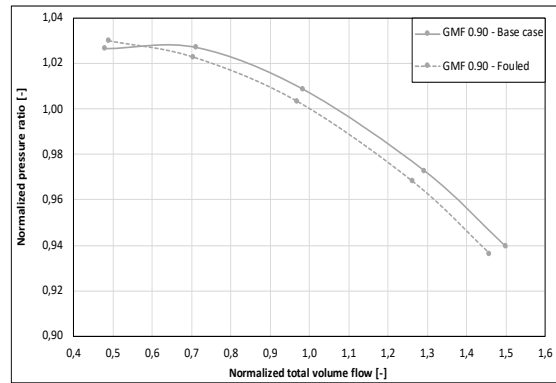


Figure 42: Normalized pressure ratio versus normalized total volume flow, base case versus fouled GMF 0.90.

The same trend is observed for the polytropic head seen in Figure 43, where a steady increase in head towards surge is demonstrated. This effect is highlighted in Figure 70 and Figure 71 in Appendix A. The results for PRTS and HRTS suggests that fouling increases the compressor stability in wet gas flow.

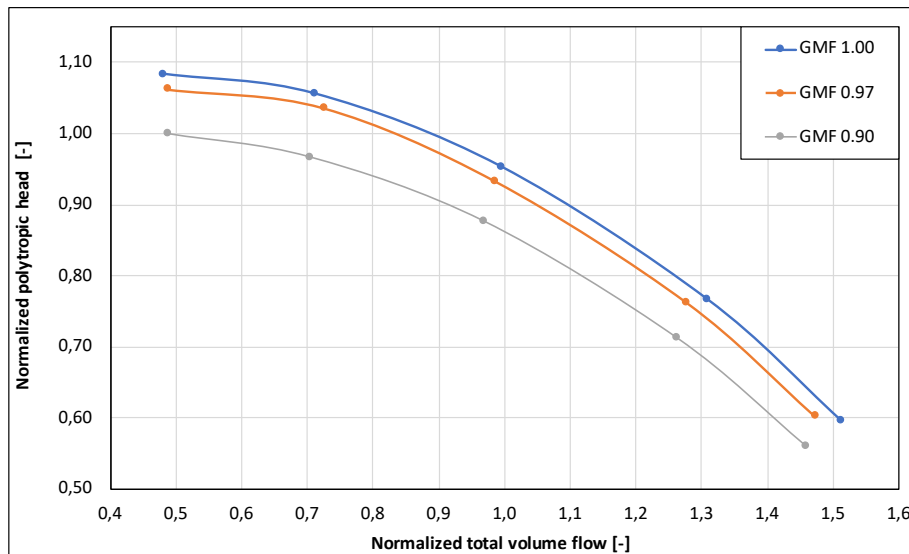


Figure 43: Normalized polytropic head versus normalized total volume flow, fouled.

5.3 Replicated Fouling

5.3.1 Test Objective

The objective of this test is to establish a method for tuning the performance characteristics. The goal is to obtain a pressure ratio versus volume flow curve which is in compliance with the fouled compressor.

As seen in last section, the fouled compressor entails a curve shifted towards lower pressure ratio in the high flow rate region and a limited maximum flow rate. The result is a steeper and narrower characteristic curve. At the same valve opening, the fouled compressor might have an operating point shifted slightly towards lower flow rate. These effects can be seen in Figure 44 where the bullets mark the same valve opening.

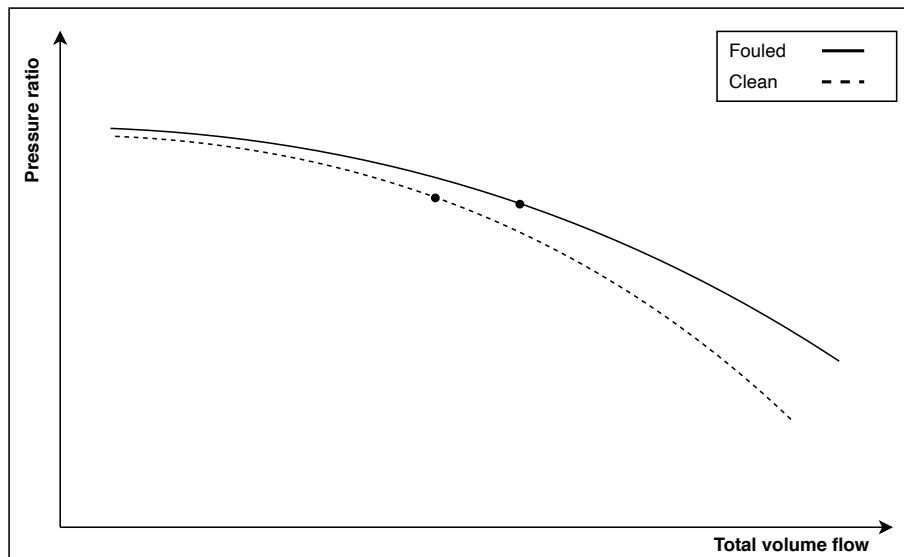


Figure 44: General trend in performance characteristics of clean and fouled compressor at same valve opening.

Traditionally, research on compressor fouling requires application of a suitable coating on the relevant surfaces of the compressor. This can be sandpaper or paint with mixed in particles. This is to replicate the thickness and surface roughness of the fouling observed. This technique of applying material to the rotating or static parts of the machine is labor-intensive and poses a risk for human beings. Running the machine with this material can also be a risk for the machine in the case of material being teared off and entering vulnerable parts of the machine.

The objective of this test is to replicate the performance characteristics of a fouled compressor with the use of compressor control techniques. To replicate this behaviour, three steps involving three different control techniques will be used. These are presented below and illustrated in Figure 45.

1. Variable inlet guide vanes to add pre-swirl which tilts the curve down in the high flow rate range
2. Variable speed drive to reduce the rotational speed which parallel shifts the curve towards origo
3. Discharge throttle valve to move along the curve to achieve the exact same operating point

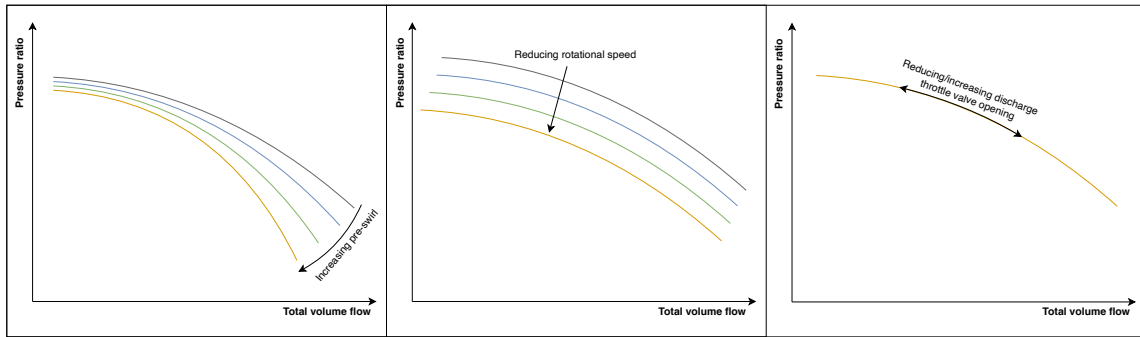


Figure 45: Three steps of replicating fouling using compressor control techniques.

If the fouled compressor characteristics can be replicated with the use of control techniques instead of actually fouling the compressor, it would be very advantageous. Primarily, it would reduce the risk for both man and machine but also simplify research on the field. In the future the findings can be included in e.g. a digital twin. Implementing known types of deterioration in the model can help the operator to recognize challenges and aid in troubleshooting in case of operational problems.

The aim is to reproduce the pressure ratio versus volume flow observed for the fouled conditions. The three steps mentioned, starts with obtaining characteristics for various degrees of pre-swirl and GMF's. This is done by setting the valve sequence tool to run the discharge throttle valve from 100% to 30% in ten minutes. This is repeated for the various IGV angles.

Compressor speed	GMF	Valve opening [%]	VIGV angle [°]
9000	1.00	100-30	10
	0.97		20
	0.90		30
			40

Table 6: Test matrix, effect of various VIGV-angles on performance characteristics in wet and dry conditions.

5.3.2 Results and Discussion

The results show that a low degree of pre-swirl is needed to replicate the slope of the fouled curve. For the dry gas case, the angle needed to replicate the curve is less than what was used in the initial test. In addition, it revealed that the rotational speed needed reduction. This is seen in Figure 46 where the lowest IGV angle is too steep and has an offset relative to the fouled curve. To improve the results, a new test was done with a 5° IGV angle. This replicated the slope perfectly. Next, the rotational speed was reduced to shift the curve. The results are seen in Figure 47.

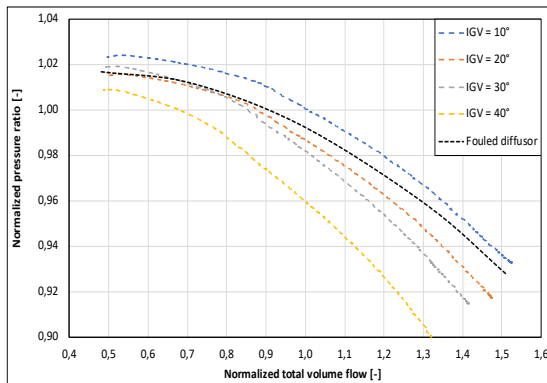


Figure 46: Normalized pressure ratio versus normalized total volume flow, various IGV angles GMF 1.00.

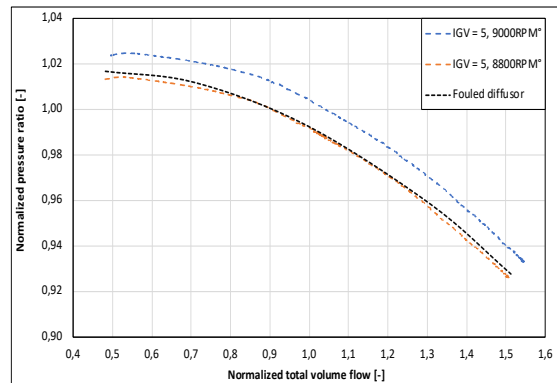


Figure 47: Normalized pressure ratio versus normalized total volume flow, IGV angle 5° GMF 1.00.

As seen from Figure 48 and Figure 49, adding pre-swirl alone was enough to replicate the fouled curve. This means that reducing the rotational speed was not necessary to achieve a good result. This is linked with the IGV pressure loss which increases as the GMF is reduced. Here, good results were achieved with an IGV angle of 10° for both GMF's.

If investigated further, it is likely that the IGV angle needed to replicate the slope of the curve depends on the GMF more strongly than observed in these results. From GMF 1.00 to GMF 0.97 a higher angle is needed, but the same angle is used for GMF 0.97 and GMF 0.90. If a high level of accuracy was needed fine tuning both the IGV and rotational speed could be used. The tests also showed that the valve opening needed to reproduce the operating point was within 1% of what was used in the fouling test. Hence, no discharge throttling was used to obtain the same operating point.

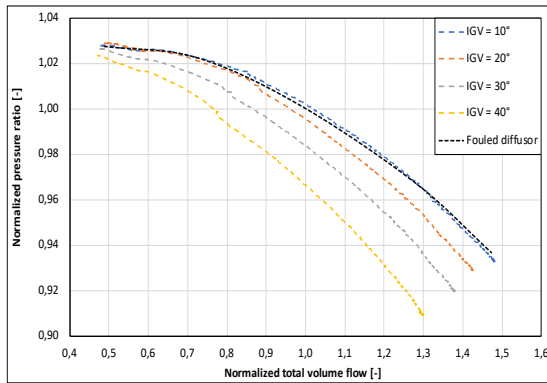


Figure 48: Normalized pressure ratio versus normalized total volume flow, various IGV angles GMF 0.97.

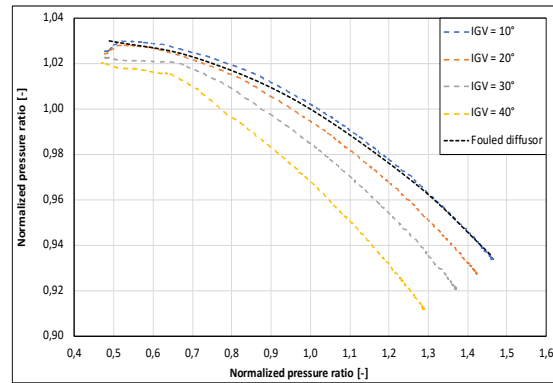


Figure 49: Normalized pressure ratio versus normalized total volume flow, various IGV angles GMF 0.90.

5.4 Uncertainty and Sources of Error

- Several steps of human interference in the data processing increases the probability of errors.
- During the experimental campaign the lab was frequently experiencing instabilities and spikes in all sensors connected to the system. By sensitivity analysis it was discovered that small deviations in pressure or temperature could change e.g. the calculated efficiency of several percentage points. In compliance with ASME PTC-10, if one of the four sensors showed large deviation, the sensor data was discarded and the other three averaged.

5.5 Summary

The results from the compressor performance tests show the immediate effects of wet gas. The main trend for decreasing GMF is increased pressure ratio, reduced polytropic head and polytropic efficiency. The wet gas also induces an increase in the slope of the pressure ratio curves, which indicates a higher PRTS and more stable operation at low flow rates.

Introducing the fouled diffuser, the impact on compressor performance was documented. Going from non-fouled to fouled the general trends are reduced total volume flow rate, pressure ratio, polytropic head and polytropic efficiency. Further, these effects are not equal in all operating points resulting in a steeper performance characteristic. Lastly, the method for replicating the performance characteristic of a fouled compressor was established and applied with success.

6 Experimental Campaign - Compressor Transients

This chapter contains the experimental campaign on compressor transients with emphasis on driver trip. The aim is to test and analyze dry and wet trip scenarios to document the compressor system behaviour. Of specific interest is how different compressor performance characteristics affect the rundown trajectory. The chapter includes test objectives, test matrices, Detailed test procedures results and discussion.

The main objectives are:

- Investigate the delay phenomena described as «Further Work» in studies done in the NTNU Test Facility
- Establish rundown trajectories in dry and wet conditions for the base case. Validate the use of the discharge throttle valve for tuning of the rundown trajectory
- Establish rundown trajectories with fouling in dry and wet conditions
- Establish rundown trajectories with the replicated fouling characteristics using variable inlet guide vanes, in dry and wet conditions

The delay phenomena mentioned is a peculiar behaviour observed during trip tests. Driver trip induces an immediate pressure reduction. However, this is not the case for the volume flow rate which is persistent for another 0.5 seconds before the decay starts. The impact of this is a vertical section at the start of the trip trajectory. The phenomena is tested and found to be due to an instrument delay in the pressure differential transmitter placed on the flow orifice. The full description of the test and results is found in Appendix A. From this conclusion, an offset of 0.5 seconds is added to the air flow measurements.

In this experimental campaign, all tests will be performed twice. This is a self-verification process to ensure consistency and detect possible errors. If significant deviation between the two runs is found, a re-test of the specific scenario will be performed. Examples of consistency in the results are shown in Appendix A.

All rundown trajectories plotted in this chapter includes a red surge line. This is positioned such that it intersects the flat part of the performance characteristic for dry gas. The time elapsed since driver trip is marked by bullets, squares and triangles. These are placed respectively 5, 10 and 15 seconds after driver trip.

The stability parameters mentioned in this chapter are:

- Time to surge - The time from driver trip to the first intersection with the surge line
- Pr - The pressure ratio at the first intersection with the surge line
- Minimum flow - How far into surge the operating point travels
- Time in surge - The time between the two intersections with the surge line
- Maximum flow - The flow gain after surge

All results in this section are normalized in one of two ways.

1. Normalized against the operational point before driver trip for the dry gas base case, #1
2. Normalized against its own operational point before driver trip

This is shown in equations (6.1) and (6.2).

$$\text{Normalized total volume flow} = \frac{Q_{tot}(t)}{Q_{tot}(t=0)_{\#1}} \quad \text{or} \quad \frac{Q_{tot}(t)}{Q_{tot}(t=0)} \quad (6.1)$$

$$\text{Normalized static pressure ratio} = \frac{Pr(t)}{Pr(t=0)_{\#1}} \quad \text{or} \quad \frac{Pr(t)}{Pr(t=0)} \quad (6.2)$$

Each of these normalizing methods has its advantages. Normalizing all data against the same starting point highlights the differences from start but hides changes that occur along the trip trajectory. Normalizing against the test's own starting point does the exact opposite. All tests get the same starting point and differences along the trip trajectory is highlighted. The figures that are normalized using the last-mentioned method will be marked with (*).

In all test scenarios the driver trip has been done both with and without tuning of the rundown trajectory. This is to reveal if the observed effects are similar in all cases. However, the emphasize is on the tests with tuning and the tests without tuning will only be mentioned if relevant findings are done.

All trip tests is done from a valve opening of 54% (BEP for dry gas). It is expected that the operating point before trip impacts the stability performance but due to the limited scope this is left as further work.

6.1 Driver Trip - Base Case

6.1.1 Test Objective

The objective of this test is to establish trip trajectories in dry and wet gas conditions. The results from these tests will be analyzed and the general wet gas impact on the trip trajectory will be documented. These tests will form a basis for the rest of the campaign. Keeping control of the changes done from the base case, the relative impact of different factors on the trip trajectory can be analyzed.

To obtain the wanted compressor behaviour the method suggested in Section 3.4 is used. Further, this method is to be reviewed and validated. To be able to validate the tuning method, the base case test parameters are chosen to be in accordance with the tests done by Navarsete [30]. Here, the tuning parameters which achieved results closest to an industrial system is chosen. The expected outcome of the tuning and an illustration of the valve sequence tool is given in Figure 50 and Figure 51.

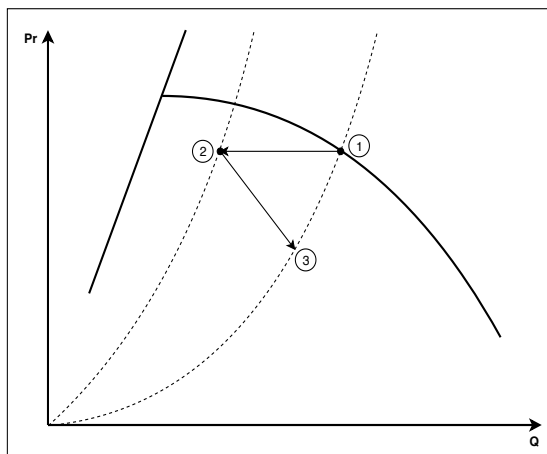


Figure 50: Effect of tuning the rundown trajectory using the discharge throttle valve.

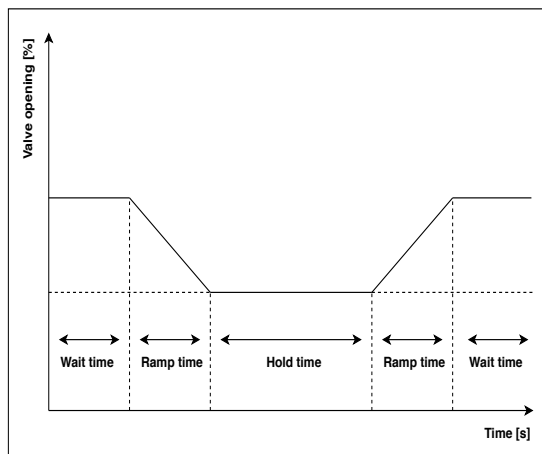


Figure 51: Valve sequence tool used to tune the rundown trajectory, NTNU Test Facility.

In Figure 50 the right dotted line is the system resistance curve before the valve sequence is initiated, while the left is the system resistance curve at the valve end position. Point 1 is the operating point before the compressor driver trip. From point 1 to point 2 the discharge throttle valve opening is reduced until point 2 is reached. This position is held for some time. After that, the discharge throttle valve opening is increased to the initial value, moving the operating point from 2 to 3.

The test matrix for this scenario can be seen in Table 7.

Test number	#1	#2	#3	#4	#5	#6
Compressor condition	Non-fouled					
Compressor speed [rpm]	9000	9000	9000	9000	9000	9000
GMF	1.00	0.97	0.90	1.00	0.97	0.90
Valve start position [%]	54	54	54	54	54	54
Valve end position [%]	54	54	54	30	30	30
Ramp time [s]	N/A	N/A	N/A	3	3	3
Hold time [s]	N/A	N/A	N/A	1	1	1

Table 7: Test matrix, driver trip - base case.

The detailed test procedure is given below.

1. Perform start-up procedure
2. Adjust discharge throttle valve to 54% (BEP)
3. Adjust the water injection valve to obtain specified GMF
4. Run until rotational speed, flow rate, suction pressure and discharge pressure are stable
5. Start logging
6. Trip the compressor manually and initiate valve sequence simultaneously
7. Run until the rotational speed reaches 3000 rpm
8. Stop logging
9. Close the water injection valve
10. Restart the compressor
11. Repeat steps 3-10 until all tests are done according to the test matrix

6.1.2 Results and Discussion

As seen in previous studies [29, 30] the compressor at the NTNU Test Facility entails a rundown trajectory very close to what predicted by the affinity laws. This is the case for both dry and wet gas when no tuning of the trajectory is done. This can be seen in Figure 52.

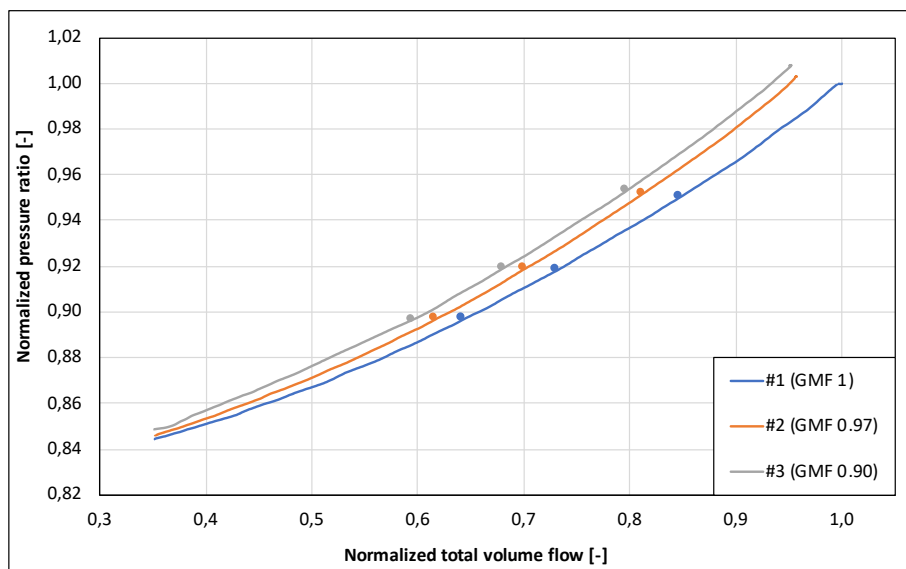


Figure 52: Trip trajectory, base case without tuning.

From the same figure, the initial wet gas impact is seen. This is equivalent to the observations in the performance tests. This includes higher pressure ratio and lower total volume flow rate. The difference is largest between #1 and #2, which seems to be the immediate effect of introducing liquid to the flow. However, increasing the liquid content further induces less change. The mentioned observations seem to be consistent in all wet gas scenarios in both performance tests and transient tests.

Figure 53 shows the base case with tuning of the trip trajectory. The results are in close compliance with Navarsete [30]. The tuning induces a change in shape from affinity-like to a shape similar to the ones observed in large-volume, high-pressure systems. The only significant deviation observed from e.g. Troll Kollsnes is a less abrupt leap into surge. This is attributed to a too long ramp down time. However, this is limited by the valve sequencing tool which does not differentiate between ramp up and ramp down. From this result it is evident that the method is suitable for the purpose.

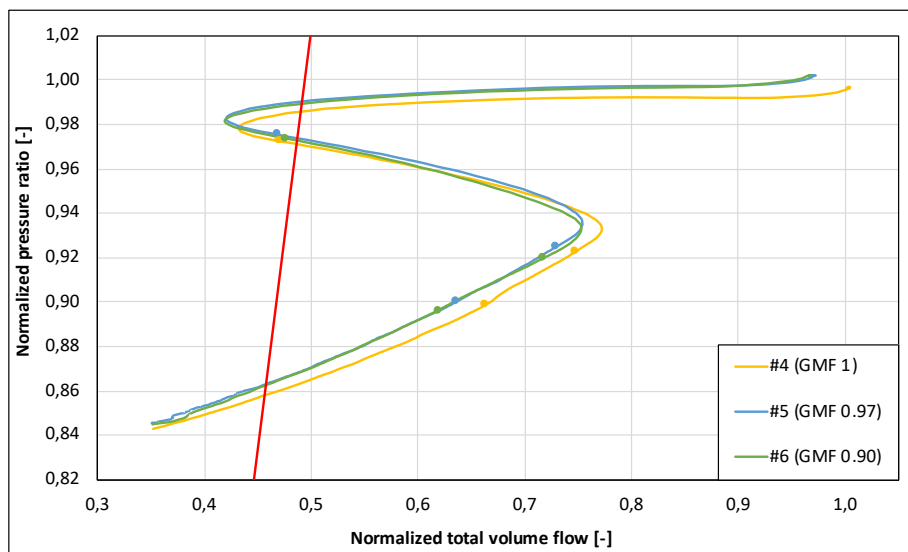


Figure 53: Trip trajectory, base case.

The immediate effect of wet gas on the trip trajectory is rather obvious. However, the effect of increasing the liquid content further is minimal. The two wet gas cases follow trajectories which are close to inseparable for most of the rundown. The only difference is seen during valve ramp up. This might be linked to the wet gas valve performance. Further, the offset between the dry and wet gas cases is persistent through the entire rundown.

Figure 54 demonstrates an increasing impeller speed decay rate when liquid is introduced. The high density ratio of the flow implies that only small amounts of liquid increases the density of the flow substantially. In this case #6 has almost 10% higher mass flow than #4. This does not affect the energy stored in the impeller, but it increases the fluid power. The result is a higher impeller speed decay rate seen from equation (6.3). The mentioned observations coincides with previous studies [29, 30].

$$\frac{d}{dt} (\omega_c^2) = -2 \frac{P_{fluid} + P_{losses}}{I_{tot}} \quad (6.3)$$

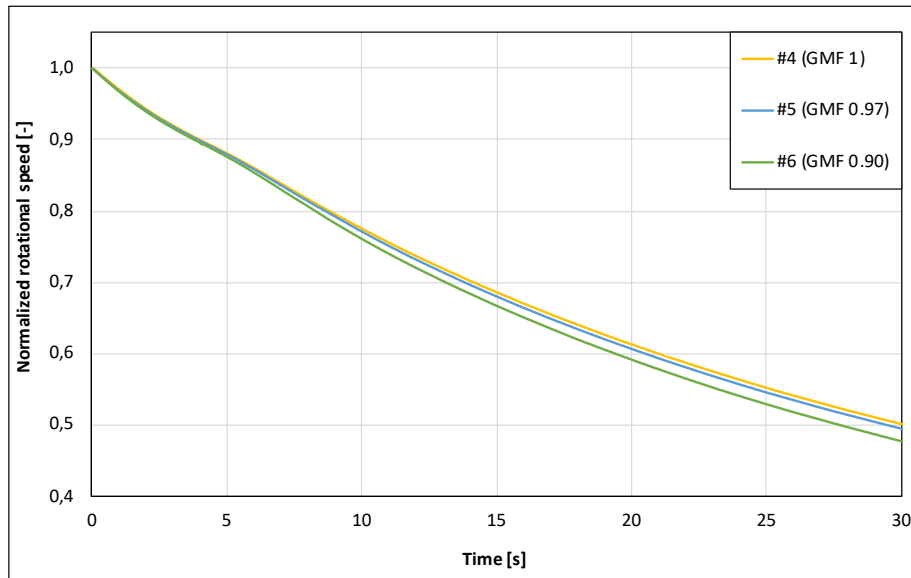


Figure 54: Normalized rotational speed versus time, base case.

Along the trip trajectory the differences between dry and wet is less obvious. However, both the total volume flow rate, in Figure 55, and the pressure ratio, in Figure 56, is observed to be reduced faster with decreasing GMF.

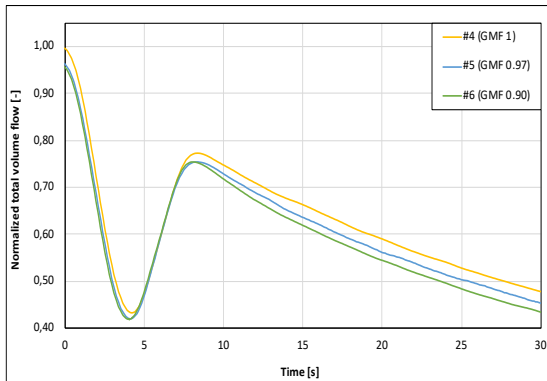


Figure 55: Total volume flow versus time, base case.

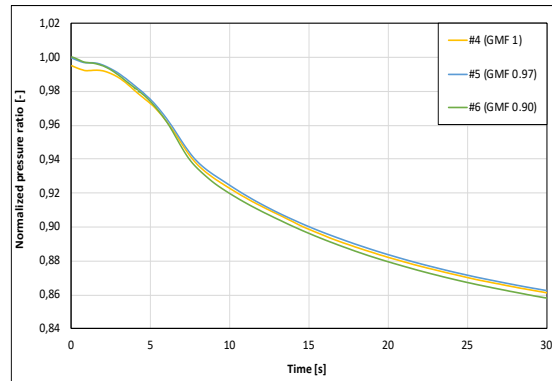


Figure 56: Pressure ratio versus time, base case.

This is linked with the mentioned increased impeller speed decay. The faster reduction in pressure ratio is in contrast with what is expected for a large-volume, high-pressure system. Here the pressure ratio will remain at its initial level if no actions are taken after driver trip. In this context a faster impeller speed decay rate will reduce the flow capacity faster and the pressure ratio will remain for

longer. This is not the case in the laboratory. Here, the compressor is not operating against a high-pressure, high-volume reservoir and the only thing maintaining the pressure ratio is the compressor itself.

From the results, the wet gas impact on compressor stability performance have been investigated. This is summarized in Table 8. Going from dry to wet, a consistent reduction in TTS is observed. This is linked with the faster reduction in volume flow rate after trip initiation. However, it is not possible to draw any further conclusions from the results. This is due to the lack of consistent and significant change in other stability related variables. It seems that the affinity-like nature of the system leads to a transient behaviour which is mostly dependent on the compressor speed.

Variable	#4 (GMF 1)	#5 (GMF 0.97)	#6 (GMF 0.90)
Time to surge	3.225s	3.150s	3.100s
Minimum flow	0.429	0.432	0.428
Pr	0.989	0.988	0.986
Time in surge	1.900s	1.825s	1.900s
Maximum flow	0.767	0.776	0.776

Table 8: Stability performance, base case(*).

Moreover, the expected wet gas impact on the stability of large-volume, high-pressure system can be predicted to a certain degree from the results in this campaign. In the performance part an increase in PRTS was observed going from dry to wet. The implication of this is that the onset of surge is further away from the operating point. In isolation this would increase the TTS but considering the faster impeller speed decay which reduces the flow faster, the net effect is probably a reduction in TTS. Regarding TIS, this is also expected to increase for wet gas. This is attributed to the larger flow reduction, seen in Figure 53, and an increased fluid response time [30]. Lastly, the possible consequences of surge is expected to be more severe in wet gas operation due to the higher density fluid.

6.2 Driver Trip - Fouling

6.2.1 Test Objective

The objective of this test is to establish trip trajectories for the fouled compressor in dry and wet conditions. Further, document how fouling affects the trip trajectory and the related stability performance. Of specific interest is the time to surge and time in surge. In a study by L.E. Bakken et al. [25], simulations of a fouled compressor have shown better stability performance in the form of increased HRTS. Similarly, an increase in both PRTS and HRTS was observed in the performance part of this experimental campaign. Yet, this effect was seen only for wet gas cases. The impact this has on the stability performance is to be investigated.

The tests done in this section are identical to the base case, only with a fouled diffuser. Because of this the procedure used for this test is the same as for the base case. The test matrix is given in Table 9.

Test number	#7	#8	#9	#10	#11	#12
Compressor condition	Fouled					
Compressor speed [rpm]	9000	9000	9000	9000	9000	9000
GMF	1.00	0.97	0.90	1.00	0.97	0.90
Valve start position [%]	54	54	54	54	54	54
Valve end position [%]	54	54	54	30	30	30
Ramp time [s]	N/A	N/A	N/A	3	3	3
Hold time [s]	N/A	N/A	N/A	1	1	1

Table 9: Test matrix, driver trip with fouled diffuser.

6.2.2 Results and Discussion

The wet gas impact in the fouled case is demonstrated in Figure 57. Compared to the base case the wet gas impact is more prominent in the fouled compressor. This is seen as a larger distance between the trajectories. The same figure shows a peculiar trend regarding the total volume flow rate. Going from GMF 1 to 0.97 induces reduction in total volume flow rate. In comparison, the base case demonstrated a flow rate reduction of over 3% when increasing the liquid content to GMF 0.97. Reducing the GMF further to 0.90 induces a sudden drop by almost 5%. The same change in the base case induced no change in the total volume flow rate. Also, note that no change in impeller speed decay was observed going from non-fouled to fouled.

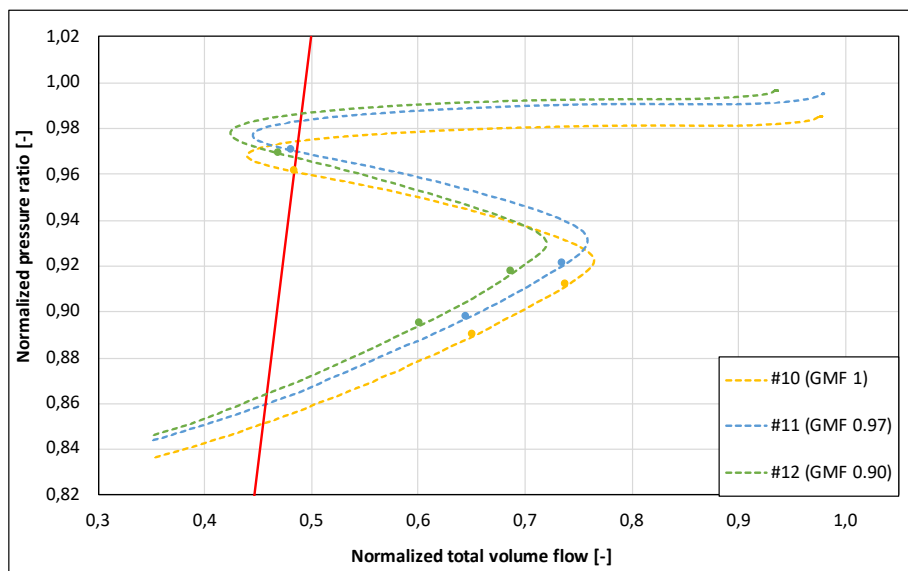


Figure 57: Trip trajectory, fouled.

These findings suggest that the onset of wet gas limiting the flow rate has migrated in the direction of lower GMF. This might be attributed to formation of a liquid film which smooths out the roughness from the fouling, reducing the frictional losses. This is not proven to be the case and the result is in contradiction to findings from the performance tests and Haugen and Paulsen [28]. The test was repeated four times with consistent results.

Similar to the base case, an increase in pressure ratio is demonstrated for both GMF 0.97 and 0.90. However, in the base case the maximum pressure ratio increase was achieved at GMF 0.97. The fouled case demonstrates a further increase in pressure ratio from GMF 0.97 to 0.90 is observed. This also substantiates the mentioned migration of the onset of wet gas effects.

Figure 58 and Figure 59 shows a comparison between non-fouled and fouled for GMF 1 and GMF 0.90. Here, the deviation between non-fouled and fouled is largest for dry gas where the fouling is clearly a limiting factor. This is markedly in both pressure ratio and volume flow rate. Looking at #12, the impact of fouling is also present, however not as markedly as for #10. Figure 59 demonstrates a significant reduction in peak flow rate, but almost no change in pressure ratio. Further, a slight decrease in pressure ratio reduction rate is observed for the fouled cases. This is attributed to the initially lower pressure ratio and lower flow rate. This is highlighted in Figure 78, Figure 79 and Figure 80 in the appendix.

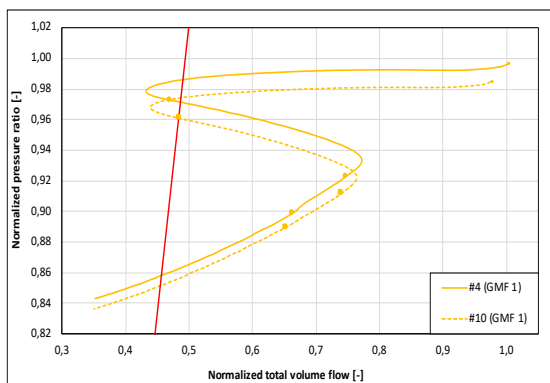


Figure 58: Trip trajectory for GMF 1, fouled versus non-fouled.

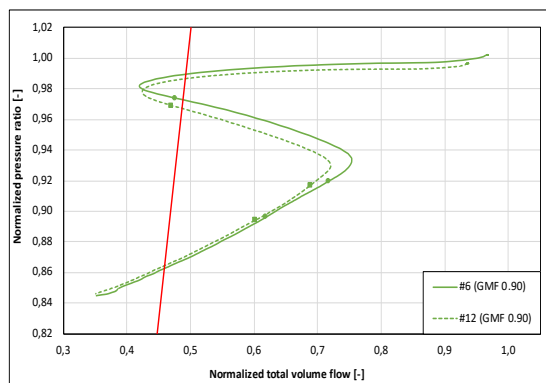


Figure 59: Trip trajectory for GMF 0.90, fouled versus non-fouled.

Table 10 summarizes the changes in stability performance from base case to the fouled case. The most interesting result is a markedly reduction in time in surge. This is linked with a higher minimum flow during valve ramp down for all three GMF's. Regarding time to surge the findings are not consistent over all the GMF's. However, the fouling impact demonstrated in the performance part of the campaign was an increase in PRTS which was observed only for the wet gas cases. This coincides with the results in Table 10 which shows an increase in TTS for GMF 0.97 and 0.90.

Variable	#10 (GMF 1)	#11 (GMF 0.97)	#12 (GMF 0.90)
Time to surge	-1.6%	+3.2%	+1.6%
Pr	+0.1%	+0.1%	+0.4%
Minimum flow	+4.5%	+4.7%	+5.7%
Time in surge	-14.5%	-12.3%	-14.5%
Maximum flow	+2.3%	-0.2%	-0.5%

Table 10: Change in stability performance from base case to fouled (*).

This indicates that the TTS is increasing for a fouled compressor in wet gas conditions. Although, the largest PRTS was observed in GMF 0.90 and the largest increase in TTS was observed for GMF 0.97. This suggests that the interaction is more complex and must be investigated further before drawing strict conclusions.

6.3 Driver Trip - Replicated Fouling

6.3.1 Test Objective

The objective of this test is to investigate if fouling behaviour can be replicated in trip tests. This includes establishing trip trajectories while using the performance tuning method established in Section 5.3. Further, compare the results with the findings from the fouled compressor.

In the performance section of the experimental campaign the method for tuning the compressor performance characteristics was established and validated. The specific changes in IGV-angle, rotational speed and valve opening needed to achieve the desired operating point for each GMF was found. This is the basis for the test matrix seen in Table 11. The test procedure is given below.

Test number	#13	#14	#15	#16	#17	#18
Compressor speed [rpm]	8800	9000	9000	8800	9000	9000
GMF	1.00	0.97	0.90	1.00	0.97	0.90
VIGV position	5°	10°	10°	5°	10°	10°
Valve start position [%]	54	54	54	54	54	54
Valve end position [%]	54	54	54	30	30	30
Ramp time [s]	N/A	N/A	N/A	3	3	3
Hold time [s]	N/A	N/A	N/A	1	1	1

Table 11: Test matrix, driver trip with replicated fouling.

1. Perform start-up procedure
2. Adjust discharge throttle valve to 54% (BEP)
3. Set the specified rotational speed
4. Adjust the variable inlet guide vanes to obtain specified angle
5. Adjust the water injection valve to obtain specified GMF
6. Run until rotational speed, flow rate, suction pressure and discharge pressure are stable
7. Start logging
8. Trip the compressor manually and initiate valve sequence simultaneously
9. Run until the rotational speed reaches 3000 rpm
10. Stop logging
11. Close the water injection valve
12. Restart the compressor
13. Repeat steps 3-12 until all tests are done according to the test matrix

6.3.2 Results and Discussion

Figure 60 shows the replicated fouling impact on the trip trajectory. Here, the wet gas impact is even more prominent than the fouled case. The reduction in volume flow rate for the wet gas cases is attributed to the formation of a liquid film on the airfoils of the IGV, reducing the effective inlet flow area.

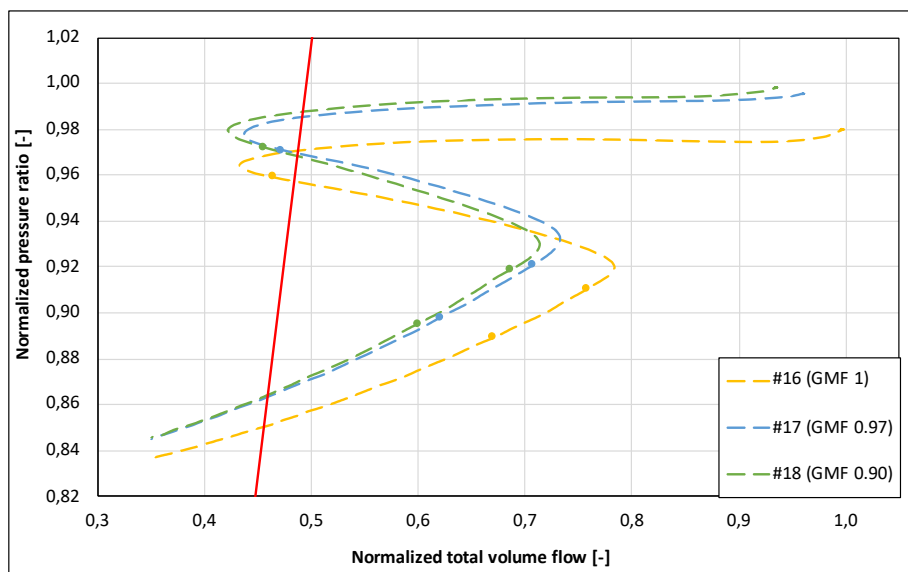


Figure 60: Trip trajectory, replicated fouling.

The results show similar trip trajectories as for the fouled cases. However, the degree of compliance varies for the different GMF's. The best fit is achieved for GMF 0.90, seen in Figure 62, where a close to perfect fit is observed. The dry gas case shows the lowest degree of compliance. This is seen from start where the curve is shifted towards lower pressure ratio and higher flow rate. In this case, better fit can probably be achieved by reducing the opening of the discharge throttle valve. This will reduce the total volume flow and increase the pressure ratio.

Along the trip trajectory the behaviour is almost inseparable. This can be seen in Figure 75, Figure 76 and Figure 77 in Appendix A.

In conclusion, these results demonstrate that the suggested method for tuning the performance characteristic is suitable to replicate the trip trajectory of a fouled compressor. However, deviation in some of the cases suggests that test parameters could have been finely tuned to achieve a better fit. Therefore, it is suggested to further investigate the impact each of the control techniques has on the compressor performance.

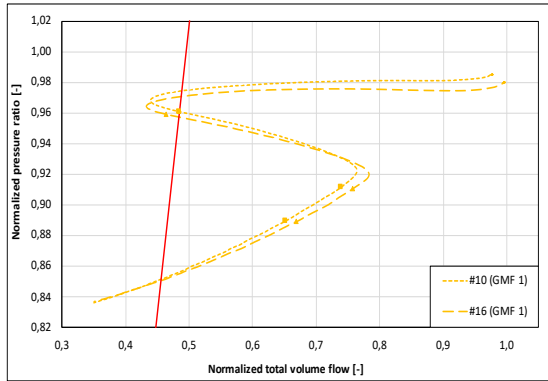


Figure 61: Trip trajectory for GMF 1, fouling versus replicated fouling.

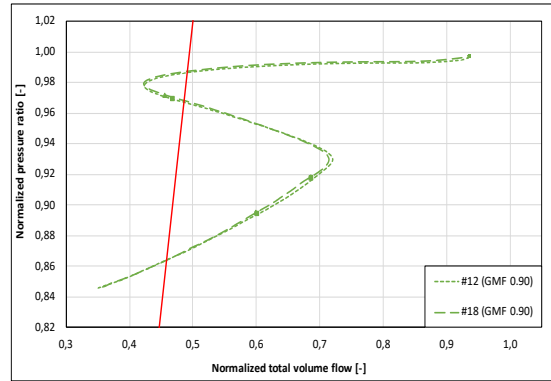


Figure 62: Trip trajectory for GMF 0.90, fouling versus replicated fouling.

The compressor stability performance was also calculated and compared to the fouled case. This can be seen in Table 12. Here, the only consistent change is an increase in TTS. Further analysis of this data is not performed but left attached for illustrative purposes.

Variable	#16 (GMF 1)	#17 (GMF 0.97)	#18 (GMF 0.90)
Time to surge	+0.8%	+1.5%	+6.4%
Pr	+0.3%	+0.1%	-0.1%
Minimum flow	-3.5%	+0.6%	-0.1%
Time in surge	+20%	-3.1%	-1.5%
Maximum flow	-0.2%	-1.7%	-0.8%

Table 12: Change in stability performance going from fouling to replicated fouling.

6.4 Uncertainty and Sources of Error

Note that the results and considerations done in this chapter are only valid for diffuser fouling and might not be applicable for fouling in other parts of the compressor.

This part of the experimental campaign involves many steps of human interaction in both test execution and computing. Some of these steps can be seen in the test procedures in Appendix B. An example of this is initiating driver trip and valve sequencing simultaneously. Also, adjusting water injection rates precisely for each case is a challenge when the process is to be repeated many times.

Further, there are always large uncertainties related to research that has never been done before. This applies for most of this experimental campaign. All results and conclusions should be taken with care, even though great efforts have been put into reducing the uncertainties. One of the implemented measures is to perform all tests twice.

Due to limitations in the test facility, the water injection valve is held constant after trip initiation. The consequence is that the GMF decreases during rundown. The change in GMF during the test can be seen in Figure 63. This GMF is calculated from air and water entering the inlet pipe. Some water accumulation in front of the compressor is observed during trip, hence the actual GMF entering the compressor is slightly higher than displayed in the figure.

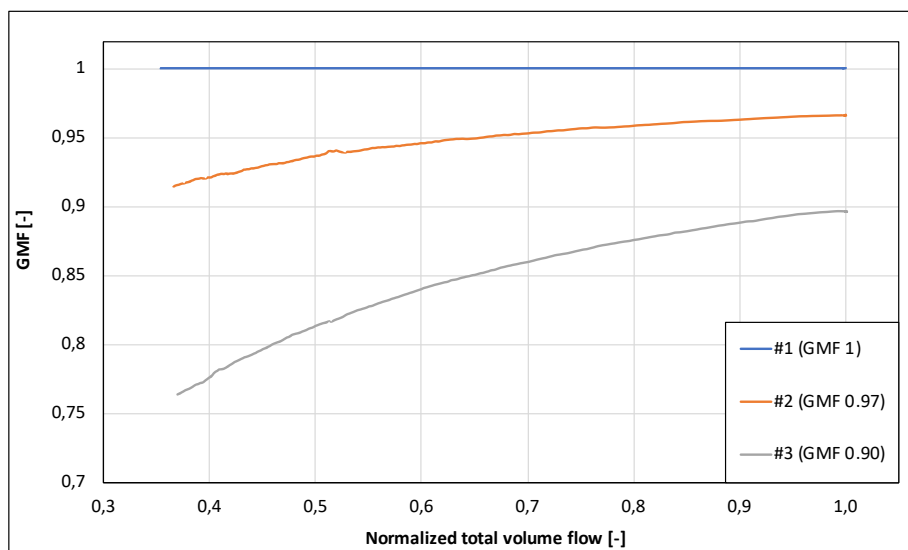


Figure 63: Change in GMF during trip test, starting at three different GMF's.

6.5 Summary

In this chapter, driver trip tests were done in three different scenarios and for three different liquid contents. The last scenario included a method for imitating the performance characteristics of a fouled compressor. This method was proven satisfactory, but with potential for improvement.

Going from dry to wet leads to:

- Increased impeller speed decay rate
- Increased pressure ratio decay rate
- Increased volume flow decay rate
- Reduced time to surge

There are two main mechanisms found to be responsible for these differences. The first is the higher mass flow of the wet gas flow increasing the impeller speed decay rate. The second is the initially higher pressure ratio of the wet gas cases.

Going from non-fouled to fouled leads to:

- Wet gas effects are more prominent
- Onset of wet gas effects has migrated towards lower GMF
- Increased minimum flow rate and reduced in time in surge
- Increased time to surge for the wet gas cases

The changes in wet gas effects is thought to be due to a formation of liquid film smoothing out the roughness of the fouling. Further, the improved stability is attributed to an increase in PRTS and a higher minimum flow rate.

7 Conclusion

In the first part of the experimental campaign compressor performance characteristics were established for three different cases. Non-fouled, fouled and a case where fouling was imitated by tuning the performance characteristics using three different control techniques. These techniques are variable inlet guide vanes, variable speed drive and discharge throttle valve. The method allows for testing challenges related to fouling without degrading the machine. In conclusion, the potential of the method is revealed and satisfactory compliance with a fouled compressor was demonstrated. However, better compliance with the fouled compressor could be achieved by tweaking the method.

In the driver trip tests a suggested method for tuning the trip trajectory utilizing the discharge throttle valve was validated. The results demonstrated a change in shape of the trip trajectory from affinity-like to the shape observed in large-volume, high-pressure systems. Using this method, trip trajectories were established for the same three cases as in the performance part. From this, the wet gas impact on the trip trajectory was investigated. The general trend when introducing liquid is a faster reduction in impeller speed decay, total volume flow rate and pressure ratio. Regarding compressor stability a reduced time to surge is observed, attributed to an increased PRTS found in the performance part of the experimental campaign.

Further, the fouling impact on the trip trajectory was documented. From start, a reduction in volume flow rate and pressure ratio is found. In contrast to the base case, the onset of wet gas effects has migrated towards lower GMF. The impeller speed decay is unaffected by the fouling and so is the volume flow reduction rate. Regarding compressor stability an improvement in several of the performance indicators is done. From the performance part, a markedly increase in PRTS was observed for the wet gas cases. The same cases showed an increase in TTS after driver trip. Further, all GMF's demonstrated a reduction in TIS, which is attributed to a higher minimum flow rate.

8 Further Work

During this project, challenges and potential improvements been exposed. Due to limitations in time and scope of work, some of these are left for future work. The aim is to further widen the understanding of important concepts regarding wet gas compression.

Implement logging of the compressor driver trip event time in the NTNU Test Facility. At this time, the trip event time is found from the impeller speed decay. The transient behaviour related to the compressor driver trip are very fast developing phenomena. The compressor can go from normal operation to surge in just fractions of a second. When studying this, an exact event time is important to determine what changes that owes to the driver trip.

Investigate the implications of keeping the GMF constant during rundown. The current lab setup utilizes manual regulation of the GMF during tests. This means that the water injection rate is adjusted to achieve the desired GMF at the start of the test. When the compressor trips the flow rate of air sucked into the compressor will be reduced, while the water injection rate remains constant. This means that the GMF is decreased during the test. It would be of interest to see if this has a significant effect on the results. To achieve this, some kind of regulation for the water injection needs to be installed.

Investigate further and document the impact of each of the three control methods suggested for replicating of fouling characteristics. This is suggested to better understand the impact of each of them and achieve better compliance with the fouled characteristics.

Study the implications of initiating compressor driver trip at different operating points. Due to the limited scope of this project, all trip tests were done from the same operating point. When the operating point before trip initiation is moved a change in the stability performance is expected. Of specific interest is the impact of operation closer to surge, which is expected to reduce stability performance.

Investigate the impact of decreased performance steepness on the compressor performance and trip trajectory. Further, evaluate the stability performance and the related TTS and TIS. Similarly, as fouling is known to increase the performance steepness, leakages can reduce the performance steepness. Investigating this is of relevance for the industry, where findings can be implemented in a digital model to be able to reveal the development of leakages.

Bibliography

- [1] Leffler, W. L., Pattarozzi, R., & Sterling, G. 2011. *Deepwater Petroleum Exploration & Production: A Nontechnical Guide*. PennWell Books.
- [2] Equinor. 2019. Equinor website. Accessed: 2019-10-01. URL: <https://www.equinor.com/en/magazine/the-final-frontier.html>.
- [3] Bjørge, T. September 2019. Subsea Compression Wet Gas Compression Theory and System Considerations.
- [4] Equinor. 2015. Equinor website. Accessed: 2019-08-26. URL: <https://www.equinor.com/en/where-we-are/norway/asgard-subsea-gas-compression.html>.
- [5] Equinor. 2015. Equinor website. Accessed: 2019-08-26. URL: <https://www.equinor.com/en/news/2015/07/03/article.html>.
- [6] Boyce, M. June 2006. *Gas Turbine Engineering Handbook*. 3rd. Elsevier Science.
- [7] Ellingsgård Johansen, K. E. Subsea Compressor Operation. Project report, NTNU, 2019.
- [8] Dixon, S. & Hall, C. 01 2010. *Fluid Mechanics and Thermodynamics of Turbomachinery*. Elsevier. URL: <https://doi.org/10.1016/C2009-0-20205-4>.
- [9] Schultz, J. M. 01 1962. The Polytropic Analysis of Centrifugal Compressors. *Journal of Engineering for Gas Turbines and Power*, 84(1), 69–82. URL: <https://doi.org/10.1115/1.3673381>.
- [10] Hundseid, Ø., Bakken, L. E., & Helde, T. 05 2006. A Revised Compressor Polytropic Performance Analysis. In *Turbo Expo: Power for Land, Sea, and Air*, Volume 5: Marine; Microturbines and Small Turbomachinery; Oil and Gas Applications; Structures and Dynamics, Parts A and B, 617–624. URL: <https://doi.org/10.1115/GT2006-91033>.
- [11] Mæland, D. & Bakken, L. E. 06 2017. Wet Gas Compression: Test Conditions and Similitude. In *Turbo Expo: Power for Land, Sea, and Air*, Volume 9: Oil and Gas Applications; Supercritical CO2 Power Cycles; Wind Energy. URL: <https://doi.org/10.1115/GT2017-64374>.
- [12] Hundseid, Ø., Bakken, L. E., Grüner, T. G., Brenne, L., & Bjørge, T. 08 2009. Wet Gas Performance of a Single Stage Centrifugal Compressor. In *Turbo Expo: Power for Land, Sea, and Air*, Volume 7: Education; Industrial and Cogeneration; Marine; Oil and Gas Applications, 661–670. URL: <https://doi.org/10.1115/GT2008-51156>.

-
- [13] Forsthoffer, W. B. 2005. *Forsthoffer's Rotating Equipment Handbooks*. Elsevier Science. URL: <https://doi.org/10.1016/B978-185617472-5/50057-5>.
- [14] Tveit, G. B., Bakken, L. E., & Bjørge, T. 06 2004. Compressor Transient Behaviour. In *Turbo Expo: Power for Land, Sea, and Air*, Volume 7: Turbo Expo 2004, 813–821. URL: <https://doi.org/10.1115/GT2004-53700>.
- [15] Vigdal, L. A. B. *An Experimental Study of Wet Gas Compressor with IGV Control*. PhD thesis, NTNU, 2018.
- [16] Leufvén, O., Eriksson, L., & Systems, V. 07 2008. Time to surge concept and surge control for acceleration performance. *Proceedings of the 17th World Congress The International Federation of Automatic Control Seoul, Korea*. URL: <https://doi.org/10.3182/20080706-5-KR-1001.00350>.
- [17] Tveit, G. B., Bakken, L. E., & Bjørge, T. 03 2005. Compressor Performance Impact on Rundown Characteristics. In *European Conference on Turbomachinery - Fluid Dynamics and Thermodynamics*.
- [18] Bakken, M. & Bjørge, T. 12 2017. Volute Flow Influence on Wet Gas Compressor Performance. In *Gas Turbine India Conference*, Volume 1: Compressors, Fans and Pumps; Turbines; Heat Transfer; Combustion, Fuels and Emissions. URL: <https://doi.org/10.1115/GTINDIA2017-4529>.
- [19] Bakken, M. & Bjørge, T. 06 2017. An Experimental Investigation on the Impact of Inlet Slugging on Wet Gas Compressor Performance. In *Turbo Expo: Power for Land, Sea, and Air*, Volume 9: Oil and Gas Applications; Supercritical CO2 Power Cycles; Wind Energy. URL: <https://doi.org/10.1115/GT2017-65094>.
- [20] Bertoneri, M., Duni, S., Ransom, D., Podestà, L., Camatti, M., Bigi, M., & Wilcox, M. 06 2012. Measured Performance of Two-Stage Centrifugal Compressor Under Wet Gas Conditions. In *Turbo Expo: Power for Land, Sea, and Air*, Volume 6: Oil and Gas Applications; Concentrating Solar Power Plants; Steam Turbines; Wind Energy, 173–180. URL: <https://doi.org/10.1115/GT2012-69819>.
- [21] Bakken, M., Bjørge, T., & Bakken, L. E. 11 2018. Wet gas compressor operation and performance. In *ASME International Mechanical Engineering Congress and Exposition*, Volume 6A: Energy. URL: <https://doi.org/10.1115/IMECE2018-86562>.
- [22] Brenne, L., Bjørge, T., Gilarranz, J. L., Koch, J., & Miller, H. R. 2005. Performance evaluation of a centrifugal compressor operating under wet gas conditions. In *Proceedings of the 34th Turbomachinery Symposium*. URL: <https://doi.org/10.21423/R1V35Z>.

-
- [23] Fabbrizzi, M., Cerretelli, C., Del Medico, F., & D’Orazio, M. 06 2009. An Experimental Investigation of a Single Stage Wet Gas Centrifugal Compressor. In *Turbo Expo: Power for Land, Sea, and Air*, Volume 5: Microturbines and Small Turbomachinery; Oil and Gas Applications, 443–453. URL: <https://doi.org/10.1115/GT2009-59548>.
- [24] Ferrara, V., Bakken, L. E., Falomi, S., Sassanelli, G., Bertoneri, M., & Scotti del Greco, A. 06 2016. Wet Compression: Performance Test of a 3D Impeller and Validation of Predictive Model. In *Turbo Expo: Power for Land, Sea, and Air*, Volume 9: Oil and Gas Applications; Supercritical CO2 Power Cycles; Wind Energy. URL: <https://doi.org/10.1115/GT2016-57976>.
- [25] Bakken, L. E., Lunde, E., & Løes, M. 06 2016. Power Dip Impact on Compressor System Stability. In *Turbo Expo: Power for Land, Sea, and Air*, Volume 9: Oil and Gas Applications; Supercritical CO2 Power Cycles; Wind Energy. URL: <https://doi.org/10.1115/GT2016-56950>.
- [26] Tveit, G. B., Bjørge, T., & Bakken, L. E. 06 2005. Impact of Compressor Protection System on Rundown Characteristics. In *Turbo Expo: Power for Land, Sea, and Air*, Volume 4: Turbo Expo 2005, 317–325. URL: <https://doi.org/10.1115/GT2005-68436>.
- [27] Schjølberg, I., Hyllseth, M., Skofteland, G., & Nordhus, H. 06 2008. Dynamic Analysis of Compressor Trips in the Snøhvit LNG Refrigerant Circuits. In *Turbo Expo: Power for Land, Sea, and Air*, Volume 7: Education; Industrial and Cogeneration; Marine; Oil and Gas Applications, 679–688. URL: <https://doi.org/10.1115/GT2008-51235>.
- [28] Paulsen Haugen, M. & Paulsen, K. Fouling Impact on Compressor Performance. Master’s thesis, NTNU, 2019.
- [29] Bakken, M., Bjørge, T., & Bakken, L. E. 06 2019. Wet Gas Compressor Model Validation. In *Turbo Expo: Power for Land, Sea, and Air*, Volume 9: Oil and Gas Applications; Supercritical CO2 Power Cycles; Wind Energy. V009T27A016. URL: <https://doi.org/10.1115/GT2019-90354>.
- [30] Navarsete, T. Transient Compressor System Analysis. Master’s thesis, NTNU, 2019.
- [31] Hundseid, Ø. & Bakken, L. E. 06 2015. Integrated Wet Gas Compressor Test Facility. In *Turbo Expo: Power for Land, Sea, and Air*, Volume 9: Oil and Gas Applications; Supercritical CO2 Power Cycles; Wind Energy. URL: <https://doi.org/10.1115/GT2015-43004>.
- [32] Grüner, T. G. & Bakken, L. E. 06 2010. Wet Gas Impeller Test Facility. In *Turbo Expo: Power for Land, Sea, and Air*, Volume 5: Industrial and Cogeneration; Microturbines and Small Turbomachinery; Oil and Gas Applications; Wind Turbine Technology, 705–712. URL: <https://doi.org/10.1115/GT2010-22618>.

-
- [33] Vigdal, L. B. & Bakken, L. E. 06 2015. Inlet Guide Vane Performance at Dry and Wet Gas Conditions. In *Turbo Expo: Power for Land, Sea, and Air*, Volume 9: Oil and Gas Applications; Supercritical CO2 Power Cycles; Wind Energy. URL: <https://doi.org/10.1115/GT2015-43225>.

Appendix A: Additional Results

Delay Phenomenon

In former studies, done in the NTNU Test Facility, a strange phenomenon has been observed. When the compressor driver is tripped, the measured response in pressure is instantaneous. However, this is not the case for the flow rate which is unchanged for some time after the trip. In Figure 64 this is seen as a vertical section at the start of the trajectory.

Test Objective

The objective of this test is to investigate the delay phenomenon observed during compressor driver trips in the NTNU Test Facility. This was suggested as further work by Navarsete [30], where a delay of approximately 0,5 seconds were observed without finding the reason. A trip trajectory where the delay is visible is plotted in Figure 64. Two main hypotheses of the cause are proposed. Since

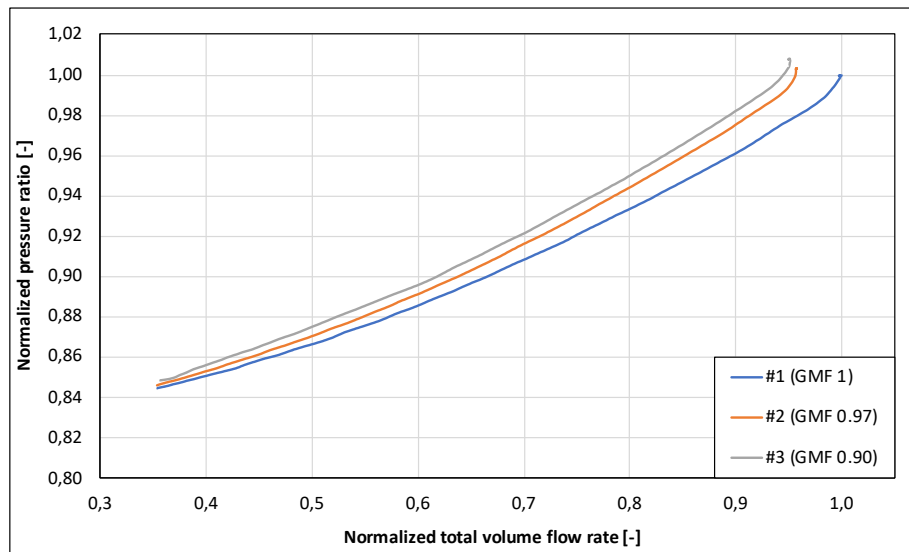


Figure 64: Trip trajectory with delay.

the flow orifice is located approximately 25 meters upstream of the compressor one hypothesis is related to the travelling time of the pressure wave and mass inertia. The pressure wave travels with the speed of sound and calculations indicate that this alone can not induce such a large delay.

The other hypothesis, which is regarded as most probable, is instrument delay. It was decided to test this first, before other hypotheses was investigated. The test consist of establishing direct connection to the sensor where delay is measured and two reference sensors using tubing. Two sensors at different locations in the system are chosen for reference. These are placed at the compressor inlet and in the middle of the loop. Further, the open ends of the tubing is connected and a number of pressure pulses is sent into the three tubes simultaneously using an air compressor. To ensure that the pressure pulses reach the three sensors simultaneously tubing of same type, diameter and length were used. If the delay is still present, this implies that the delay is due to the instrument itself. The test is done twice to ensure consistency. The detailed test procedure can be seen below.

1. Establish direct connection to all three sensors using identical air tubes
2. Connect the end of the three tubes with a 4-way fitting
3. Start logging
4. Use an air compressor to provide a number of pressure pulses with a few seconds in between
5. Stop logging

Results and Discussion

The results from the test can be seen in Figure 65 and Figure 66.

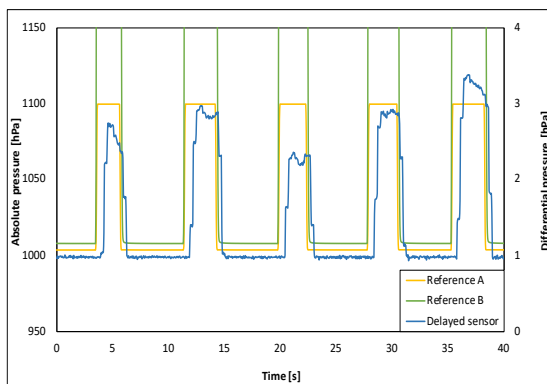


Figure 65: Response from pressure pulses.

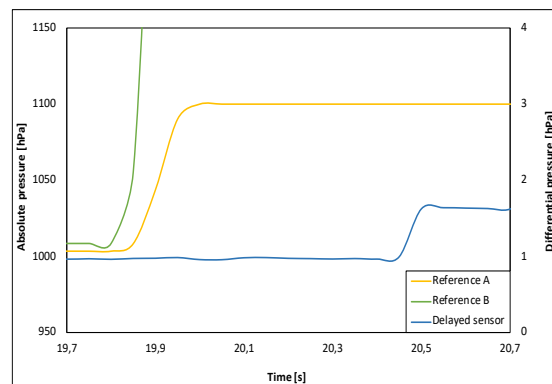


Figure 66: Response from pressure pulses, zoomed in.

Here, a consistent pressure pulse response is observed. No significant time delay between the pressure sensor from the compressor inlet and the reference sensors is observed. However, the PDT-sensor at the orifice plate shows a time delay of 0,5 - 0,6 seconds. The three sensors have different measuring ranges which causes different height of the recorded pulses.

Since the delay is present also in this test, the conclusion is that it is caused by the instrument itself and not a physical phenomena in the fluid flow. Following from this conclusion, all results in this experimental campaign is compensated for this delay. This is achieved by offsetting the flow measurement with -0.5 seconds. The result of this offset can be seen by looking at Figure 64 and Figure 67 which is the same data respectively before and after correcting for delay.

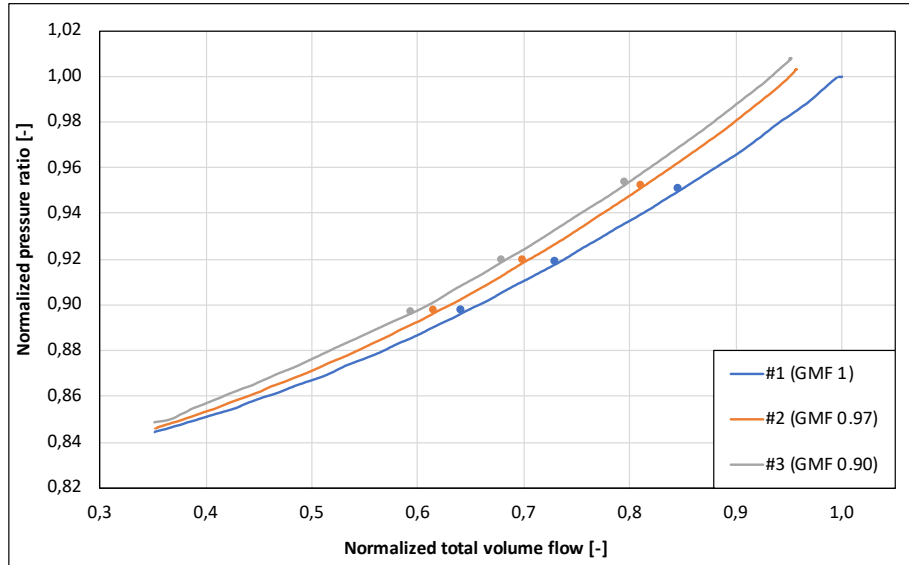


Figure 67: Trip trajectory after correcting for delay.

Performance - Fouling

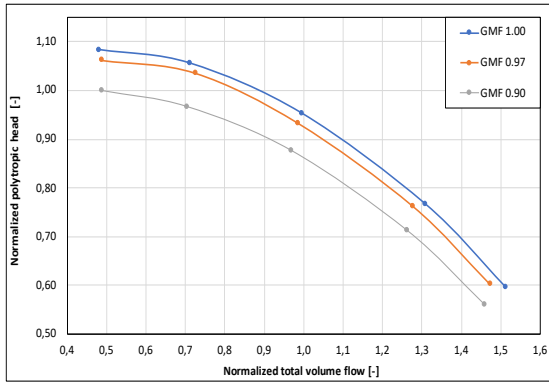


Figure 68: Normalized polytropic head versus normalized total volume flow, fouled.

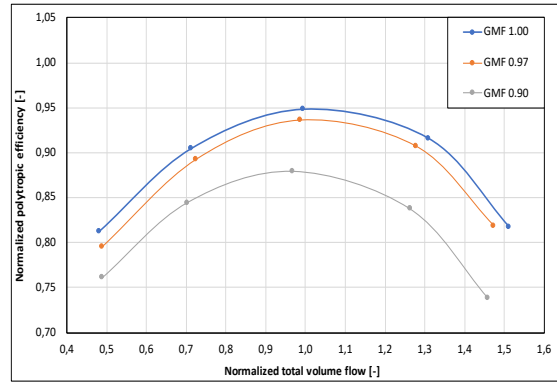


Figure 69: Normalized polytropic efficiency versus normalized total volume flow, fouled.

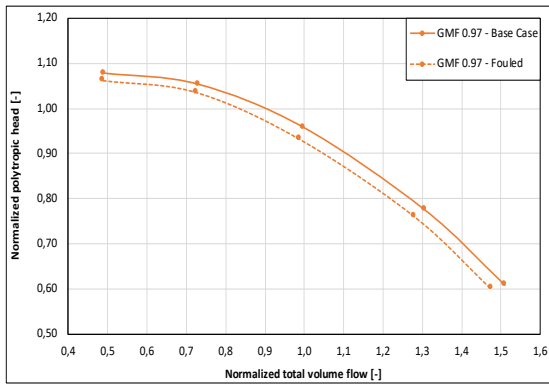


Figure 70: Normalized polytropic efficiency versus normalized total volume flow, base case versus fouled GMF 0.97.

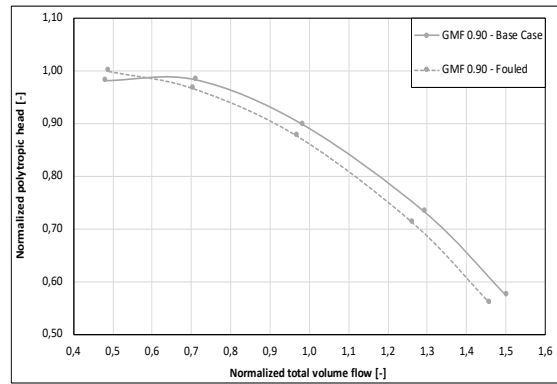


Figure 71: Normalized polytropic efficiency versus normalized total volume flow, base case versus fouled GMF 0.90.

Trip Trajectories

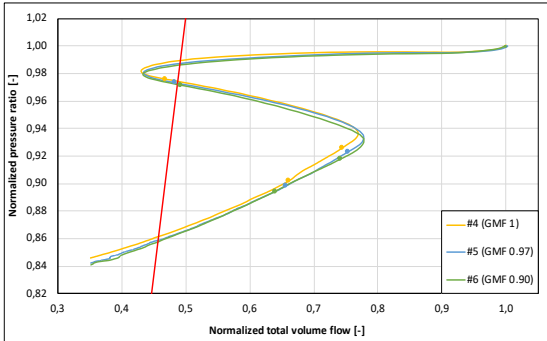


Figure 72: Trip trajectory for all GMF's, base case (*).

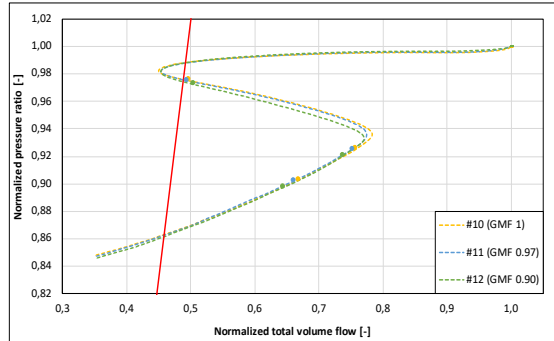


Figure 73: Trip trajectory for all GMF's, fouled (*).

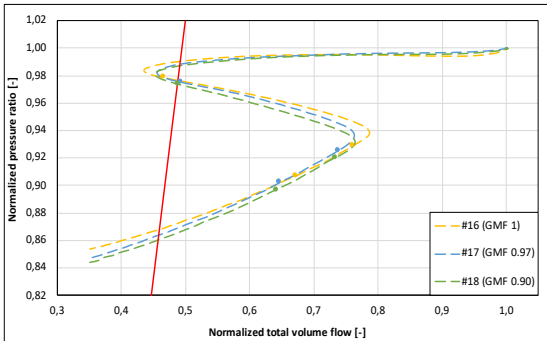


Figure 74: Trip trajectory for all GMF's, replicated fouling (*).

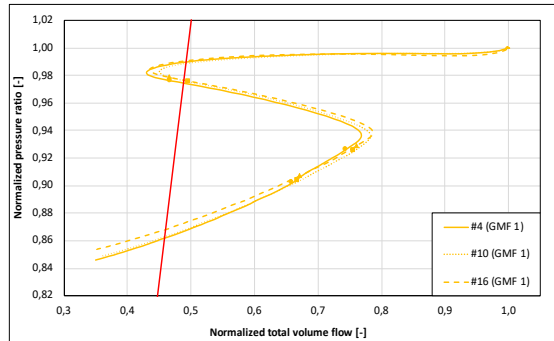


Figure 75: Trip trajectory for all scenarios, GMF 1 (*).

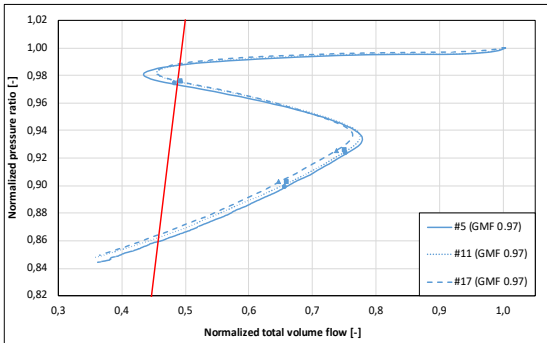


Figure 76: Trip trajectory for all scenarios, GMF 0.97 (*).

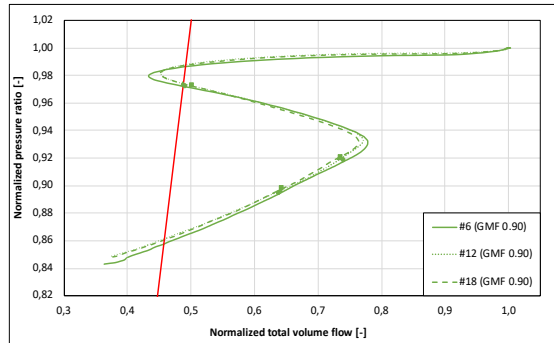


Figure 77: Trip trajectory for all scenarios, GMF 0.90 (*).

Pressure Ratio and Volume Flow

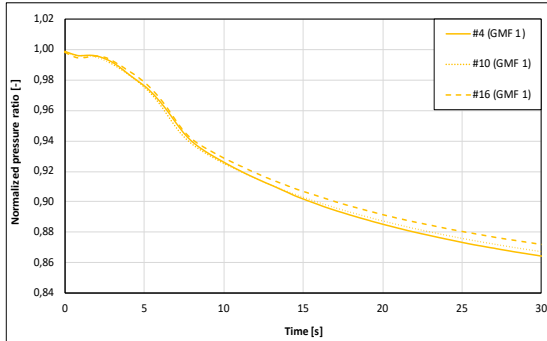


Figure 78: Pressure ratio versus time, GMF 1 (*).

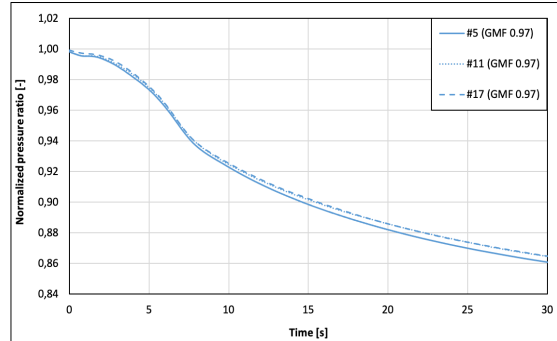


Figure 79: Pressure ratio versus time, GMF 0.97 (*).

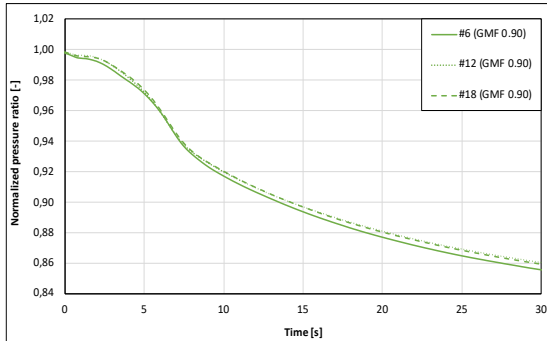


Figure 80: Pressure ratio versus time, GMF 0.90 (*).

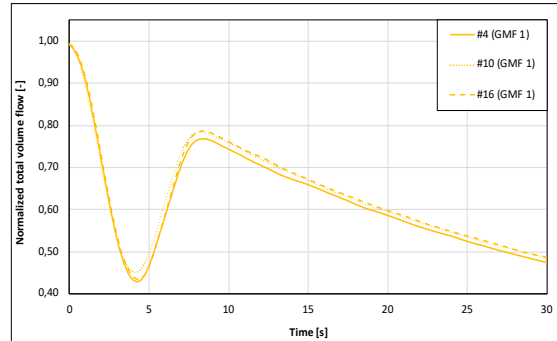


Figure 81: Total volume flow versus time, GMF 1 (*).

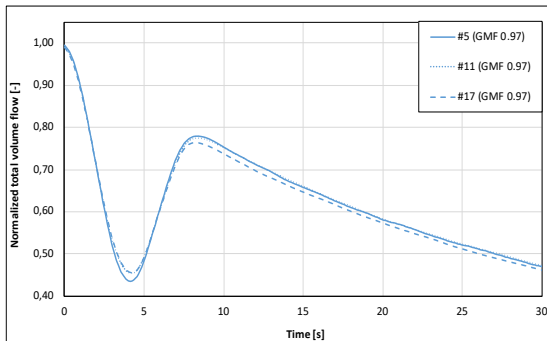


Figure 82: Total volume flow versus time, GMF 0.97 (*).

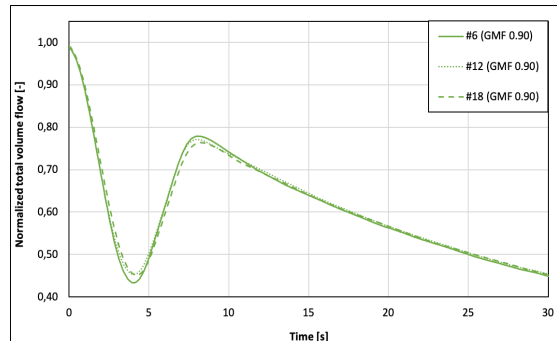


Figure 83: Total volume flow versus time, GMF 0.90 (*).

Consistency in Trip Tests

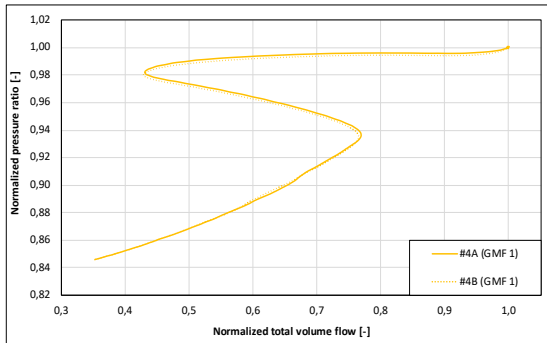


Figure 84: Consistency in test scenario #4 (*).

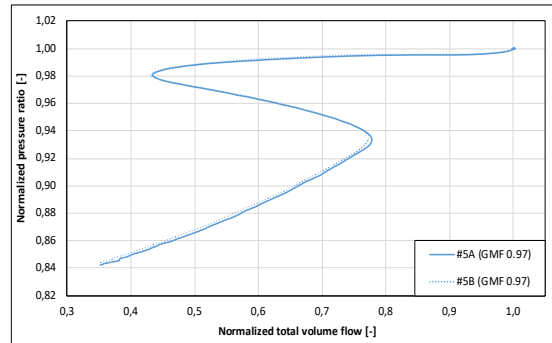


Figure 85: Consistency in test scenario #5 (*).

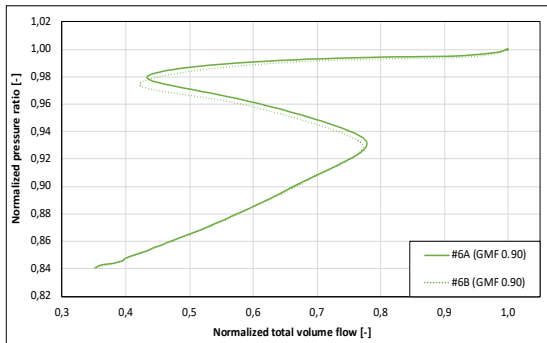


Figure 86: Consistency in test scenario #6 (*).

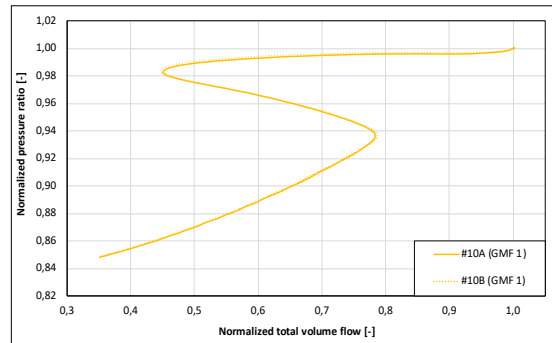


Figure 87: Consistency in test scenario #10 (*).

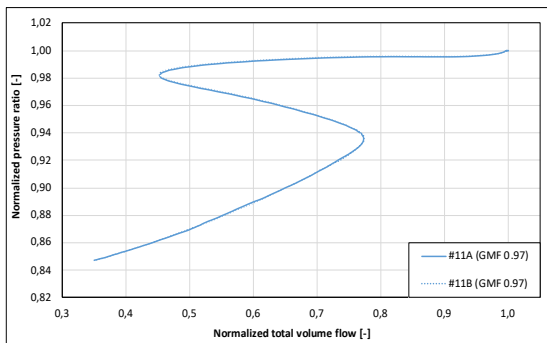


Figure 88: Consistency in test scenario #11 (*).

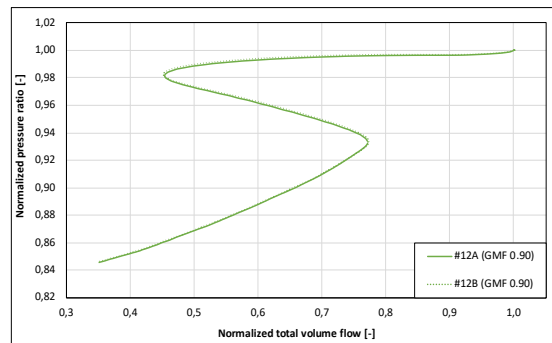


Figure 89: Consistency in test scenario #12 (*).

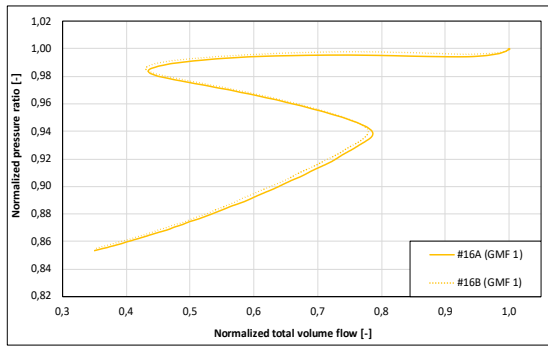


Figure 90: Consistency in test scenario #16 (*).

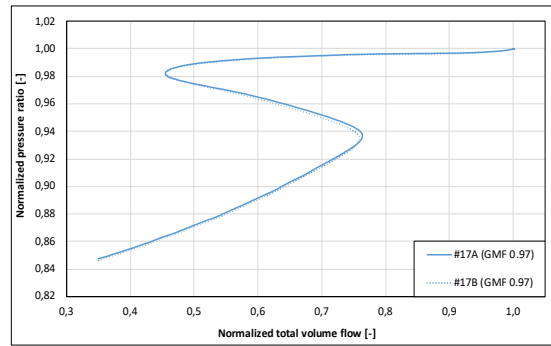


Figure 91: Consistency in test scenario #17 (*).

Appendix B: Test Procedures

Preparations

Still Test

Before starting the compressor a still test is performed. This is a logging with all equipment running except the compressor. This is done to validate the consistency and correctness of the instrumentation. Since the machine is not running, the readings of pressure and temperature should be approximately ambient. An example of this is checking that the 4 pressure sensors at the inlet and outlet of the compressor shows equal readings. This allows us to reveal any potential problems with the instruments before the test.

Reference Point

Before the actual test is started a reference point is tested. This is to check for compliance with earlier tests to ensure that they are comparable. This is done by running a specific operating point until pressure and temperatures are stable. Before proceeding with the planned tests, performance calculations are performed for validation.

Start-up Procedure

1. Start engine lubrication and the electric drive
2. Perform «still test»
3. Start the compressor at 2000 rpm with the discharge valve fully open
4. Accelerate to wanted rotational speed in steps. Check instrumentation and vital values for each step.

Compressor Performance

Base Case and Fouled

For the dry gas performance tests the order is from small valve opening to large valve opening. This is because the discharge temperature is at its highest in the low flow rate cases. By starting at this end, stability for the later points will be achieved faster.

1. Perform start-up procedure
2. Start logging
3. Adjust discharge throttle valve to obtain wanted operating point
4. Open water injection valve and adjust water valve to obtain wanted GMF
5. Run for minimum 5 minutes for wet gas or 30 minutes for dry gas
6. Stop logging
7. Close water injection valve
8. Repeat steps 2-6 until five operating points is recorded according to the test matrix
9. Repeat steps 2-7 for all GMF's according to the test matrix

Replicated Fouling

1. Perform start-up procedure
2. Start logging
3. Adjust the variable inlet guide vanes to obtain wanted angle
4. Open water injection valve and adjust water valve to obtain wanted GMF
5. Set discharge throttle valve to go from 100% to 30% in 10 minutes
6. Continuously adjust water injection valve to maintain the wanted GMF
7. Close water injection valve
8. Stop logging

Driver Trip

Base Case and Fouled

1. Perform start-up procedure
2. Adjust discharge throttle valve to 54% (BEP)
3. Adjust the water injection valve to obtain specified GMF
4. Run until rotational speed, flow rate, suction pressure and discharge pressure are stable
5. Start logging
6. Trip the compressor manually. For the tests including tuning of rundown trajectory, the valve sequence is initiated simultaneously with the driver trip
7. Run until the rotational speed reaches 3000 rpm
8. Stop logging
9. Close the water injection valve
10. Restart the compressor
11. Repeat steps 3-10 until all tests are done according to the test matrix

Replicated Fouling

1. Perform start-up procedure
2. Adjust discharge throttle valve to 54% (BEP)
3. Set the specified rotational speed
4. Adjust the variable inlet guide vanes to obtain specified angle
5. Adjust the water injection valve to obtain specified GMF
6. Run until rotational speed, flow rate, suction pressure and discharge pressure are stable
7. Start logging
8. Trip the compressor manually. For the tests including tuning of rundown trajectory, the valve sequence is initiated simultaneously with the driver trip
9. Run until the rotational speed reaches 3000 rpm
10. Stop logging
11. Close the water injection valve
12. Restart the compressor
13. Repeat steps 3-12 until all tests are done according to the test matrix

Appendix C: Wet Gas Compressor Test Facility

Table 13: Main dimensions, NTNU Test Facility.

Dimension	Value	Unit
Impeller outlet diameter (D_2)	400	mm
Diffuser with (b)	20	mm
Diffuser ratio (D_3/D_2)	1.7	-
Inlet hub diameter	250	mm
Outlet pipe diameter	200	mm
Inlet hub diameter	250	mm
Drive, electric motor	450	kW

Table 14: Instrumentation accuracy, NTNU Test Facility.

Location	Instrument	Accuracy	Unit
Ambient air	Temperature	± 0.2	$^{\circ}\text{C}$
	Pressure	± 0.15	hPa
	Relative humidity	± 1	%
Compressor inlet	Pressure	± 0.3	%
	Temperature	± 0.005	$^{\circ}\text{C}$
Compressor outlet	Pressure	± 0.3	%
	Temperature	± 0.005	$^{\circ}\text{C}$
Diffusor	Dynamic pressure	± 0.14	mbar
	Static pressure	± 0.002	bar
	Total temperature	± 0.009	$^{\circ}\text{C}$
	Three hole probe	± 0.11	%
Flow element	Temperature	± 0.15	$^{\circ}\text{C}$
	Differential pressure	± 0.04	%
Shaft	Speed	± 5	%
	Torque	± 0.05	%
Water supply	Flow	± 0.5	%

Appendix D: Orifice Plate

The air flow into the NTNU test facility is measured using an orifice plate with corner tappings. A detailed description of mass flow calculations through this orifice is given below.

The mass flow through the orifice plate is given by:

$$\dot{m} = C\epsilon\rho A_1 \sqrt{\frac{2\Delta p}{\rho(1-\beta^4)}} \quad (1)$$

Where the orifice factor β is defined as the ratio of the smallest to the largest diameter of the orifice

$$\beta = \frac{d_1}{d_2} \quad (2)$$

The general formula for the discharge coefficient is:

$$C = 0.5961 + 0.0261\beta^2 - 0.216\beta^8 + 0.000521 \left(\frac{10^6\beta}{Re_D}\right)^{0.7} + (0.0188 + 0.0063A)\beta^{3.5} \left(\frac{10^6}{Re_D}\right)^{0.3} \\ + (0.043 + 0.080e^{-10L_1} - 0.123e^{-7L_1})(1 - 0.11A) \frac{\beta^4}{1 - \beta^4} - 0.031(M_2' - 0.8M_2'^{1.2})\beta^{1.3} \quad (3)$$

Where:

$$M_2' = \frac{2L_2'}{1 - \beta}$$

For an orifice plate with corner tappings:

$$L_1 = L_2' = 0$$

Then the discharge coefficient for an orifice plate with corner tappings is:

$$C = 0.5961 + 0.0261\beta^2 - 0.216\beta^8 + 0.000521 \left(\frac{10^6\beta}{Re_D}\right)^{0.7} + (0.0188 + 0.0063A)\beta^{3.5} \left(\frac{10^6}{Re_D}\right)^{0.3} \quad (4)$$

This factor is commonly simplified by excluding the terms that involves the Reynolds number. Including the terms requires an iterative procedure. This requires computer power and for large sets of data the cost might outweigh the reward. The simplifying leads to a calculated flow rate which is too low. As seen from the equation for C, the Reynolds number appears in the denominator. This implies that the deviation will increase with decreasing Reynolds number. In Figure 92 the deviation from excluding these terms is seen. The figure shows that when the Re-terms are included the flow rate is 1-1,7% higher than without. The expansion factor ϵ is defined as:

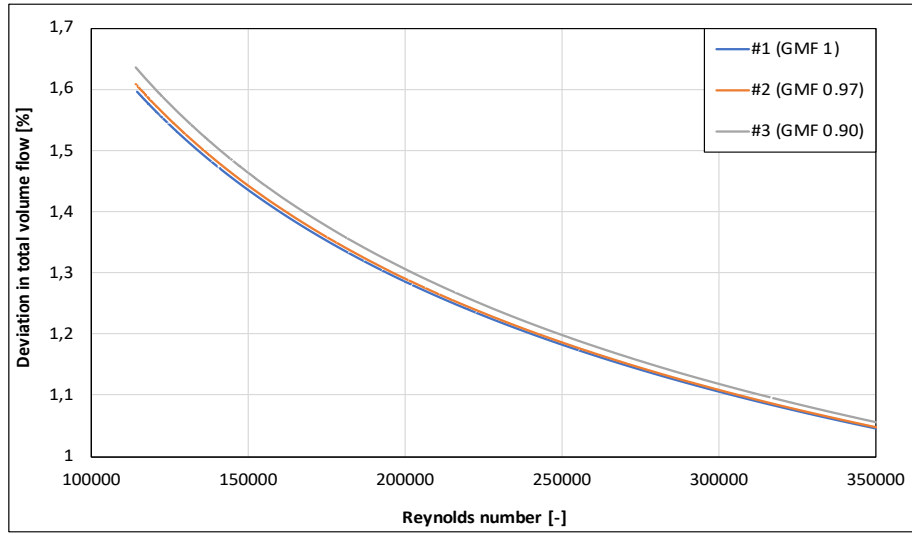


Figure 92: Effect of correcting the discharge coefficient for Reynolds' number.

$$\epsilon = 1 - \left(0.351 + 0.256\beta^4 + 0.93\beta^8 \right) \left(1 - \left(\frac{p_2}{p_1} \right)^{\frac{1}{\kappa}} \right) \quad (5)$$

Appendix E: Data Processing

When analyzing the polytropic performance of the compressor there are several ways to do the calculation based on what information is available. One option is to use both inlet and outlet temperatures. Another is to use inlet temperature and the compressor power. For dry gas tests the time for the system to achieve thermal equilibrium can be very long. Knowing this, it was decided to use the compressor power and inlet temperature to calculate the performance. Before start, it was validated that the two methods yielded the same result. From this validation it was found a deviation of less than 1% in polytropic head between the methods. The same method is used for wet gas cases but with different justification. The reason why the use of outlet temperature is avoided here is the previously mentioned challenging nature of temperature measurement in multiphase flows.

The data acquisition is done through the software Diadem by National Instruments. Diadem reads the log files from the experiments and permits data processing. In this project the pre-processing of the data is done here. This consists of checking the data for consistency, averaging values where there are more than one sensor and re-sampling data with different time scales. Some data also need smoothing to remove high frequency noise. The data collected from the acquisition system is:

- Ambient air pressure, temperature and relative humidity
- Differential pressure over the orifice plate
- Water injection volume flow and temperature
- Compressor inlet pressure and temperature
- Compressor outlet pressure and temperature
- Compressor torque and rotational speed

The sensor data acquired from Diadem is then put into the HYSYS-model for performance calculations by the Schultz' method. This model, its specifications and how it is used is described in detail in Appendix C. The output from the model is polytropic head and polytropic efficiency. Eventually, the data is collected in Excel for processing and visualization of results.

Appendix F: Simulation Model

At NTNU the simulation tool HYSYS by Aspen Tech is available. This is a process simulator which allows for both steady-state and dynamic simulations. This makes the tool applicable for many purposes. A wide variety of equations of state is available which in HYSYS are named fluid packages. These equations provide a representation of the thermodynamic relationship between pressure, specific volume and temperature. Picking the most suitable equation of state can be quite a considerable task in itself. The choice is normally done based on experience with the relevant components and operating conditions. Examples of fluid packages in frequent use are Peng-Robinson (PR) and Suave-Redlich-Kwong (SRK).

A steady-state simulation model of the NTNU Test Facility is made and validated against actual results from experiments done in the facility. SRK is the chosen fluid package. This is due to simulations with SRK have shown close compliance with results attained from wet gas compression of air/water mixtures in the NTNU test facility [28]. In the project leading up to this master's thesis the simulation model was tested with measured values from the lab. The aim was to check if the simulation results coincided with values attained in the lab. The results showed compliance with the results attained from the lab, with small deviations [7]. From this the model was concluded to be adequate for its purpose. The tool also enables the use of different methods for performance calculations. In this project the previously mentioned Schultz' method is used. The model is seen in Figure 93. The model starts with the «Dry Air» stream which only has one specification; the

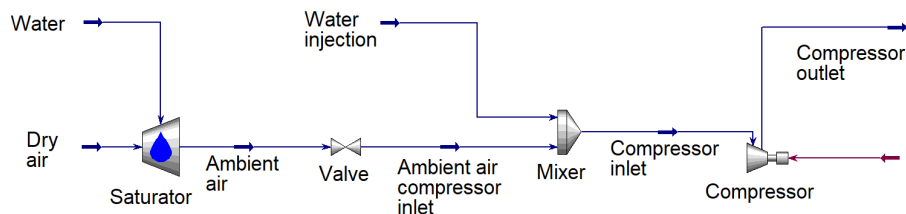


Figure 93: HYSYS simulation model.

composition. The stream enters a saturator. Here, water is injected to obtain the relative humidity measured in the room at the given temperature and pressure. This temperature and pressure is specified in the «Ambient air» stream. Also the mass flow of is specified here. This is the flow measured at the orifice plate. Now this stream is a full replica of the humid air entering the inlet duct of the compressor. Further, the stream pass through a valve. This valve has no specifications and its objective is to lower the pressure of the stream down to the suction pressure of the compressor. The

pressure difference over the valve will be solved automatically by specifying the compressor inlet pressure. Up until this point everything is equal for wet gas and dry gas scenarios.

Then the air stream «Ambient air compressor inlet» enters the mixer. This stream has no specifications and is fully determined by other streams. The «Water Injection» stream has its composition specified. Here the difference between dry gas and wet gas cases starts. The dry gas case uses the measured inlet temperature directly into "Compressor inlet". While the wet gas case uses the temperature of «Water Injection» and «Ambient air compressor inlet». From this, the mixer calculates the compressor inlet temperature assuming thermal equilibrium between the phases. This is done due to challenges measuring the temperature in wet gas as mentioned. Using these specifications the evaporative cooling effect of the injected water is accounted for. Further, the specifications are identical for wet and dry. None of the streams into the mixer has pressure specifications. This is solved by giving the compressor inlet pressure and using the automatic pressure alignment option «Equalize all» in the mixer. The last specifications are the compressor outlet pressure, compressor torque and rotational speed. The model is fully defined and solves. The compressor performance calculations are set to be done by the use of Schultz' method. The data collected from the model is polytropic head and polytropic efficiency. The model input specifications as described is given in Table 15.

Stream/equipment	Specification
Dry air	Composition
Water	Composition
Saturator	Relative humidity
Ambient air	Pressure Temperature
Valve	No specification
Ambient air compressor inlet	No specification
Water injection	Composition Mass flow rate Temperature (only for wet gas)
Mixer	Equalize all pressures
Compressor inlet	Pressure Temperature (only for dry gas)
Compressor	Torque Rotational speed
Compressor outlet	Pressure

Table 15: Simulation model specifications.

Appendix G: Schultz' Approach

Traditionally the thermodynamic design and test evaluation of centrifugal compressors is frequently based on polytropic analysis employing perfect-gas relations [9]. The assumption of perfect-gas may in many cases be inaccurate. To account for this John M. Schultz derived real-gas equations for polytropic analysis. The background of this work was to show it's application to centrifugal compressor testing and design. In his work, to supplement the compressibility factor Z he defined two additional functions, X and Y.

$$X = \frac{T}{V} \left(\frac{\partial V}{\partial T} \right)_P - 1 \quad (6)$$

$$Y = -\frac{P}{V} \left(\frac{\partial V}{\partial P} \right)_T \quad (7)$$

In practical applications a weighted average between inlet, midpoint and outlet are used.

$$X = \frac{X_1 + 2X_m + X_2}{4} \quad (8)$$

$$Y = \frac{Y_1 + 2Y_m + Y_2}{4} \quad (9)$$

These two functions are used to improve the accuracy of the polytropic approach. The aim is to account for the polytropic exponents dependence of temperature and pressure which is changing through the process. The relations between polytropic exponents and compressibility functions X and Y are given below.

$$\frac{n_T - 1}{n_T} = \frac{\kappa - 1}{\kappa} \frac{\left(\frac{1}{\eta_P} + X \right) Y}{(1 + X)^2} \quad (10)$$

$$n_v = \frac{1 + X}{Y \left[\frac{1}{\kappa} \left(\frac{1}{\eta_P} + X \right) - \left(\frac{1}{\eta_P} - 1 \right) \right]} \quad (11)$$

Using the compressibility functions does not fully account for the change in polytropic volume exponent along the compression path. To account for this variation Schultz suggested a correction factor which was assumed equal for both isentropic and polytropic analysis.




$$f = f_s = \frac{h_{2s} - h_1}{\frac{\kappa_v}{\kappa_v - 1} [p_2 v_{2s} - p_1 v_1]} \quad (12)$$

Including the Schultz correction factor the polytropic head becomes:

$$H_P \approx f \frac{n_v}{n_v - 1} \frac{Z_1 R_0 T_1}{MW} \left[\left(\frac{p_2}{p_1} \right)^{\frac{n-1}{n}} - 1 \right] \quad (13)$$

The international standards ASME PTC-10 and ISO 5389 have both included the works by Schultz.

Appendix H: Risk Assessment

 NTNU  HSE/IKS	<h3 style="margin: 0;">Risk assessment</h3>	Prepared by	Number	Date
		HSE section	HMSRV/2603E	04.02.2011
		Approved by	Replaces	01.12.2006
		The Rector		
				

Unit: Department of Energy and Process Engineering

Line manager: Terese Løvås (head of department)

Participants in the identification process: Knut Erik Ellingsgård Johansen (student), Erik Langørgeren (lab engineer)



Short description of the main activity/main process: Subsea Compressor Transients - Master project for Knut Erik Ellingsgård Johansen

Is the project work purely theoretical?: No

Signatures: Responsible supervisor: *[Signature]*

Student: *[Signature]*

Activity	Potential undesirable incident/strain	Likelihood: (1-5)	Consequence:			Risk Value (human)	Comments/status Suggested measures
			Human (A-E)	Environment (A-E)	Economy/ material (A-E)		
Dry and wet gas experiments in compressor test facility	PMMA section breakage	1	D	A	A	D1	Use of protective glasses at all times Keep away from the volute during compressor operation
Dry and wet gas experiments in compressor test facility	Hearing damage	1	D	A	B	D1	Use of hearing protection at all times
Dry and wet gas experiments in compressor test facility	Mechanical failure due to wear/fatigue	1	D	A	D	D1	Routinely inspection and maintenance
Dry and wet gas experiments in compressor test facility	Mechanical failure due to sudden overload	1	D	A	D	D1	Run tests within safe operating limits
Dry and wet gas experiments in compressor test facility	Mechanical failure due to vibrations/pulsations	1	D	A	D	D1	Run tests within safe operating limits

NTNU		Prepared by	Number	Date
		HSE section	HMSRV/2603E	04.02.2011
HSE/KS		Approved by		Replaces
		The Rector		01.12.2006
Risk assessment				

Dry and wet gas experiments in compressor test facility	Emergency brake disabled. Can lead to higher consequences during incidents where emergency stop is triggered	1	D	A	D	D1	Limit the number of tests running with emergency brake disabled. Keep away from rotating parts during operation.
---	--	---	---	---	---	----	--

- Likelihood, e.g.:**
1. Minimal
 2. Low
 3. Medium
 4. High
 5. Very high
- Consequence, e.g.:**
- A. Safe
 - B. Relatively safe
 - C. Dangerous
 - D. Critical
 - E. Very critical
- Risk value (each one to be estimated separately):**
- Human = Likelihood x Human Consequence
 Environmental = Likelihood x Environmental consequence
 Financial/material = Likelihood x Consequence for Economy/material

Potential undesirable incident/strain
 Identify possible incidents and conditions that may lead to situations that pose a hazard to people, the environment and any materiel/equipment involved.

Criteria for the assessment of likelihood and consequence in relation to fieldwork

Each activity is assessed according to a worst-case scenario. Likelihood and consequence are to be assessed separately for each potential undesirable incident. Before starting on the quantification, the participants should agree what they understand by the assessment criteria:

Likelihood					
Minimal 1	Low 2	Medium 3	High 4	Very high 5	
Once every 50 years or less	Once every 10 years or less	Once a year or less	Once a month or less	Once a week	

Consequence				
Grading		Human	Environment	Financial/material
E Very critical		May produce fatality/ies	Very prolonged, non-reversible damage	Shutdown of work >1 year.
D Critical		Permanent injury, may produce serious health damage/sickness	Prolonged damage. Long recovery time.	Shutdown of work 0.5-1 year.

NTNU	Prepared by		Number	Date
	HSE section		HMSRV2603E	04.02.2011
HSE/KS	Approved by			Replaces
	The Rector			01.12.2006
Risk assessment				
				

C Dangerous	Serious personal injury	Minor damage. Long recovery time	Shutdown of work < 1 month
B Relatively safe	Injury that requires medical treatment	Minor damage. Short recovery time	Shutdown of work < 1week
A Safe	Injury that requires first aid	Insignificant damage. Short recovery time	Shutdown of work < 1day

The unit makes its own decision as to whether opting to fill in or not consequences for economy/material, for example if the unit is going to use particularly valuable equipment. It is up to the individual unit to choose the assessment criteria for this column.

Risk = Likelihood x Consequence

Please calculate the risk value for "Human", "Environment" and, if chosen, "Economy/material", separately.

About the column "Comments/status, suggested preventative and corrective measures":

Measures can impact on both likelihood and consequences. Prioritise measures that can prevent the incident from occurring; in other words, likelihood-reducing measures are to be prioritised above greater emergency preparedness, i.e. consequence-reducing measures.

